

# Quadrature methods in kinetic theory: Limitations of the relaxation time approximation

Victor E. Ambruş

West University of Timișoara



Universitatea de Vest  
din Timișoara

Introduction

Boltzmann equation

Quadrature-based FDLB

Multiphase flows: Van der Waals fluid

Multicomponent systems: Cahn Hilliard model

Rarefied gas flows through micro-channels

Shock wave propagation

Relativistic fluid dynamics

# Section 1

## Introduction

# LB team in Timișoara



Victor Sofonea<sup>1</sup>



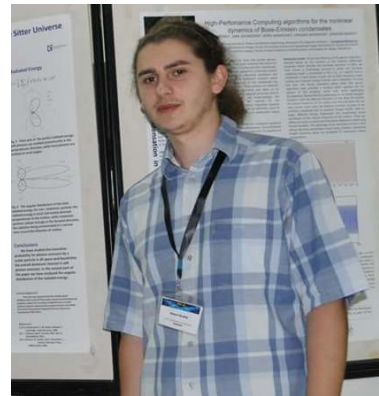
Adrian Neagu<sup>2</sup>



Artur Cristea<sup>1</sup>



Victor Ambruș<sup>3</sup>



Robert Blaga<sup>3</sup>



Sergiu Busuioc<sup>1,3</sup>

## Lattice Boltzmann study of the one-dimensional boost-invariant expansion with anisotropic initial conditions

Victor E. Ambruș<sup>1,3</sup> and Călin G. Guga-Rodica<sup>3,4</sup>

<sup>1</sup>Department of Physics, West University of Timișoara, Bd. Ștefi Pârvan 4, Timișoara 300223, Romania

<sup>2</sup>Corresponding author: Victor.Ambrus@westu.ro

<sup>3</sup>rodica@upit.ro

**Abstract:** A numerical algorithm for the implementation of anisotropic distributions in the frame of the relativistic Boltzmann equation is presented. The implementation relies on the expansion of the Rosenzweig-Strickland distribution with respect to spherical polynomials, which is evolved using the lattice Boltzmann algorithm. The validation of our proposed scheme is performed in the context of the one-dimensional boost-invariant expansion. Explicit results are given for various values of the ratio of the shear viscosity to the energy density. This study is limited to the case of massive particles obeying Maxwell-Boltzmann statistics.

### INTRODUCTION

Following the seminal work of Bodev and Shovel [1], relativistic viscous fluid dynamics has been consistently developed for a wide range of applications, including nuclear collisions [2], neutron starshells [3], cosmology [4] and the spin Hall effect [5] [6] [7] [8] [9] [10] [11] [12] [13] [14] [15] [16] [17] [18] [19] [20] [21] [22] [23] [24] [25] [26] [27] [28] [29] [30] [31] [32] [33] [34] [35] [36] [37] [38] [39] [40] [41] [42] [43] [44] [45] [46] [47] [48] [49] [50] [51] [52] [53] [54] [55] [56] [57] [58] [59] [60] [61] [62] [63] [64] [65] [66] [67] [68] [69] [70] [71] [72] [73] [74] [75] [76] [77] [78] [79] [80] [81] [82] [83] [84] [85] [86] [87] [88] [89] [90] [91] [92] [93] [94] [95] [96] [97] [98] [99] [100].

The lattice Boltzmann method was recently employed to obtain solutions of the relativistic Boltzmann equation, including for the one-dimensional boost-invariant longitudinal expansion [16] [17]. The implementation in Ref. [17] was validated against the semi-analytic solution of the Boltzmann flow presented in Ref. [16] for massive particles obeying Maxwell-Boltzmann statistics or a relativistic distribution for only the case of anisotropic initial conditions. In this paper, we extend the lattice Boltzmann algorithm to a more general situation, namely to anisotropic initial conditions. It is shown that the scheme developed in Ref. [17] is unable to handle anisotropic initial conditions, which is remedied by using the Rosenzweig-Strickland form [18]. This is the main result of this paper. The resulting scheme is validated by comparison with first and second order hydrodynamic results at small  $q$ , analytic expressions in the free-streaming regime and the semi-analytic procedure derived in Ref. [16] everywhere else.

<sup>1</sup>Centre for Fundamental and Advanced Technical Research, Romanian Academy  
<sup>2</sup>Victor Babeș University of Medicine and Pharmacy Timisoara, Romania  
<sup>3</sup>Department of Physics, West University of Timișoara, Romania



# Introduction

## RTA: Pros

- ▶ Easy to implement
- ▶ Easy to compute
- ▶ Versatile
- ▶ Accurate close to eq.  
(and beyond?)
- ▶ ...

# Introduction

## RTA: Pros

- ▶ Easy to implement
- ▶ Easy to compute
- ▶ Versatile
- ▶ Accurate close to eq.  
(and beyond?)
- ▶ ...

## RTA: Cons

- ▶ None.

# Introduction

## RTA: Pros

- ▶ Easy to implement
- ▶ Easy to compute
- ▶ Versatile
- ▶ Accurate close to eq.  
(and beyond?)
- ▶ ...

## RTA: Cons

- ▶ Requires equilibrium  $f^{(\text{eq})}$
- ▶ Requires transport coeffs.:  
 $\mu, \lambda, \dots$
- ▶ Smears over collision details
- ▶ Derived for flows close to eq.
- ▶ ...

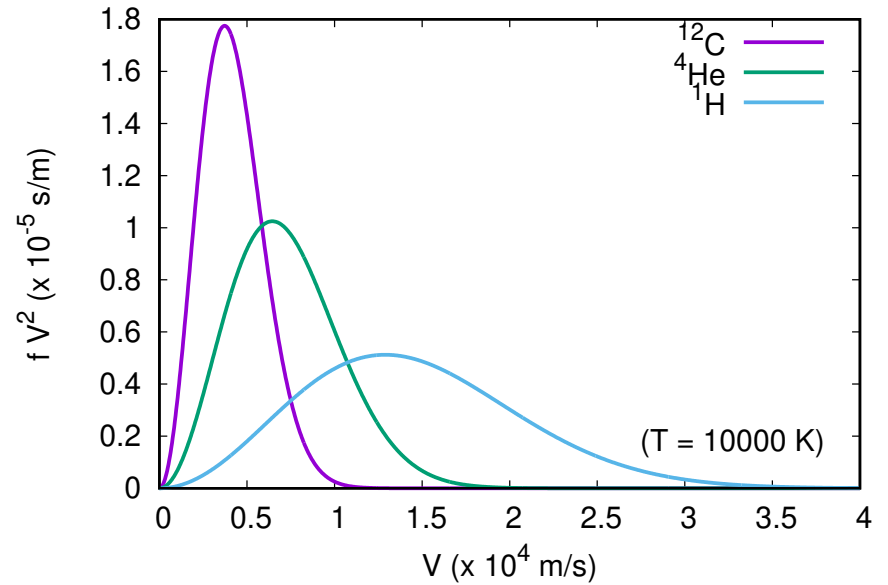
## Section 2

### Boltzmann equation

# Mesoscale approach



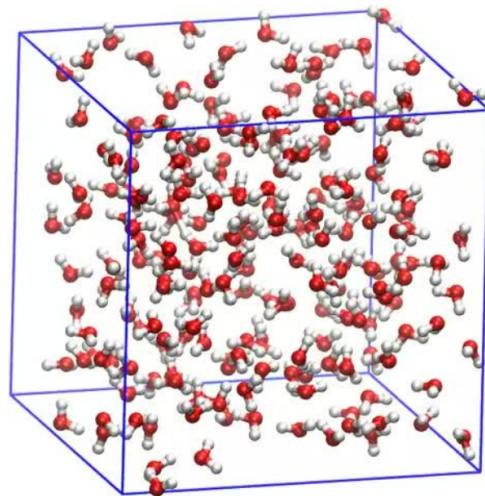
Macroscopic:  $n$ ,  $\mathbf{u}$ ,  $T$   
(Navier-Stokes-Fourier)



Mesoscopic:  $f(\mathbf{x}, \mathbf{p}, t)$   
(Boltzmann)

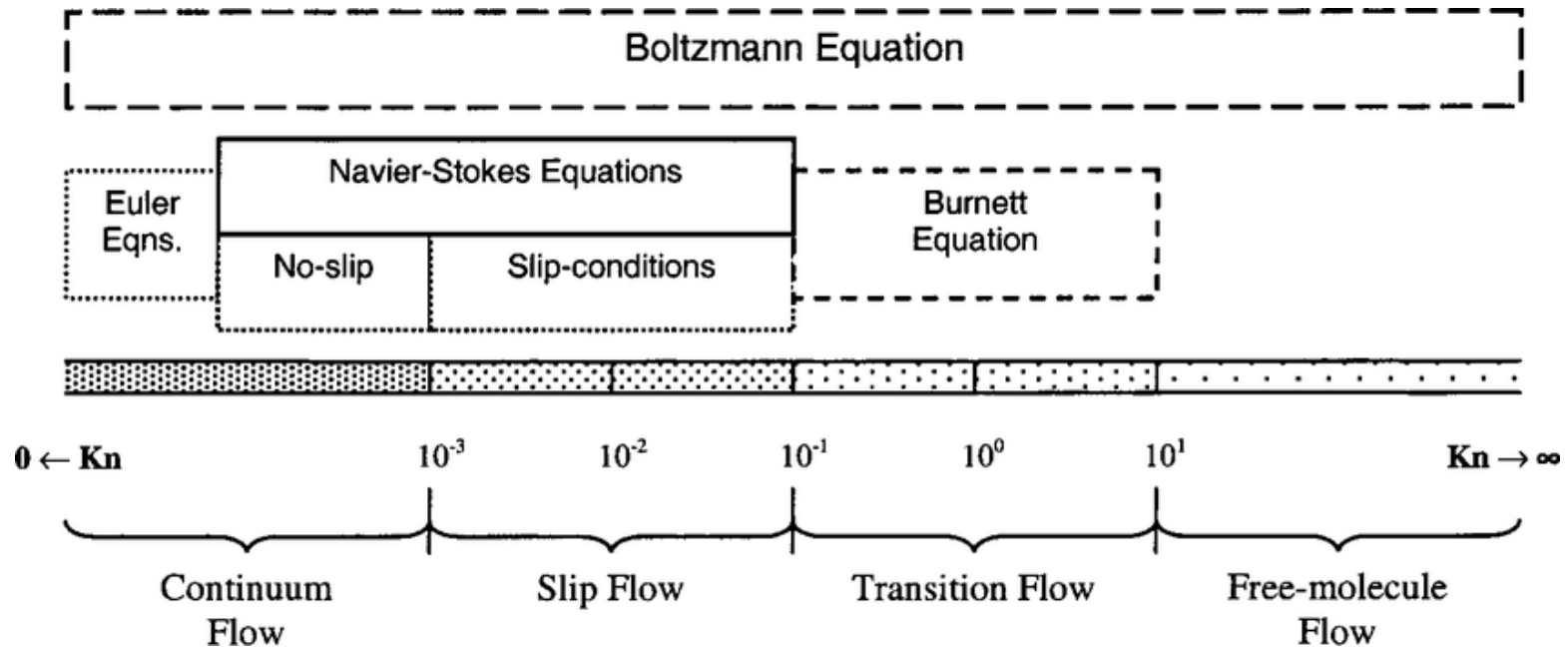


$$N_A = 6.02 \times 10^{23}$$



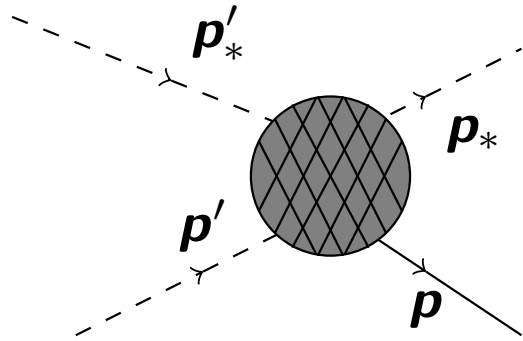
Microscopic:  $(\mathbf{x}_i, \mathbf{p}_i)$   
(MD)

# Rarefied flows: Knudsen number ( $Kn$ )

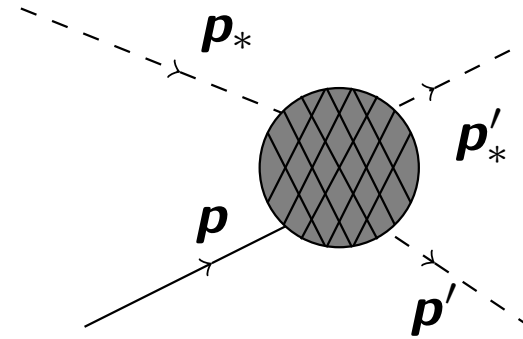


- ▶  $Kn = \lambda/r_p$  ( $\lambda \equiv$  mean free path;  $r_p \equiv$  characteristic channel length).
- ▶ Hydrodynamic regime (NSF):  $Kn \rightarrow 0$ .
- ▶ Ballistic regime (Vlasov):  $Kn \rightarrow \infty$ .

# Boltzmann Equation



$\Gamma_+$ : Part. w.  $\mathbf{p}$  after a collision.



$\Gamma_-$ : Part. w.  $\mathbf{p}$  before a collision.

- ▶ The Boltzmann eq. governs the evol. of the PDF  $f \equiv f(\mathbf{x}, \mathbf{p}, t)$ :<sup>1</sup>

$$\frac{df}{dt} = \partial_t f + \frac{1}{m} \mathbf{p} \cdot \nabla f + \mathbf{F} \cdot \nabla_{\mathbf{p}} f = J[f], \quad J[f] = \Gamma_+ - \Gamma_-. \quad (1)$$

- ▶ The collision op.  $J[f]$  accounts for changes to  $f$  due to collisions.
- ▶ For ideal gases:

$$J[f] = \int d^3 p_* d^3 p' d^3 p'_* \delta^3(\mathbf{p} + \mathbf{p}_* - \mathbf{p}' - \mathbf{p}'_*) \delta(E + E_* - E' - E'_*) \times W(\mathbf{p}, \mathbf{p}_* | \mathbf{p}', \mathbf{p}'_*) (f' f'_* - f f_*). \quad (2)$$

---

<sup>1</sup>C. Cercignani, *The Boltzmann equation and its applications* (Springer, New York, 1988).

# Thermodynamic equilibrium

- ▶ The  $H$  theorem ensures that the state of maximum entropy is described by the thermodynamic equilibrium distribution.
- ▶ For non-relativistic ideal gases, this is the Maxwell-Boltzmann distribution:

$$f^{(\text{eq})}(\mathbf{x}, \mathbf{p}, t) = \frac{n}{(2\pi m K_B T)^{\frac{3}{2}}} \exp \left[ -\frac{(\mathbf{p} - m\mathbf{u})^2}{2m K_B T} \right]. \quad (3)$$

- ▶ Other simple equilibrium distributions can be derived in a similar manner:
  - ▶ Non-relativistic Fermi-Dirac and Bose-Einstein distributions (Uehling-Uhlenbeck collision term);
  - ▶ Maxwell-Jüttner distribution for relativistic ideal gases;
  - ▶ Relativistic Fermi-Dirac and Bose-Einstein distributions.
- ▶ The main features of  $J[f]$  can be captured using simple RTAs:

Non-relativistic, BGK:<sup>1</sup>

$$J_{\text{BGK}}[f] = -\frac{1}{\tau} [f - f^{(\text{eq})}].$$

Relativistic, Anderson-Witting:<sup>2</sup>

$$J_{\text{A-W}}[f] = \frac{\mathbf{p} \cdot \mathbf{u}}{\tau c^2} [f - f^{(\text{eq})}].$$

---

<sup>1</sup>P. L. Bhatnagar, E. P. Gross, M. Krook, Phys. Rev. **94**, 511–525 (1954).

<sup>2</sup>J. L. Anderson, H. R. Witting, Physica **74** (1974) 466–488; 489–495.



# Moments of $f$

- ▶ The macroscopic properties of the fluid can be written in terms of moments of order  $N$  of  $f$ :

$$N = 0 : \quad \text{number density:} \quad n = \int d^3 p f, \quad (4a)$$

$$N = 1 : \quad \text{velocity:} \quad \mathbf{u} = \frac{1}{\rho} \int d^3 p f \mathbf{p}, \quad (4b)$$

$$N = 2 : \quad \text{temperature:} \quad T = \frac{2}{3n} \int d^3 p f \frac{\xi^2}{2m}, \quad (4c)$$

$$\text{viscous tensor:} \quad \sigma_{\alpha\beta} = \int d^3 p \frac{\xi_\alpha \xi_\beta}{m} f - P \delta_{\alpha\beta}, \quad (4d)$$

$$N = 3 : \quad \text{heat flux:} \quad \mathbf{q} = \int d^3 p f \frac{\xi^2}{2m} \frac{\xi}{m}, \quad (4e)$$

where  $\xi = \mathbf{p} - m\mathbf{u}$  is the peculiar velocity and  $P = nk_B T$  is the ideal gas pressure.

# Macroscopic equations: Navier-Stokes limit

- ▶ The collision operator  $J[f]$  admits the collision invariants  $\psi \in \{1, \mathbf{p}, \mathbf{p}^2/2m\}$ , i.e.:

$$\int d^3p J[f]\psi = 0. \quad (5)$$

- ▶ This allows the evolution equations of  $n$ ,  $\mathbf{u}$  and  $T$  to be derived:

Continuity: 
$$\frac{Dn}{Dt} + n(\nabla \cdot \mathbf{u}) = 0, \quad (6)$$

Cauchy eq.: 
$$\rho \frac{Du_i}{Dt} = nF_i - \nabla_i P - \nabla_j \sigma_{ij},$$

Energy eq.: 
$$n \frac{D}{Dt} \left( \frac{3}{2} K_B T \right) + \nabla \cdot \mathbf{q} + P \nabla \cdot \mathbf{u} + \sigma_{ij} \nabla_i u_j = 0,$$

where  $D/Dt = \partial_t + \mathbf{u} \cdot \nabla$  is the material derivative.

- ▶ At small  $\tau$ , the Navier-Stokes-Fourier (NSF) regime is recovered through the Chapman-Enskog (CE) expansion:

$$\sigma_{ij} \simeq -\eta \left( \partial_j u_i + \partial_i u_j - \frac{2}{3} \delta_{ij} \nabla \cdot \mathbf{u} \right), \quad \mathbf{q}_i \simeq -\kappa \partial_i T, \quad (7)$$

where  $\eta = \tau P$  and  $\kappa = \frac{5}{2m} \tau K_B P$  are the coefficients of shear viscosity and heat conductivity.

## Section 3

### Quadrature-based FDLB

# FDLB in a nutshell

Ingredients:

1. Discretisation of the momentum space (Gauss quadratures);
2. Polynomial representation of  $f^{(\text{eq})}$  in the collision term;
3. Replacement of  $\nabla_{\mathbf{p}} f$  using a “suitable” expression;
4. Numerical method for time evolution and spatial advection;
5. Boundary conditions.

Scope:

- ▶ Only macroscopic moments are important;
- ▶ Exact recovery of the conservation eqs;
- ▶ Achieve accurate results using minimal quadrature orders.

# Gauss-Hermite quadrature: discretisation

- ▶ All macroscopic quantities are obtained as moments of the distribution function.
- ▶ A quadrature method is required to evaluate such integral following the discretisation of the momentum space.
- ▶ A popular choice is the Gauss-Hermite quadrature:<sup>2</sup>

$$\int_{-\infty}^{\infty} \frac{dx}{\sqrt{2\pi}} e^{-x^2/2} P_s(x) \simeq \sum_{k=1}^Q w_k P_s(x_k) \quad (8)$$

where the equality is exact when  $Q > 2s$ ,  $x_k$  are the roots of  $H_Q(x)$  and the q. weights  $w_k$  are

$$w_k = \frac{Q!}{H_{Q+1}^2(x_k)}. \quad (9)$$

- ▶ The density is thus computed as:

$$n = \int d^3 p f = \sum_{i=1}^{Q_x} \sum_{j=1}^{Q_y} \sum_{k=1}^{Q_z} f_{ijk}, \quad f_{ijk} = \frac{w_i^{Q_x} w_j^{Q_y} w_k^{Q_z}}{e^{-\bar{\mathbf{p}}^2/2}} f(\mathbf{p}), \quad (10)$$

where  $\bar{p}_\alpha = p_\alpha / p_{0,\alpha}$  is defined w.r.t. a reference momentum scale.

<sup>2</sup>X.W. Shan, X.F. Yuan, H.D. Chen, J. Fluid Mech. **550** (2006) 413–441.

## Gauss-Hermite quadrature: $f^{(\text{eq})}$

- ▶ The MB distribution can be factorised w.r.t.  $\mathbf{p}$ :

$$f^{(\text{eq})} = n g_x g_y g_z, \quad g_\alpha = \frac{1}{\sqrt{2\pi m K_B T}} \exp \left[ -\frac{(p_\alpha - m u_\alpha)^2}{2m K_B T} \right]. \quad (11)$$

- ▶ After discretisation,  $f^{(\text{eq})} \rightarrow f_{ijk}^{(\text{eq})} = n g_{x,i} g_{y,j} g_{z,k}$ .
- ▶ The collision invariants are preserved as long as:

$$\sum_{i,j,k} f_{ijk}^{(\text{eq})} = n, \quad \sum_{i,j,k} f_{ijk}^{(\text{eq})} \mathbf{p}_{ijk} = \rho \mathbf{u}, \quad \sum_{i,j,k} f_{ijk}^{(\text{eq})} \frac{\xi_{ijk}^2}{2m} = \frac{3}{2} n K_B T. \quad (12)$$

- ▶ The functions  $g_\alpha$  can be expanded w.r.t. the Hermite polynomials:

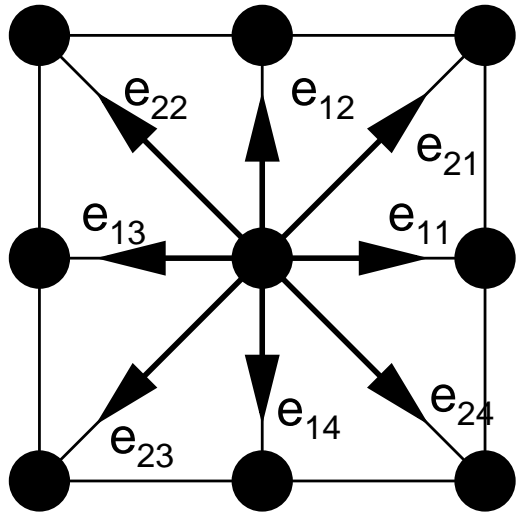
$$g_\alpha = \frac{e^{-\bar{p}_\alpha^2/2}}{\sqrt{2\pi p_{0,\alpha}}} \sum_{\ell=0}^{\infty} \frac{1}{\ell!} \mathcal{G}_\ell H_\ell(\bar{p}_\alpha), \quad \mathcal{G}_\ell = \int_{-\infty}^{\infty} dp_\alpha g_\alpha H_\ell(\bar{p}_\alpha). \quad (13)$$

- ▶ Since  $\langle H_\ell, H_{\ell'} \rangle = \ell! \delta_{\ell,\ell'}$ , only  $\ell \in \{0, 1, 2\}$  contribute to Eq. (12).
- ▶ **The collision invariants are preserved when  $g_\alpha$  is truncated at  $N_\alpha$ .**
- ▶  $N_\alpha = 2$  for Euler, 3 for isothermal NS, 4 for thermal NS,...

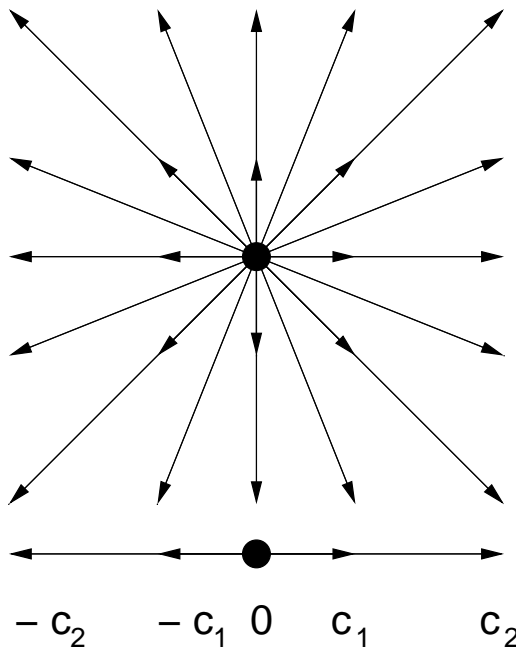
- ▶ Analytic expr.:<sup>3</sup>  $g_k = \sum_{\ell=0}^N \sum_{s=0}^{\lfloor \ell/2 \rfloor} \frac{w_k H_\ell(\bar{p}_k)}{2^s s! (\ell - 2s)!} \left( \frac{T}{T_0} - 1 \right)^2 \left( \frac{m u}{p_0} \right)^{\ell - 2s}$ .

<sup>3</sup>V. E. Ambruş, V. Sofonea, J. Comput. Phys. **316** (2016) 1–29.

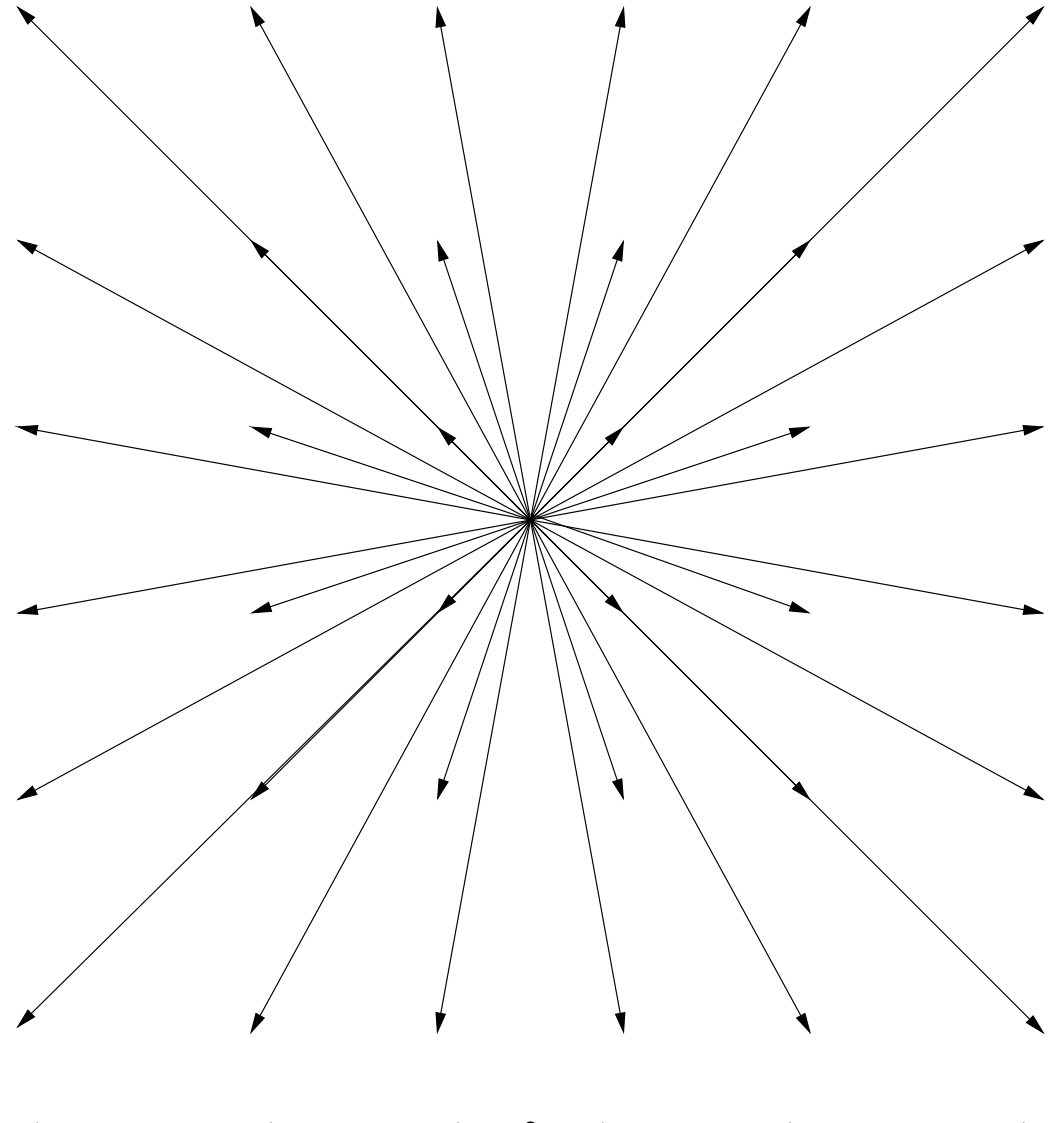
# HLB models in 2D: momentum sets



$Q = 3$



$Q = 5$



$Q = 6$

# Quadrature w.r.t. spherical coordinates

- ▶ Another convenient factorisation of the momentum space can be performed w.r.t.  $(p, \theta, \varphi)$ :

$$\int d^3p \rightarrow \int_0^\infty dp p^2 \int_{-1}^1 d(\cos \theta) \int_0^{2\pi} d\varphi. \quad (14)$$

- ▶ The  $\varphi$  integral can be recovered using the Mysovskikh quadrature:<sup>4</sup>

$$\int_0^{2\pi} d\varphi (\cos \varphi)^n (\sin \varphi)^m \simeq \frac{2\pi}{Q_\varphi} \sum_{i=1}^{Q_\varphi} (\cos \varphi_i)^n (\sin \varphi_i)^m, \quad (15)$$

where  $\varphi_i = \varphi_0 + 2\pi i / Q_\varphi$  ( $\varphi_0$  is an arbitrary offset angle) and the equality is achieved when  $Q_\varphi > m$  and  $Q_\varphi > n$ .

- ▶ The  $\xi = \cos \theta$  integral can be recovered using the Gauss-Legendre quadrature:

$$\int_{-1}^1 d\xi P_s(\xi) \simeq \sum_{j=1}^{Q_\xi} w_j^\xi P_s(\xi_j), \quad w_j^\xi = \frac{2(1 - \xi_j^2)}{(Q_\xi + 1)^2 [P_{Q_\xi+1}(\xi_j)]^2}, \quad (16)$$

where equality is exact for  $Q_\xi > 2s$  and when  $P_{Q_\xi}(\xi_j) = 0$ .

---

<sup>4</sup>I. P. Mysovskikh, Soviet Math. Dokl. **36** (1988) 229–322.



# Radial quadrature

- ▶ The quadrature rules are used to recover moments of  $f$  and  $f^{(\text{eq})}$  w.r.t.  $\mathbf{p} = p \sin \theta (\cos \varphi \mathbf{i} + \sin \varphi \mathbf{j}) + p \cos \theta \mathbf{k}$ .
- ▶ After the  $\varphi$  and  $\xi$  integration, only even powers of  $p$  contribute to the  $p$  integral, such that the Gauss-Laguerre quadrature can be applied w.r.t.  $x = \bar{p}^2$  ( $\bar{p} = p/p_0$ ):

$$\int_0^\infty dp p^2 e^{-\bar{p}^2} P_s(\bar{p}^2) = \int_0^\infty \frac{dx}{2} x^{1/2} e^{-x} P_s(x) \simeq \sum_{k=1}^{Q_L} w_k^L P_s(x_k),$$

$$w_k^L = \frac{x_k \Gamma(Q_L + 3/2)}{Q_L! (Q_L + 1)^2 [L_{Q_L+1}^{(1/2)}(x_k)]^2}, \quad (17)$$

where the equality is exact when  $Q_L > 2s$  and  $L_{Q_L}^{(1/2)}(x_k) = 0$ .

- ▶ The density is obtained as follows:

$$n = \sum_{k=1}^{Q_L} \sum_{j=1}^{Q_\xi} \sum_{i=1}^{Q_\varphi} f_{ijk}, \quad f_{ijk} = \frac{2\pi w_j^\xi w_k^L}{Q_\varphi e^{-\bar{p}_k^2}} f(p_k, \xi_j, \varphi_i). \quad (18)$$

## Construction of $f^{(\text{eq})}$

- ▶ Starting from the decomposition  $f^{(\text{eq})} = nF(p; T)E(\mathbf{p}, \mathbf{u})$ , where

$$F = \frac{e^{-p^2/2mK_B T}}{(2\pi mK_B T)^{3/2}}, \quad E = \exp \left[ -\frac{m\mathbf{u}^2}{2K_B T} + \frac{\mathbf{u} \cdot \mathbf{p}}{K_B T} \right], \quad (19)$$

the functions  $E$  and  $F$  can be expanded as follows:

$$E = \sum_{j=0}^{\infty} \frac{1}{j!} \left( -\frac{m\mathbf{u}^2}{2K_B T} \right)^j \sum_{r=0}^{\infty} \frac{1}{r!} \left( \frac{\mathbf{p} \cdot \mathbf{u}}{K_B T} \right)^r, \quad (20)$$

while  $F$  can be expanded w.r.t. the Laguerre polynomials:

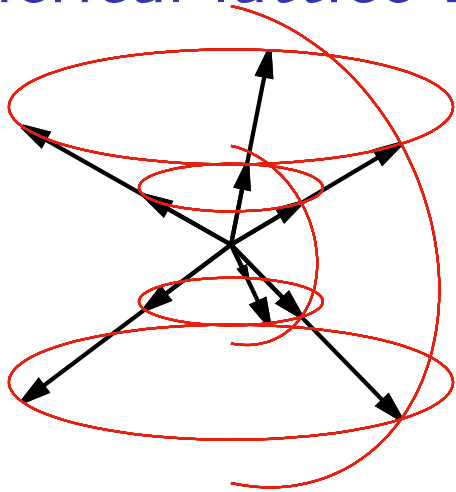
$$F = \frac{e^{-x}}{\pi^{3/2}} \sum_{\ell=0}^{\infty} \left( 1 - \frac{2mK_B T}{p_0^2} \right)^{\ell} L_{\ell}^{(1/2)}(x). \quad (21)$$

- ▶ After discretisation,  $f^{(\text{eq})} \rightarrow f_{ijk}^{(\text{eq})} = nF_k E_{ijk}$ , while  $E_{ij}$  and  $F_k$  are obtained by truncating Eqs. (20) and (21):

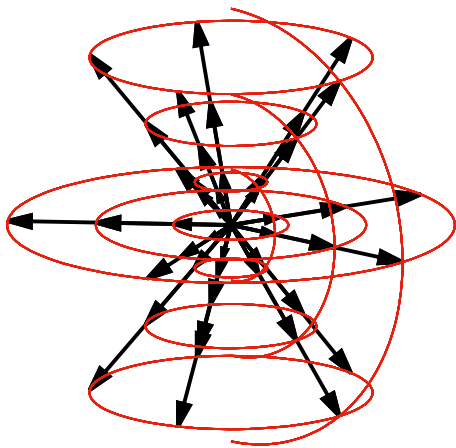
$$F_k = \frac{w_k^L}{Q_{\varphi} \sqrt{\pi}} \sum_{\ell=0}^{N_L} \left( 1 - \frac{2mK_B T}{p_0^2} \right)^{\ell} L_{\ell}^{(1/2)}(x_k),$$

$$E_{ij} = w_j^{\xi} \sum_{j=0}^{\lfloor N_{\Omega}/2 \rfloor} \frac{1}{j!} \left( -\frac{m\mathbf{u}^2}{2K_B T} \right)^j \sum_{r=0}^{N_{\Omega}-2r} \frac{1}{r!} \left( \frac{\mathbf{p}_{ijk} \cdot \mathbf{u}}{K_B T} \right)^r. \quad (22)$$

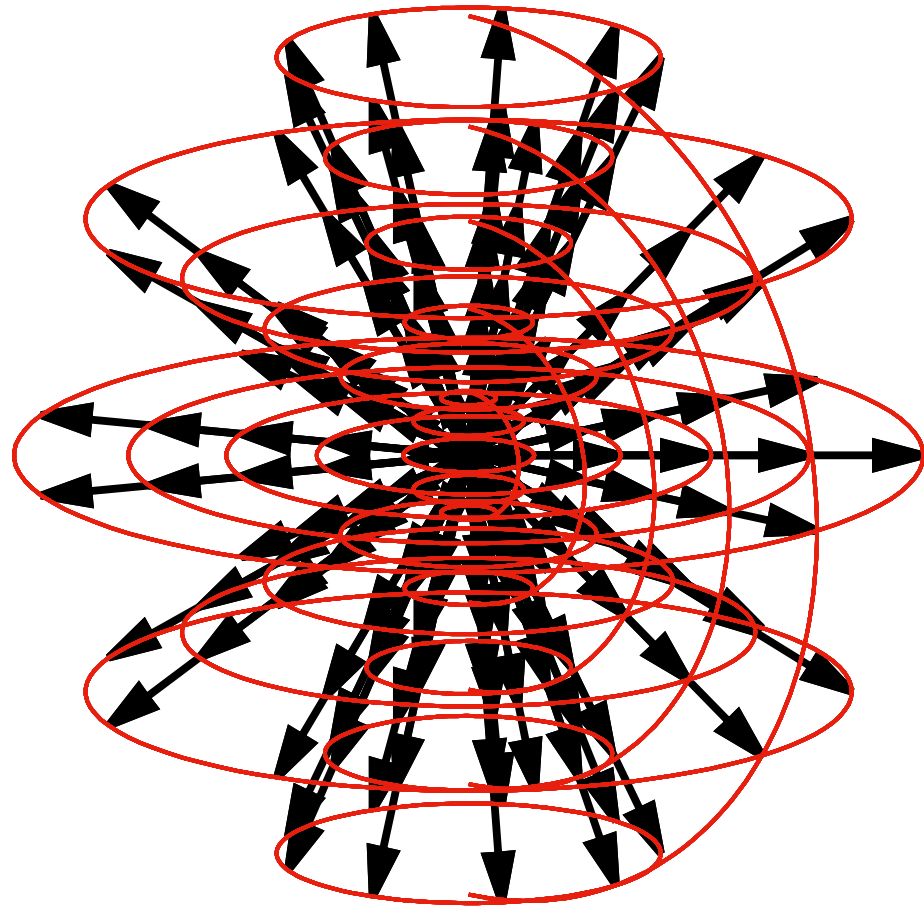
# Spherical lattice Boltzmann (SLB) models<sup>6</sup>



SLB(2, 2, 3)



SLB(3, 3, 5)



SLB(5, 5, 9)

A similar model was developed by Romatschke et al.<sup>5</sup> for ultrarelativistic flows.

---

<sup>5</sup>P. Romatschke, M. Mendoza, S. Succi, Phys. Rev. C **84** (2011) 034903.

<sup>6</sup>V. E. Ambruş, V. Sofonea, Phys. Rev. E **86** (2012) 016708.

# LB: Conclusions

- ▶ The key to the success of LB is the correlation between  $f^{(\text{eq})}$  and the chosen quadrature.
- ▶ Depending on the problem at hand, one may desire various separation of variables:
  - ▶ Cartesian  $(p_x, p_y, p_z)$ ;
  - ▶ Spherical  $(p, \theta, \varphi)$ ;
  - ▶ ...
- ▶ The scheme is easily extendable to higher orders, as all operations are analytical.

## Section 4

Multiphase flows: Van der Waals fluid

# Van der Waals equation of state

- ▶ In deriving the ideal gas EOS, the particles are assumed to be pointlike and long-range interactions are neglected.
- ▶ The assumption leading to the ideal EOS are valid for dilute gases.
- ▶ The van der Waals EOS provides an empirical extension to dense gases by taking into account two factors:
  1. The particles have finite volume, such that the average volume per particle  $\tilde{V} = 1/\tilde{n}$  is decreased by the *covolume*:  $\tilde{V} \rightarrow \tilde{V} - \tilde{b}$ .
  2. The inter-particle attraction forces increase the fluid compressibility and thus the isotropic pressure is increased:  $\tilde{P} \rightarrow \tilde{P} + \tilde{a}/\tilde{V}^2$ .
- ▶ The vdV EOS can be written as a cubic eq. for  $\tilde{V}$ :

$$\tilde{V}^3 - \left( \frac{\tilde{K}_B \tilde{T}}{\tilde{P}} + \tilde{b} \right) \tilde{V}^2 + \frac{\tilde{a}}{\tilde{P}} - \frac{\tilde{a}\tilde{b}}{\tilde{P}} = 0. \quad (23)$$

- ▶ The 3 roots coincide at the critical point:

$$\tilde{n}_c = \frac{1}{3\tilde{b}}, \quad \tilde{K}_B \tilde{T}_c = \frac{8\tilde{a}}{27\tilde{b}}. \quad (24)$$

- ▶ Below the CP, the 3 roots are real  $\Rightarrow$  phase separation.
- ▶ Non-dimensionalising the vdW EOS via  $\tilde{P}_{\text{ref}} = \tilde{n}_c \tilde{K}_B \tilde{T}_c$  gives:

$$P_{\text{Waals}} = \frac{3nT}{3-n} - \frac{9}{8}n^2, \quad (25)$$

## RTA strategy

- ▶ The main difference between the vdW and ideal fluids is that in the former, spontaneous (spinodal) phase separation can occur.
- ▶ The popular BGK model for the collision term corresponds to an ideal Newtonian fluid.
- ▶ A standard (minimal) approach is to introduce the vdW interaction via an external force:

$$\mathbf{F} = n\sigma\nabla(\Delta n) - \nabla(P_{\text{Waals}} - P_{\text{ideal}}), \quad (26)$$

such that the Cauchy equation becomes:

$$\rho \frac{Du_i}{Dt} = n\sigma\nabla_i(\Delta n) - \nabla_i P_{\text{waals}} - \nabla_j \sigma_{ij}, \quad (27)$$

where  $\sigma$  controls the surface tension.

- ▶ The drawback of this approach is that the pressure entering the energy equation is still that corresponding to the ideal gas:

$$n \frac{De}{Dt} + \nabla \cdot \mathbf{q} + P_{\text{ideal}}(\nabla \cdot \mathbf{u}) + \sigma_{ij} \nabla_i u_j = 0, \quad (28)$$

where  $e$  is the specific energy.

## (Minimal) LB implementation

- ▶ The C-E expansion shows that  $N = 4$  ( $Q = 5$ ) is required for thermal flows.<sup>7</sup>
- ▶ For 2D flows,  $\text{HLB}(5) \times \text{HLB}(5)$  is sufficient.
- ▶ The Boltzmann eq. becomes:

$$\partial_t f_{ij} + \frac{1}{m} \mathbf{p}_{ij} \cdot \nabla f_{ij} + \mathbf{F} \cdot (\nabla_{\mathbf{p}} f)_{ij} = -\frac{1}{\tau} [f_{ij} - f_{ij}^{(\text{eq})}], \quad (29)$$

where  $f_{ij}^{(\text{eq})} = n g_{x,i} g_{y,j}$  (expanded up to  $N_x = N_y = 4$ ).

- ▶ The force term must be projected w.r.t. the Hermite polynomials.
- ▶ For a  $\partial_{p_x} f$ , we have:

$$f = \frac{e^{-\bar{p}_x^2/2}}{\sqrt{2\pi}} \sum_{\ell=0}^{\infty} \frac{1}{\ell!} \mathcal{F}_{\ell}(p_y) H_{\ell}(\bar{p}_x) \Rightarrow \frac{\partial f}{\partial p_x} = -\frac{e^{-\bar{p}_x^2/2}}{\sqrt{2\pi}} \sum_{\ell=0}^{\infty} \frac{1}{\ell!} \mathcal{F}_{\ell}(p_y) H_{\ell+1}(\bar{p}_x).$$

- ▶ After discretisation,  $\mathcal{F}_{\ell;j} = \sum_{i=1}^{Q_x} f_{ij} H_{\ell}(\bar{p}_{x,i})$ , such that:

$$(\partial_{p_x} f)_{ij} = \sum_{i'=1}^{Q_x} \mathcal{K}_{i,i'} f_{i',j}, \quad \mathcal{K}_{i,i'} = -w_i^H \sum_{\ell=0}^{Q_x-1} \frac{1}{\ell!} H_{\ell+1}(\bar{p}_i) H_{\ell}(\bar{p}_{i'}). \quad (30)$$

---

<sup>7</sup>V. E. Ambrus, V. Sofonea, Phys. Rev. E **86** (2012) 016708.



# Finite difference schemes

- ▶ Phase-field models are known to be plagued by spurious fluctuations around the interface regions.
- ▶ Since they are numerical in nature, high order schemes can be used to reduce their amplitude.
- ▶ The time stepping is performed using an explicit TVD RK-3 integration due to Shu and Osher.<sup>8</sup>
- ▶ The advection is performed using the fifth-order WENO scheme.<sup>9</sup>
- ▶ The pressure difference gradient  $\nabla_i(P_{\text{Waals}} - P_{\text{ideal}})$  is performed using a 49-point stencil (6th order accurate and 8th order isotropic).<sup>10</sup>
- ▶ The gradient of the Laplacian  $\nabla_i(\Delta n)$  is computed using a 49-point stencil (4th order accurate and 6th order isotropic).<sup>11</sup>

---

<sup>8</sup>C.-W. Shu, S. Osher, J. Comput. Phys. **77** (1988) 439–471.

<sup>9</sup>G. S. Jiang, C. W. Shu, J. Comput. Phys. **126** (1996) 202.

<sup>10</sup>S. Leclaire, M. El-Hachem, J. Trepanier, M. Reggio, J. Sci. Comput. **59** (2014) 545–573.

<sup>11</sup>M. Patra, M. Karttunen, Num. Meth. Diff. Eqs. **22** (2006) 936–953.

# Validation 1: shear waves damping

- ▶ At  $t = 0$ :

$$n = \text{const},$$

$$T = \text{const},$$

$$u_y = U_0 \cos kx.$$

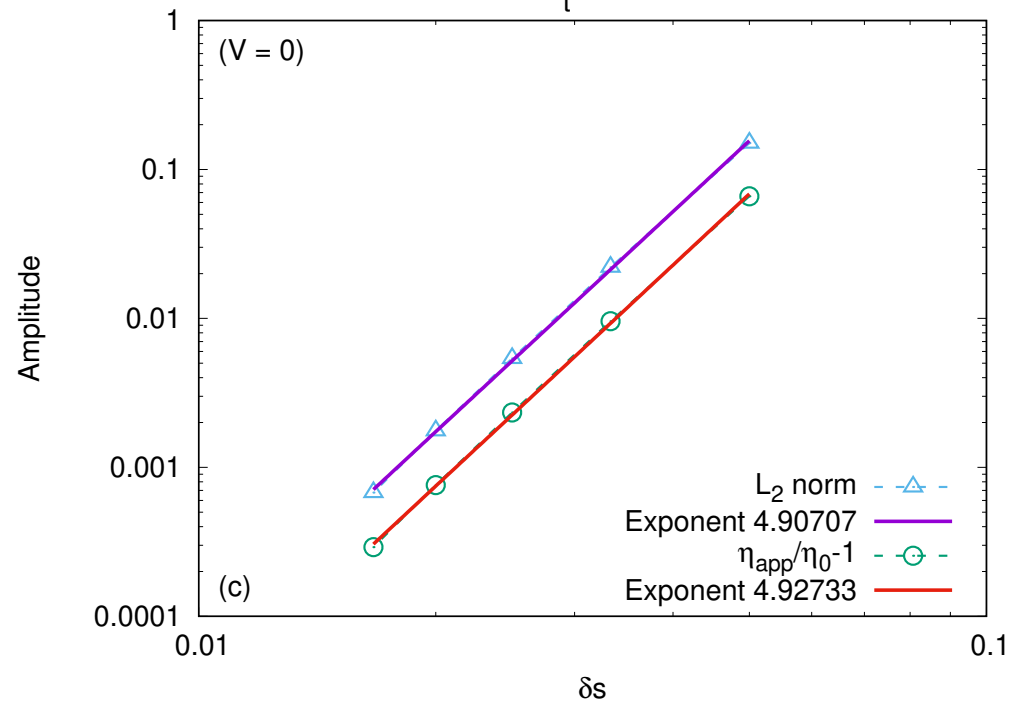
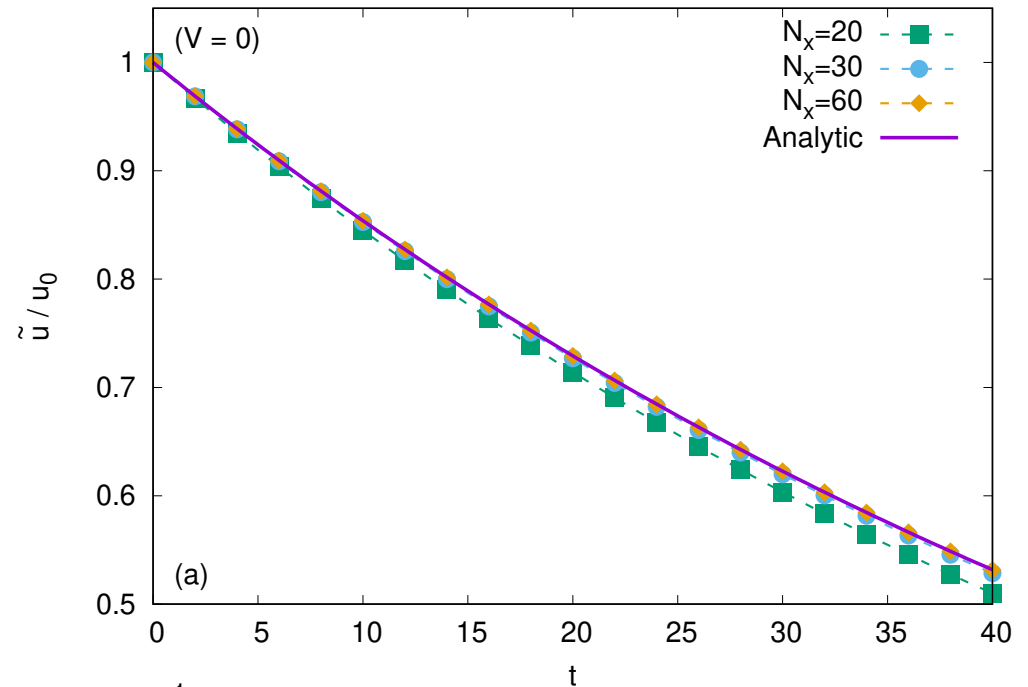
- ▶ In the linearised regime ( $U_0 \ll 1$ ),  $n$  and  $T$  remain const, while

$$u_y(x, t) = U(t) \cos kx,$$

$$U(t) = e^{-\alpha t},$$

$$\alpha = k^2 \eta / \rho.$$

- ▶  $\alpha$  is recovered for ideal fluid, vdW vapour and vdW liquid.
- ▶ Fifth order accuracy is seen in all cases.



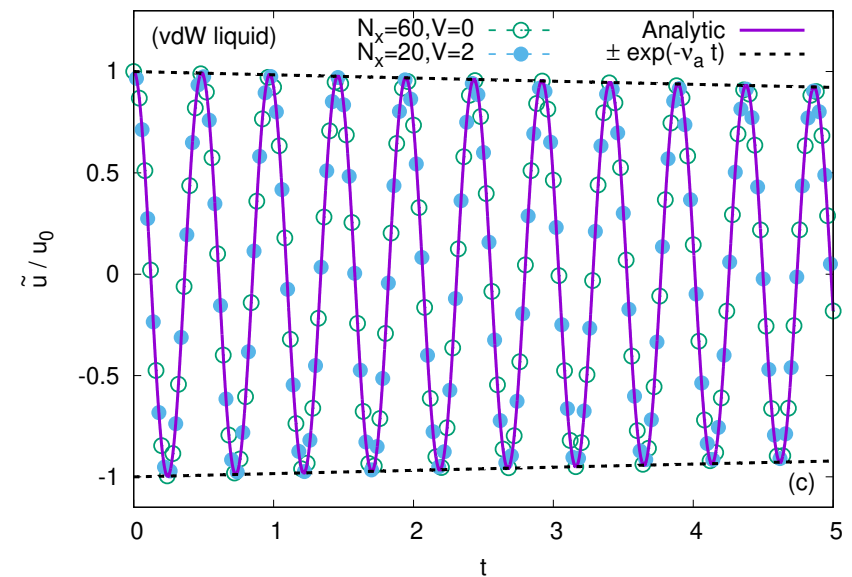
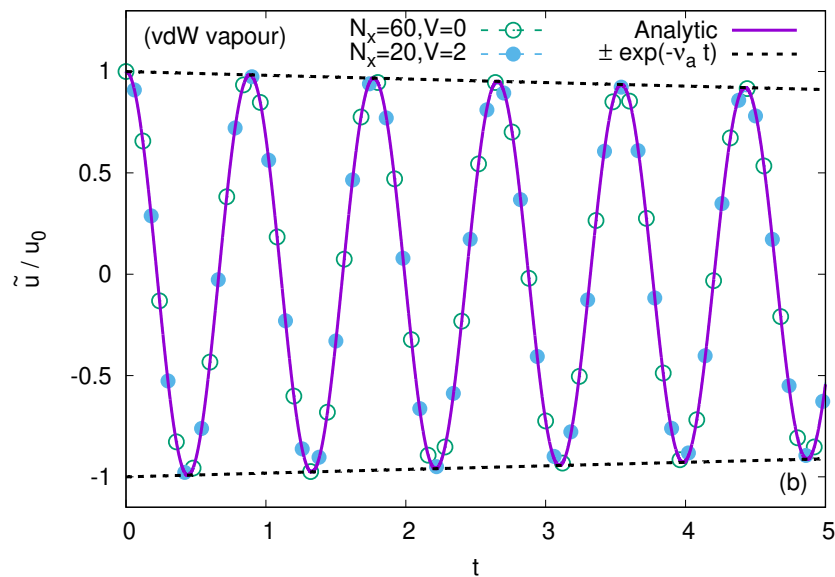
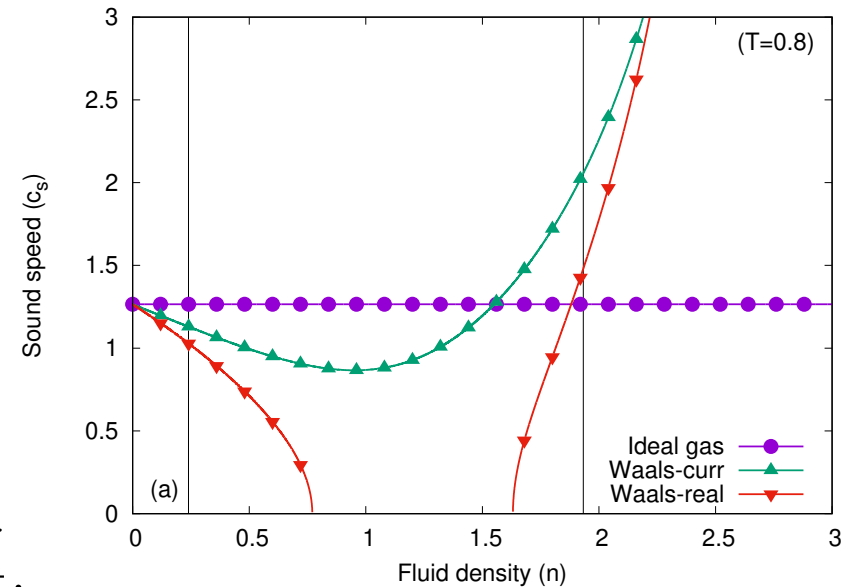
# Validation 2: longitudinal waves

- ▶ The implementation has three major drawbacks:

1.  $C_V = 2K_B T$  (2D fluid);
2.  $Pr = 1$ ;
3. The energy equation is written w.r.t.  $P_{ideal}$ .

- ▶ These affect the sound speed:

$$c_s^2 = \frac{\partial P_{Waals}}{\partial \rho} + \frac{P_{ideal}}{n\rho} \frac{\partial P_{waals}}{\partial T} + \frac{nk^2\sigma}{m}.$$

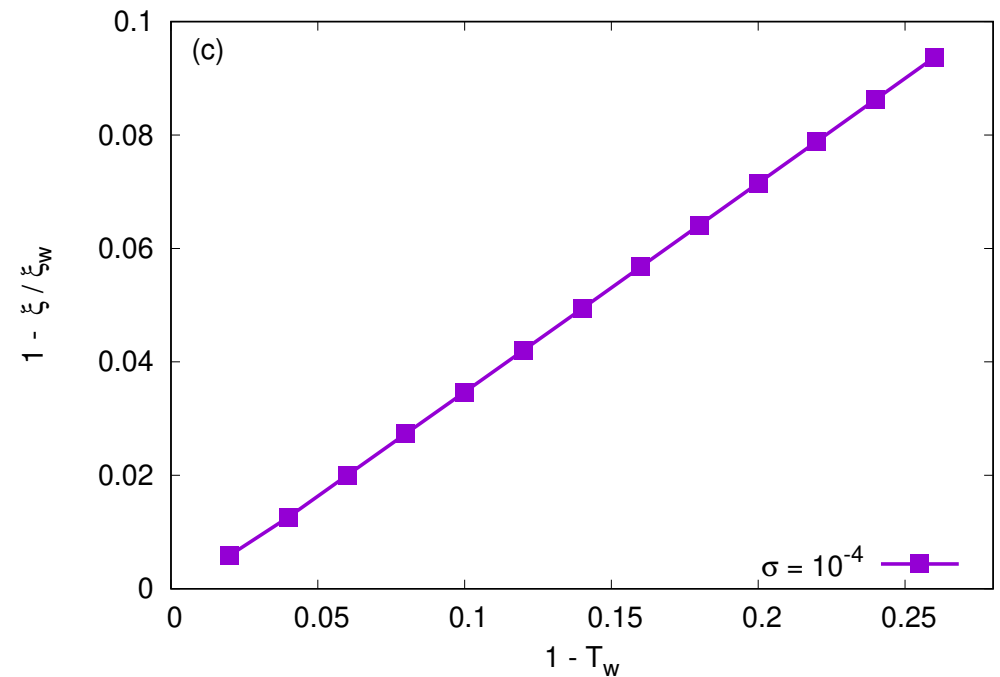
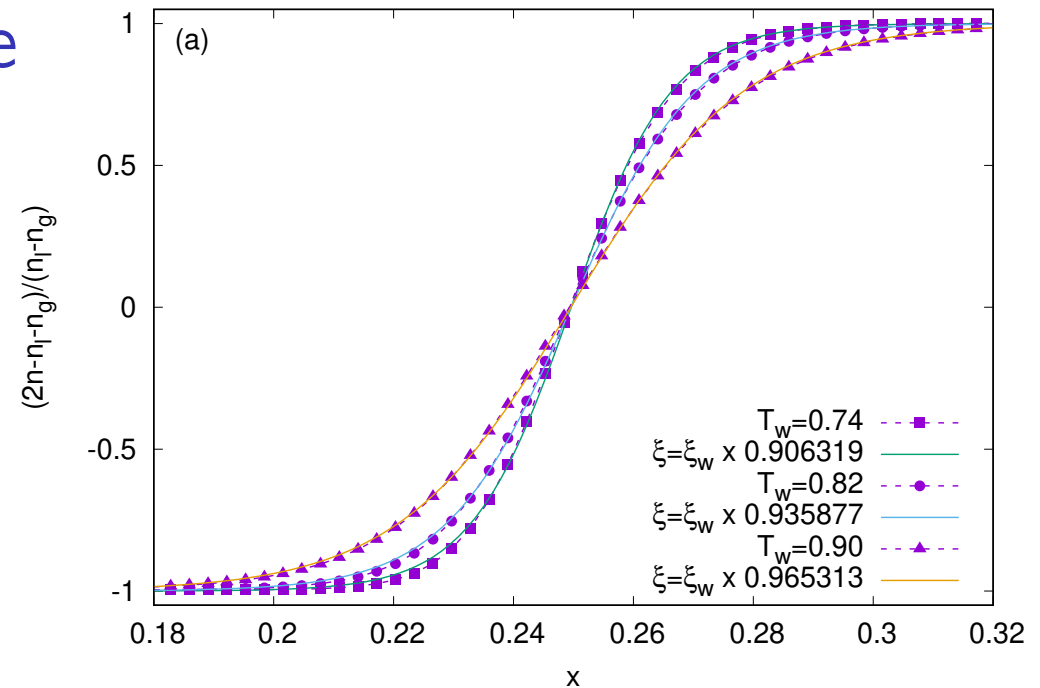


## Validation 3: Planar interface

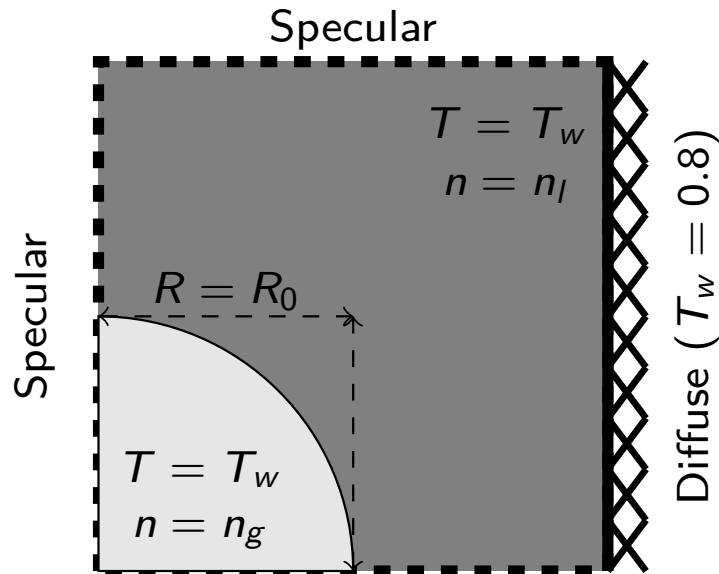
- ▶ Let us consider the fluid enclosed between two plates at  $T_w = 0.8$ .
- ▶ Due to the symmetry, only the right half is considered.
- ▶ The system is homogeneous w.r.t.  $y$ .
- ▶ The interface is initialised at  $x_0 = 0.25 = x_w/2$ .
- ▶ An approximate formula (valid when  $T \rightarrow 1$ ) is:

$$n(x) = n_g + \frac{n_l - n_g}{2} \times \left[ 1 + \tanh \frac{(x - x_0)}{\xi} \right],$$

$$\xi_w = \sqrt{\frac{8\sigma}{9(1 - T_w)}}.$$



# Validation 4: Surface tension

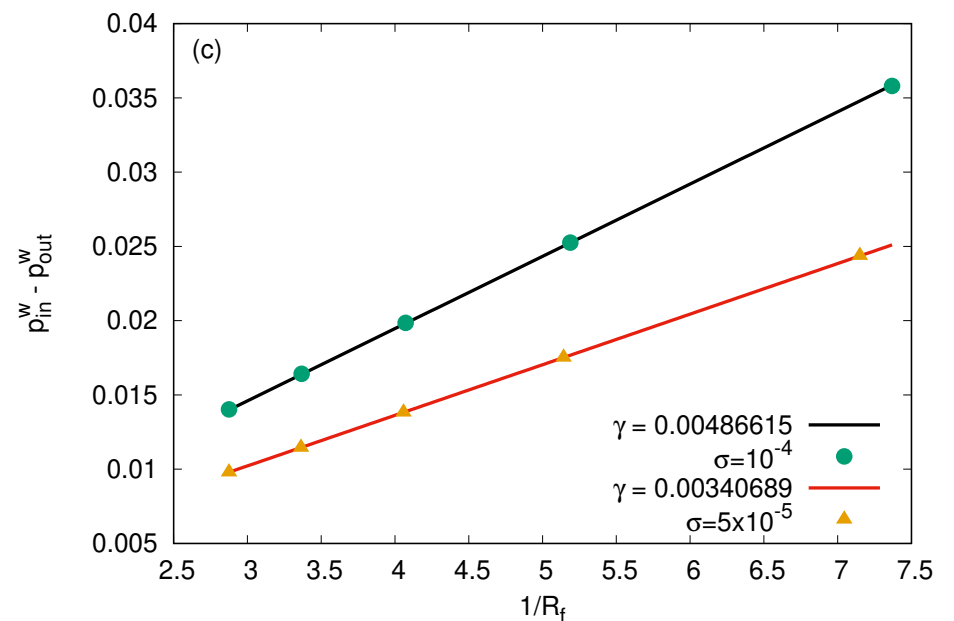
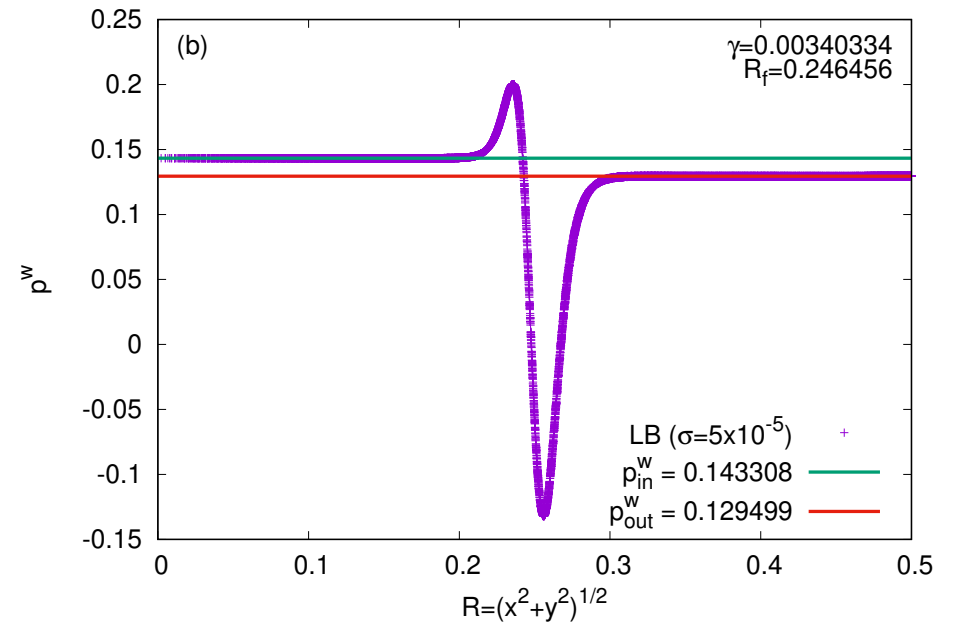


- ▶ Laplace's law:

$$P_{\text{in}}^w - P_{\text{out}}^w = \frac{\gamma_{\text{Lap}}}{R}.$$

- ▶ For the planar interface:

$$\gamma_{\text{pl}} = \sigma \int dx \left( \frac{dn}{dx} \right)^2.$$



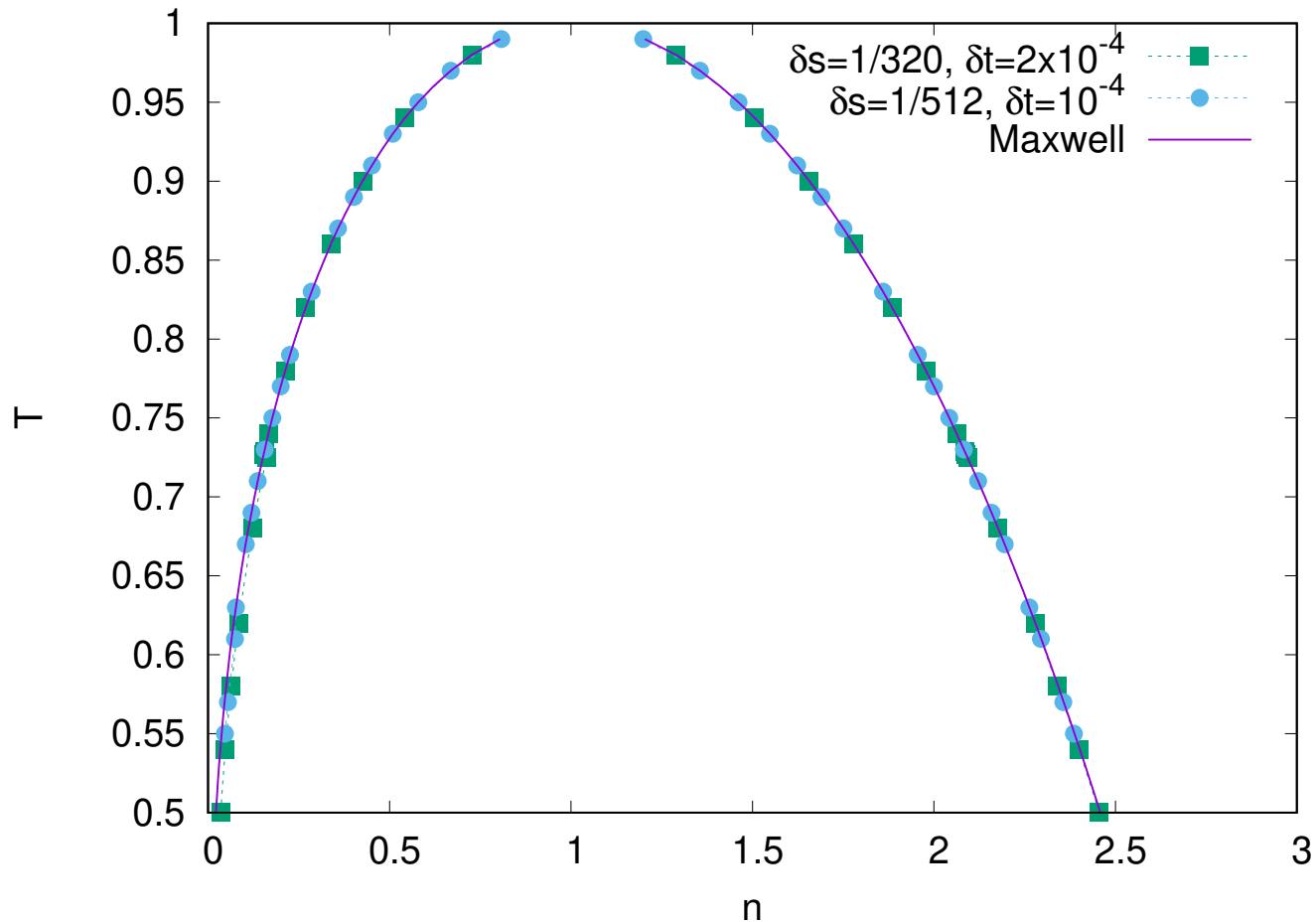
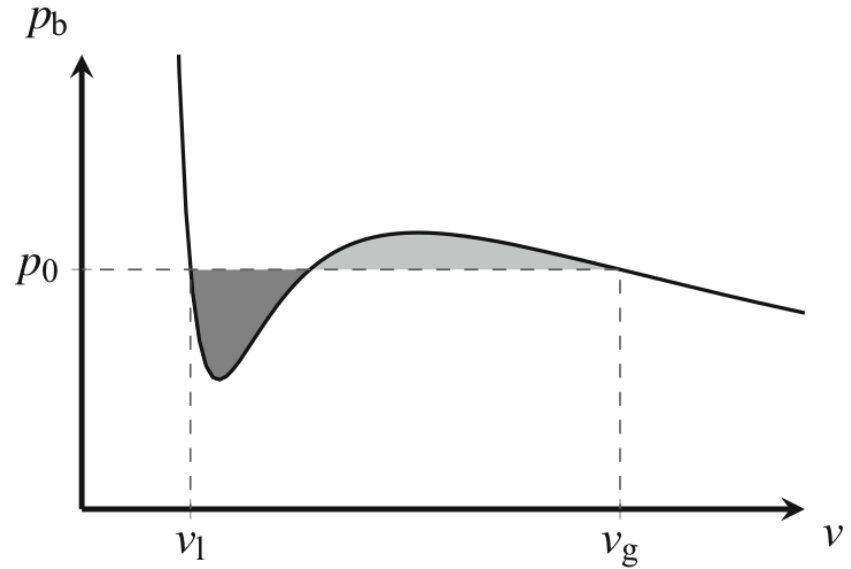
$\sigma$	$\gamma_{\text{pl}}$	$\gamma_{\text{Lap}}$
$5 \times 10^{-5}$	$3.386731 \times 10^{-3}$	$3.40689 \times 10^{-3}$
$10^{-4}$	$4.883771 \times 10^{-3}$	$4.86615 \times 10^{-3}$

# Validation 5: Phase diagram

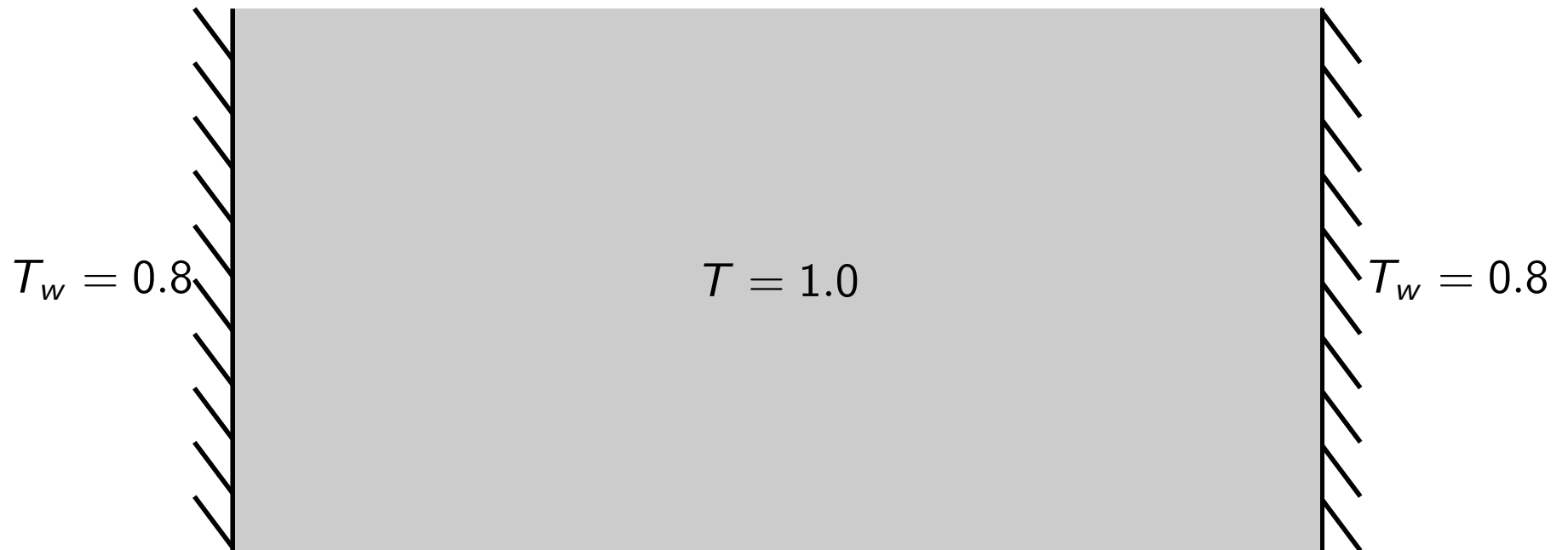
$n_g$  and  $n_l$  are given through the Maxwell construction:

$$\int_{1/n_l}^{1/n_g} [P_{\text{Waals}} - P_{\text{Waals}}^0] dV = 0,$$

where  $V = 1/n$ .

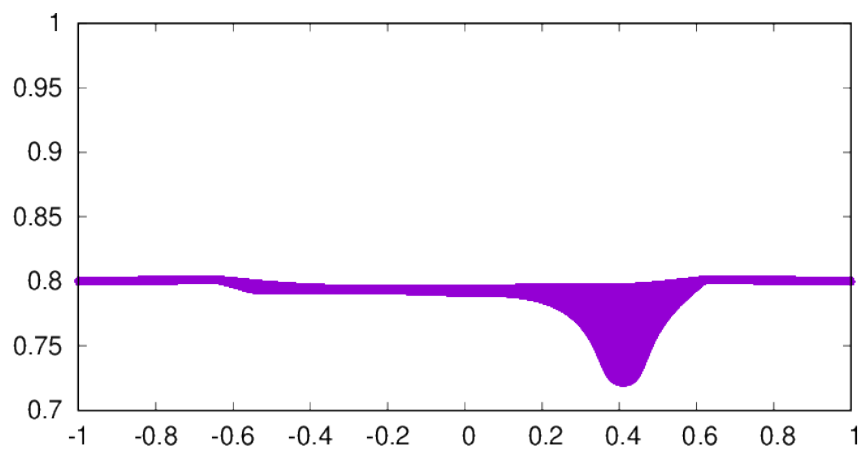
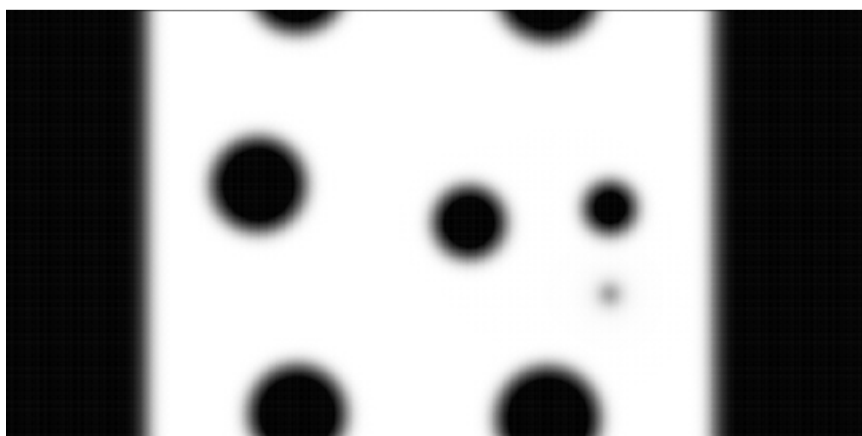
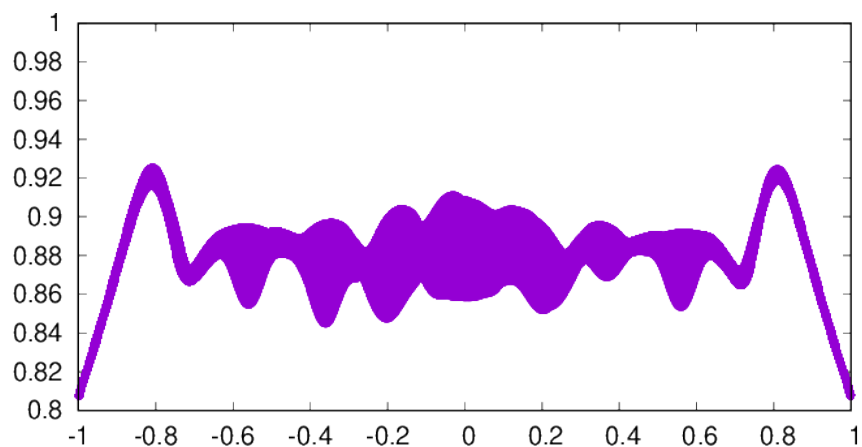
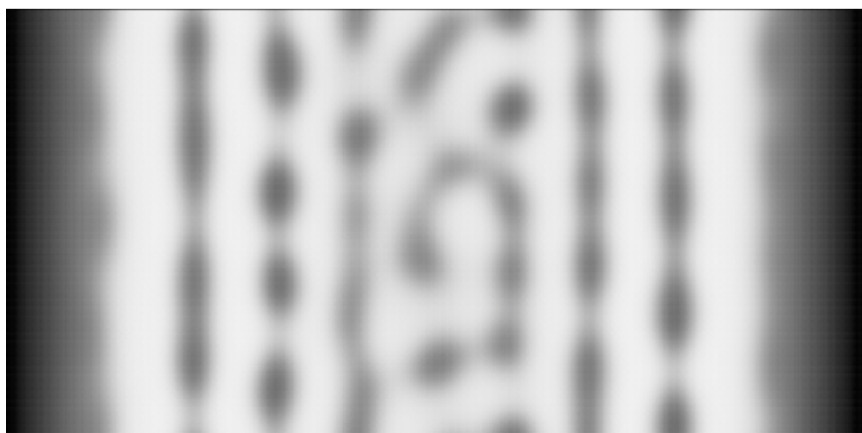
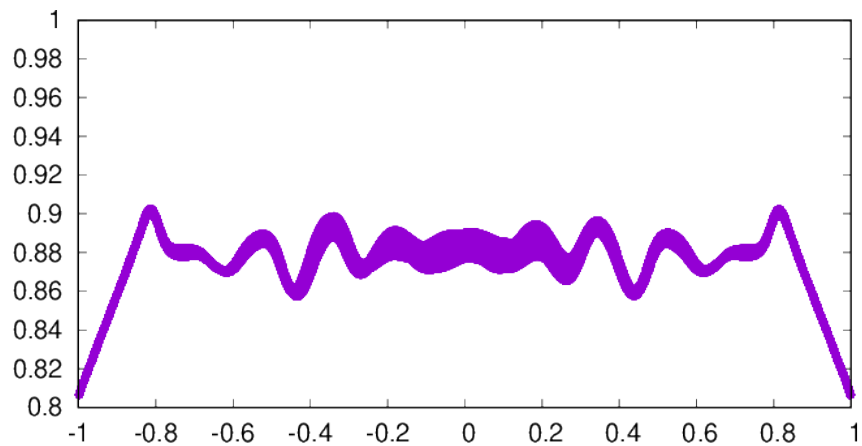
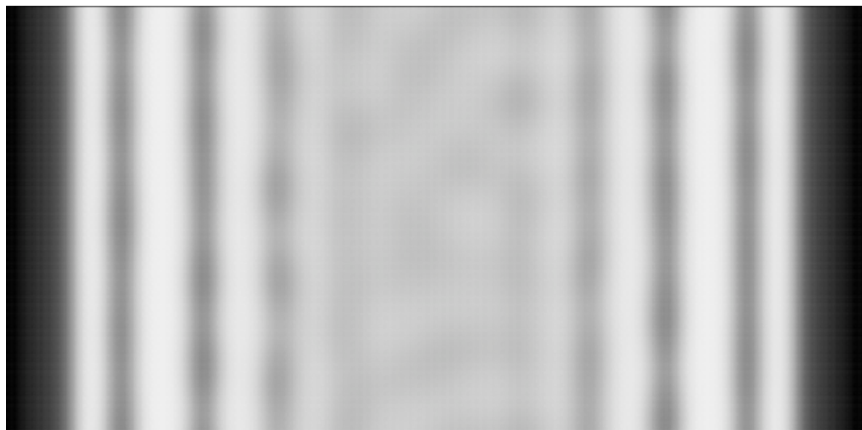


# Phase separation between parallel plates<sup>12</sup>



---

<sup>12</sup>S. Busuioc, V. E. Ambruş, T. Biciuşcă, V. Sofonea, arXiv: 1702.01690 [physics.flu-dyn].



(density)

(temperature)



# Multiphase flows: Conclusions

- ▶ Lattice Boltzmann (LB) simulations provide a convenient tool for the investigation of interface phenomena and heat transfer in multiphase systems.
- ▶ The single distribution function of order  $N = 4$  ( $Q = 5$ , 25 velocities) is able to tackle multiphase thermal flows.
- ▶ To reduce spurious numerical effects, we employed the following high order schemes:
  - ▶ WENO-5 for advection;
  - ▶ RK-3 for time stepping;
  - ▶ 6th order accurate (8th order isotropic) stencil for  $\nabla\delta P$ ;
  - ▶ 4th order accurate (6th order isotropic) stencil for  $\nabla(\Delta n)$ .

## Section 5

Multicomponent systems: Cahn Hilliard model

# Multicomponent flows: Binary immiscible fluids

- ▶ Multicomponent flows contain two (*binary*) or more (ternary, etc) different substances which do not interconvert.
- ▶ The distinction between the components is made using an order parameter  $\phi$ , e.g. (for binary fluids):

$$\phi = \frac{\rho^{(1)} - \rho^{(2)}}{\rho^{(1)} + \rho^{(2)}},$$

where  $\rho^{(1)}$  and  $\rho^{(2)}$  are the *local* densities of components 1 and 2.

- ▶ The bulk phase densities  $\rho_b^{(1)}$  and  $\rho_b^{(2)}$  correspond to the case of pure components, such that:

$$\phi = \begin{cases} 1, & \text{component 1, } \rho^{(1)} = \rho_b^{(1)}, \rho^{(2)} = 0, \\ -1, & \text{component 2, } \rho^{(1)} = 0, \rho^{(2)} = \rho_b^{(2)}. \end{cases}$$

- ▶ *Immiscible fluids* form regions of pure phases separated by internal interfaces characterised by surface tension.
- ▶ The diffusion between these components must be taken into account.

# Landau free energy model

- ▶ Assuming that  $\rho_b^{(1)} = \rho_b^{(2)} = \rho_b$ , the simplest model for multicomponent systems is the Landau free energy model:

$$\Psi = \int_V (\psi_b + \psi_g) dV = \int_V \left[ c_s^2 \rho \ln \rho + \frac{A}{4} (\phi^2 - 1)^2 + \frac{\kappa}{2} (\nabla \phi)^2 \right] dV,$$

where  $\psi_b$  and  $\psi_g$  are responsible for the bulk and interface properties, respectively.

- ▶ The parameter  $A$  is positive ( $A < 0$  corresponds to miscible fluids).
- ▶  $\psi_b$  has two minima:  $\phi = \pm 1$ , corresponding to the pure phases.
- ▶ The fluid evolution must lead to the minimisation of  $\Psi$ .
- ▶ At equilibrium, the chemical potential  $\mu$  reaches a constant value:

$$\mu = \frac{\delta(\psi_b + \psi_g)}{\delta\phi} = -A\phi(1 - \phi^2) - \kappa\Delta\phi = \text{const.}$$

# Advection-diffusion model

- ▶ The time evolution of  $\phi$  is given by the Cahn-Hilliard equation:

$$\partial_t \phi + \nabla \cdot (\mathbf{u}\phi) = \nabla \cdot (M\nabla\mu).$$

- ▶ The C-H equation governs the **advection** of  $\phi$  along  $\mathbf{u}$  and the **diffusion** of  $\phi$  due to inhomogeneities in  $\mu$  ( $M$  is the mobility parameter).
- ▶ The fluid itself evolves according to the Navier-Stokes equations:

$$\partial_t \rho + \nabla \cdot (\mathbf{u}\rho) = 0, \quad \rho(\partial_t u^i + u^j \nabla_j u^i) = -\nabla_j (P^{ij} + \sigma^{ij}),$$

where  $\sigma_{ij} = -\eta(\nabla_i u_j + \nabla_j u_i - \delta_{ij} \nabla_k u_k)$  is the viscous stress for a 2D fluid and the non-ideal stress  $P_{ij}$  is:

$$P_{ij} = \left[ P_b - \frac{\kappa}{2} (\nabla\phi)^2 - \kappa\phi\Delta\phi \right] \delta_{ij} + \kappa(\nabla_i\phi)(\nabla_j\phi).$$

- ▶ The **bulk pressure** is

$$P_b = P_{\text{ideal}} + A \left( -\frac{1}{2}\phi^2 + \frac{3}{4}\phi^4 \right),$$

where  $P_{\text{ideal}} = nK_B T$  is the ideal gas pressure.

- ▶ The surface tension is governed by the  $\kappa$  term.

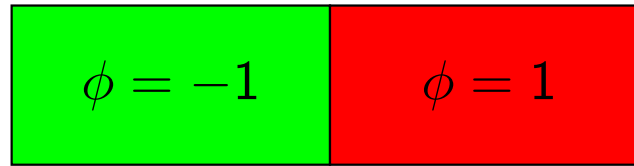
# Hybrid LB algorithm

- ▶ The system is isothermal ( $T$  is fixed when constructing  $f^{(\text{eq})}$ ).
- ▶ According to C-E, the isothermal NS eqs. can be recovered with  $N = 3$  and  $Q = 4 \Rightarrow \text{HLB}(4) \times \text{HLB}(4)$ .
- ▶ The fluid properties are obtained from  $f$ :

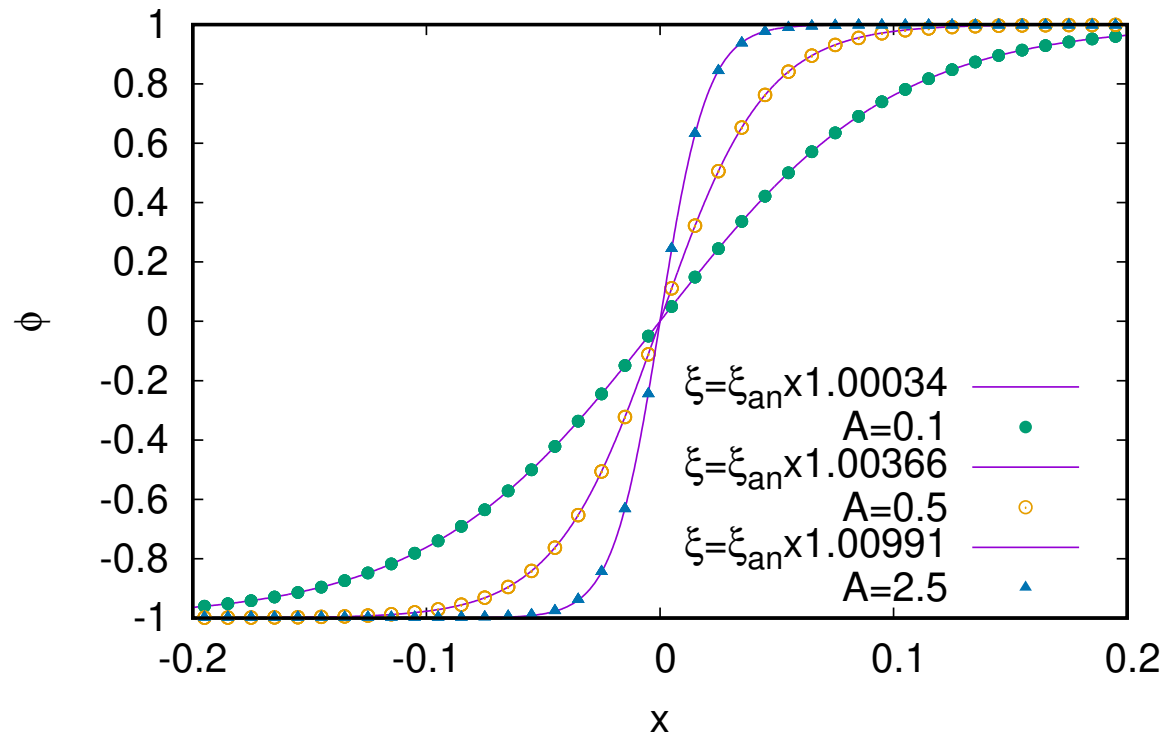
$$\begin{pmatrix} n \\ \rho u_\alpha \\ P_{\text{ideal}}\delta_{\alpha\beta} + \sigma_{\alpha\beta} \end{pmatrix} = \sum_{i,j} \begin{pmatrix} 1 \\ p_i \\ \xi_i \xi_j / m \end{pmatrix} f_{ij}.$$

- ▶ The evolution eq. for  $\phi$  is solved using FD.

# Validation 1: Planar interface

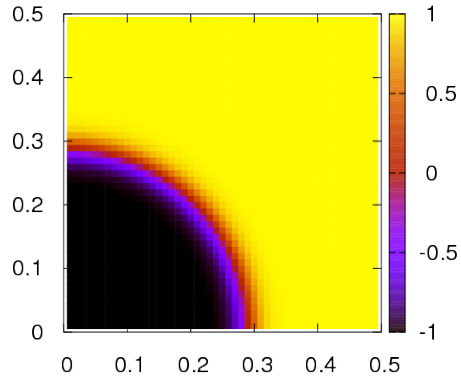


$\kappa=5e-4, \Gamma=1.0, \tau=2.5e-3, Q=4$



$$\phi = \tanh\left(\frac{x}{\xi\sqrt{2}}\right), \quad \xi = \sqrt{\frac{\kappa}{A}}$$

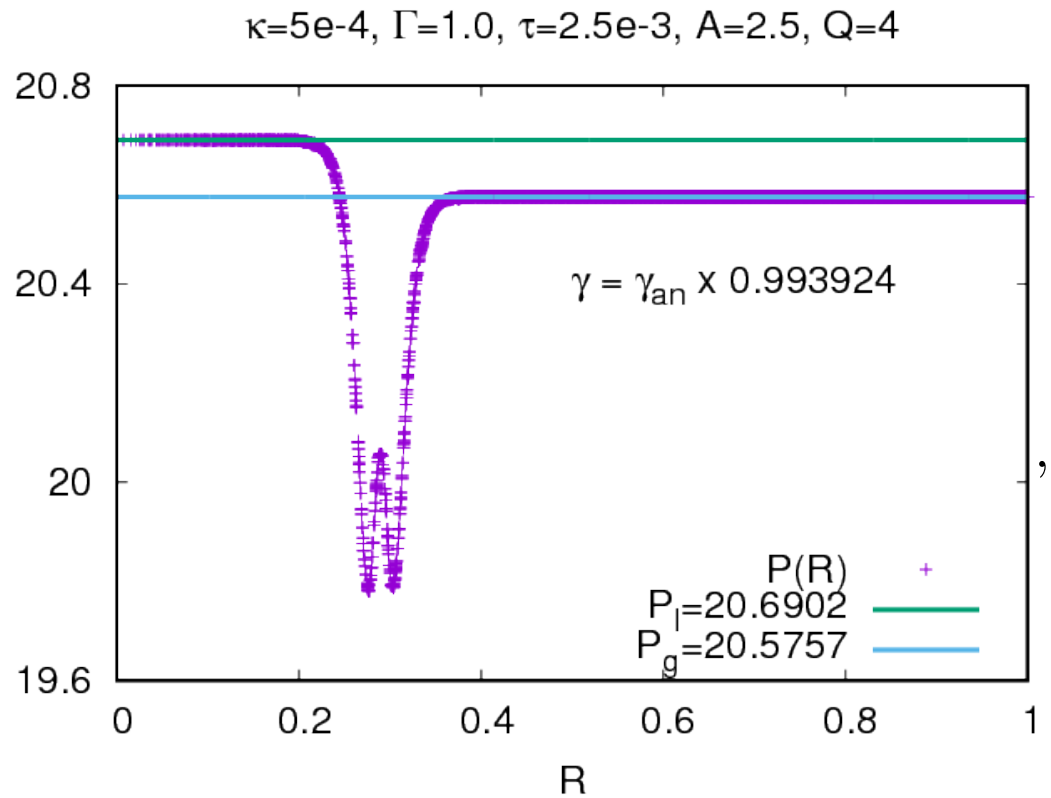
# Validation 2: Laplace pressure test



Laplace pressure law:

$$P_{\text{in}} - P_{\text{out}} = \frac{\gamma}{R},$$

$$\gamma = \sqrt{\frac{8\kappa A}{9}}.$$

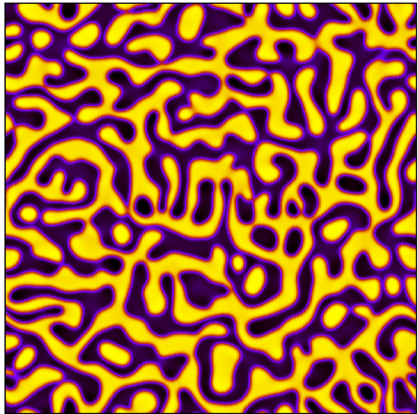




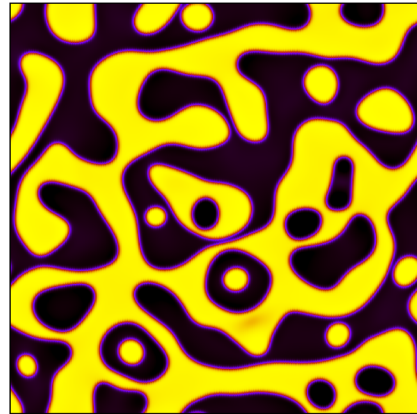
## Validation 3: Spinodal decomposition ( $\phi_0 = 0$ )

$\phi(t = 0, x, y) = \phi_0 + \delta\phi(x, y)$ ,  $-0.1 < \delta\phi < 0.1$  randomly distributed.

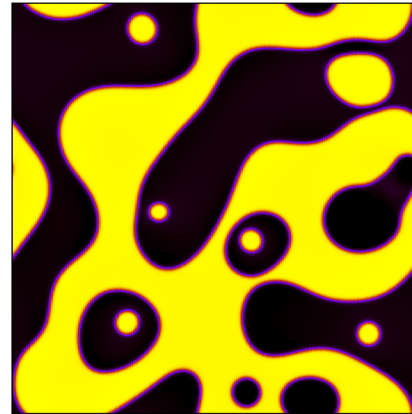
With hydro:



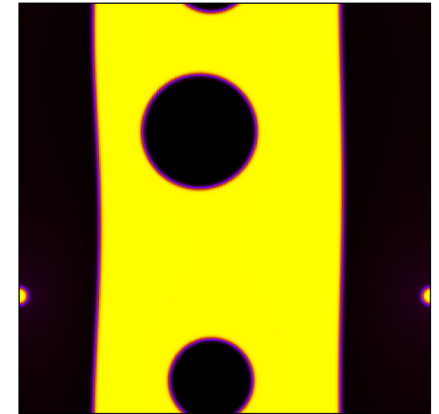
$t = 40$



$t = 100$

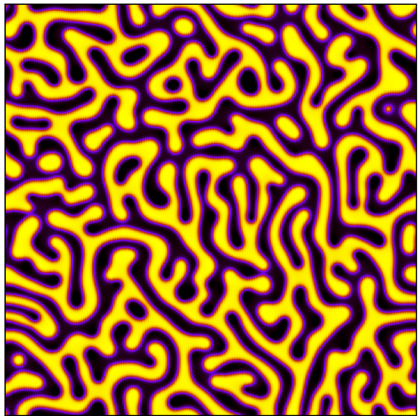


$t = 250$

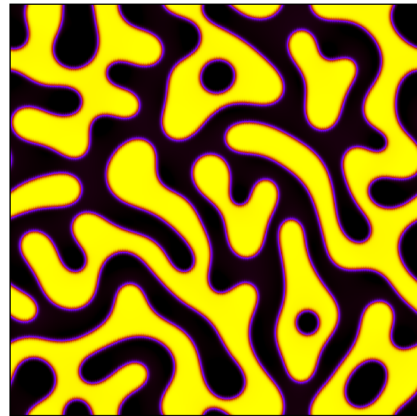


$t = 3000$

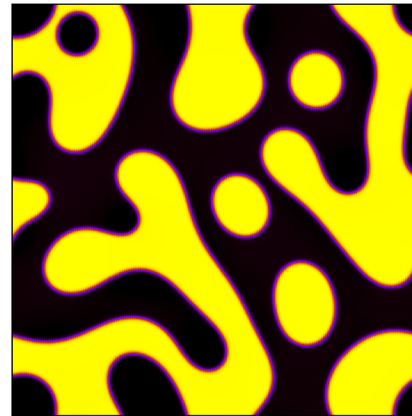
Without hydro:



$t = 300$



$t = 2700$

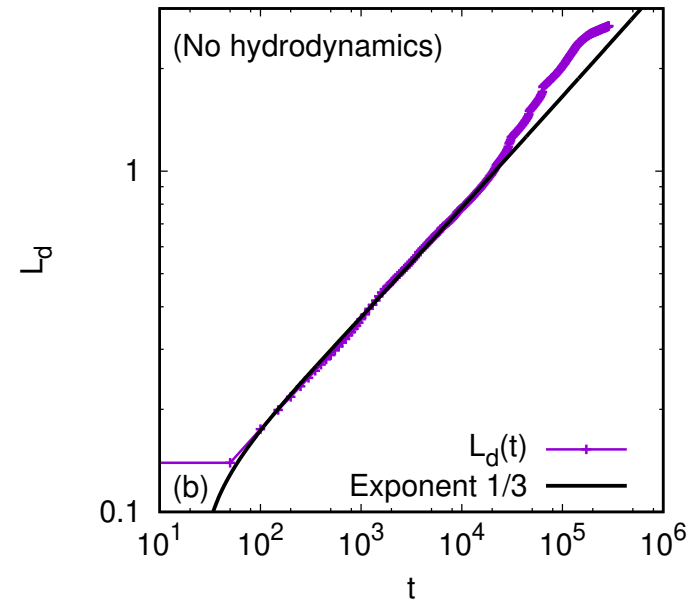
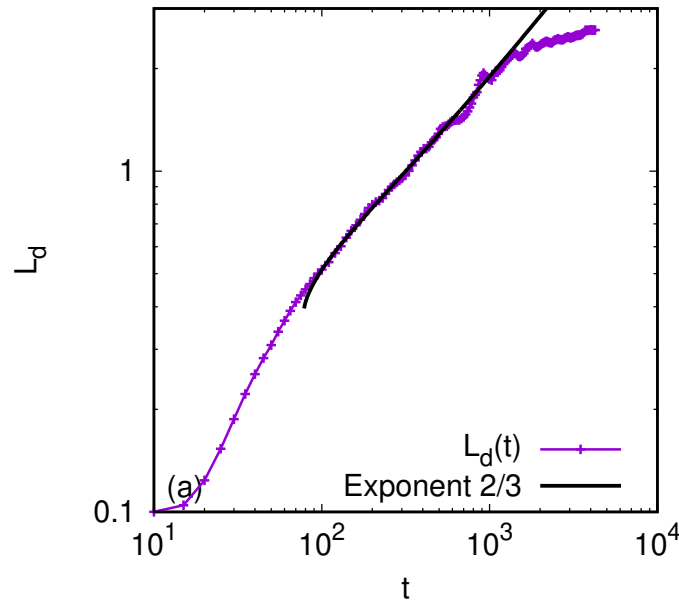


$t = 15000$



$t = 168000$

# Growth exponent



- ▶ The domain sizes can be characterised by the interface length  $\ell$ .
- ▶  $L_d = L_x L_y / \ell$  is an increasing function of time.
- ▶  $L_d \sim t^{2/3} \Rightarrow$  inertial regime.
- ▶  $L_d \sim t^{1/3} \Rightarrow$  diffusive regime.

# Curved surface: torus

- ▶ A torus can be parametrised using  $\theta$  and  $\varphi$ :

$$x = (R + r \cos \theta) \cos \varphi, \quad y = (R + r \cos \theta) \sin \varphi, \quad z = r \sin \theta,$$

giving rise to the line element:

$$ds^2 = [dx^2 + dy^2 + dz^2]_{\text{torus}} = (R + r \cos \theta)^2 d\varphi^2 + r^2 d\theta^2.$$

- ▶ It is convenient to employ the following vielbein field:

$$e_{\hat{\varphi}} = \frac{\partial_{\varphi}}{R + r \cos \theta}, \quad e_{\hat{\theta}} = r^{-1} \partial_{\theta},$$

with respect to which  $p^i = e^i_{\hat{a}} p^{\hat{a}}$ .

- ▶ The momentum space is discretised with respect to  $p^{\hat{\theta}}$  and  $p^{\hat{\varphi}}$ .

# Lattice Boltzmann equation on the torus

- ▶  $f_{\kappa}$  obeys the LB equation:

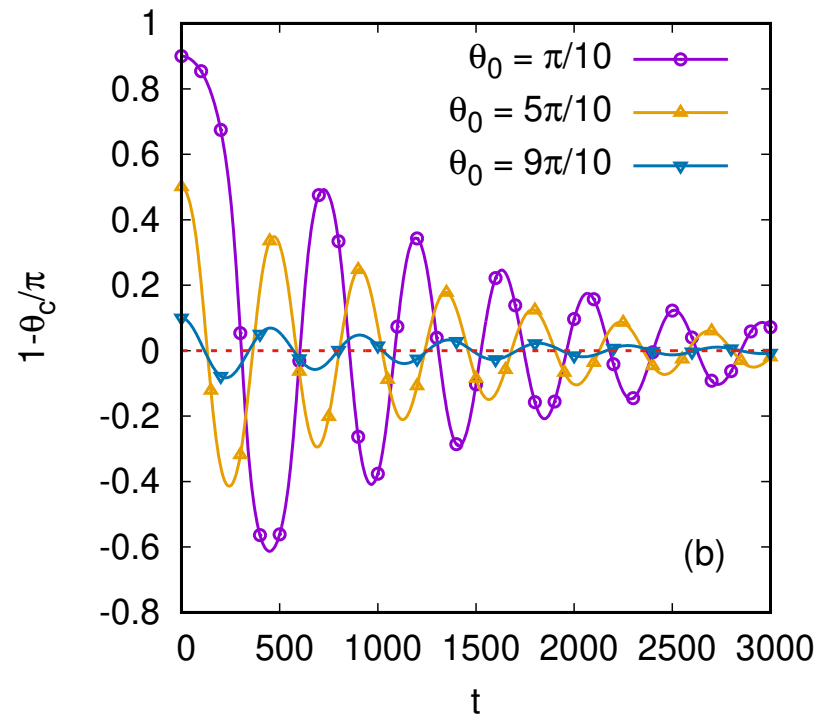
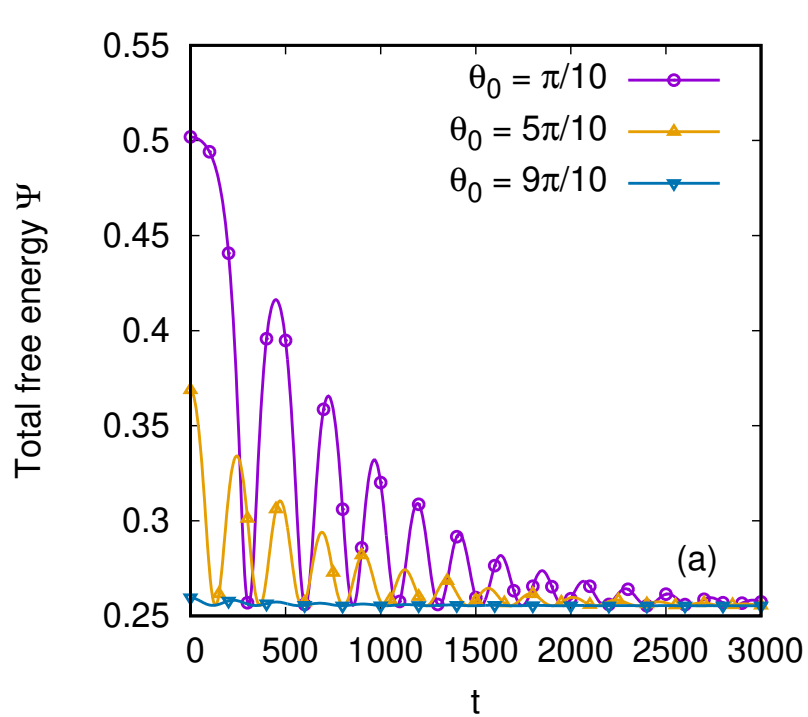
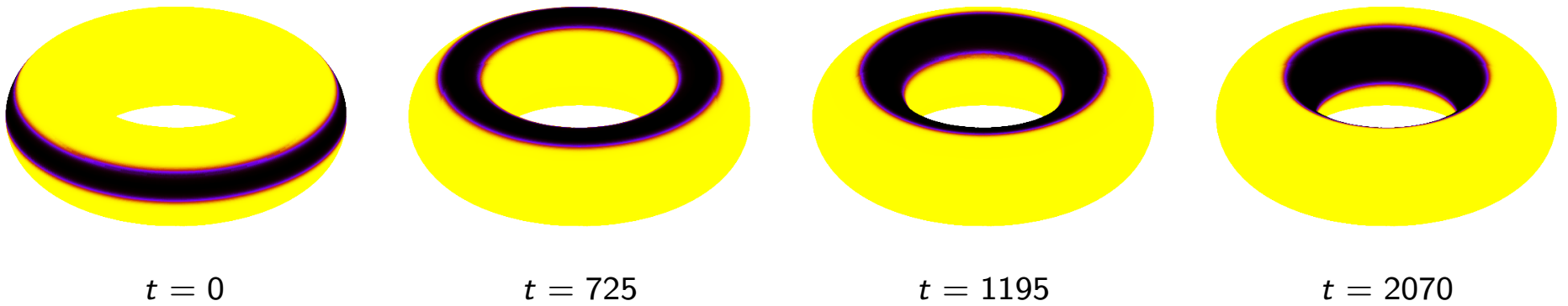
$$\begin{aligned} \frac{\partial f_{\kappa}}{\partial t} + \frac{p_{k_{\varphi}}}{m(R + r \cos \theta)} \frac{\partial f_{\kappa}}{\partial \varphi} + \frac{p_{k_{\theta}}}{mr(R + r \cos \theta)} \frac{\partial [f_{\kappa}(R + r \cos \theta)]}{\partial \theta} \\ - \frac{\sin \theta}{m(R + r \cos \theta)} \left[ p^{\hat{\varphi}} \frac{\partial (fp^{\hat{\varphi}})}{\partial p^{\hat{\theta}}} - p^{\hat{\theta}} \frac{\partial (fp^{\hat{\varphi}})}{\partial p^{\hat{\varphi}}} \right]_{\kappa} \\ + F^{\hat{\theta}} \left( \frac{\partial f}{\partial p^{\hat{\theta}}} \right)_{\kappa} + F^{\hat{\varphi}} \left( \frac{\partial f}{\partial p^{\hat{\varphi}}} \right)_{\kappa} = -\frac{1}{\tau} [f_{\kappa} - f_{\kappa}^{(\text{eq})}], \end{aligned}$$

undergoing **advection** under the action of **inertial** and **Cahn-Hilliard** forces, as well as **relaxation** (BGK approximation).

- ▶  $f^{(\text{eq})} = \frac{n}{2\pi m K_B T} e^{-\xi^2/2mT}$  is replaced by a 3<sup>rd</sup> tensor Hermite polynomial expansion:

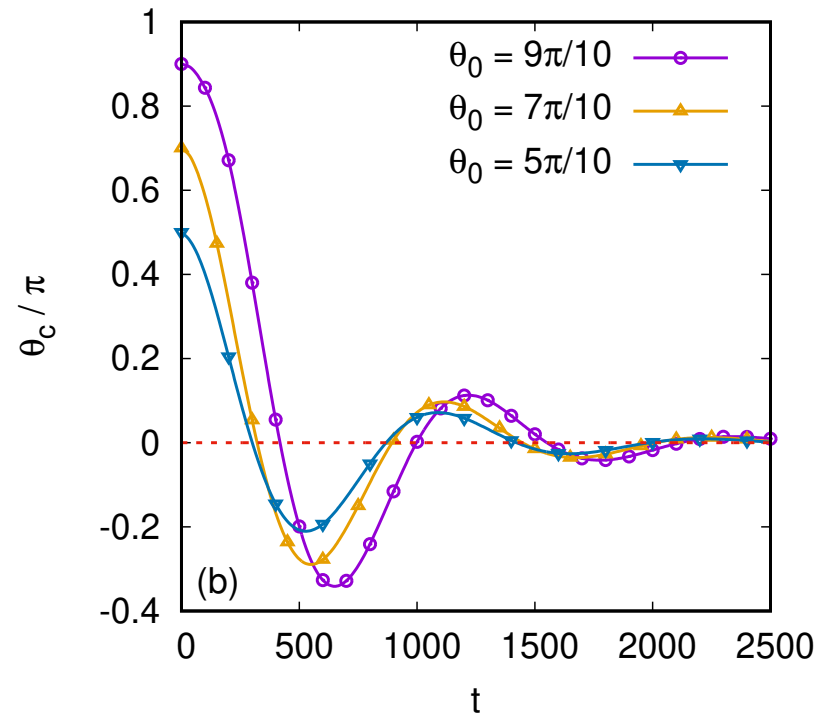
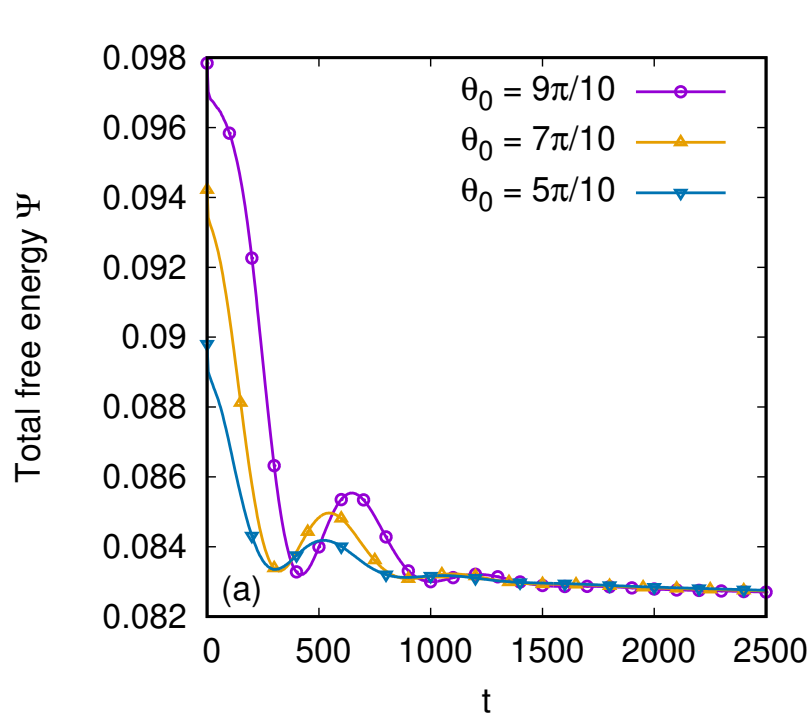
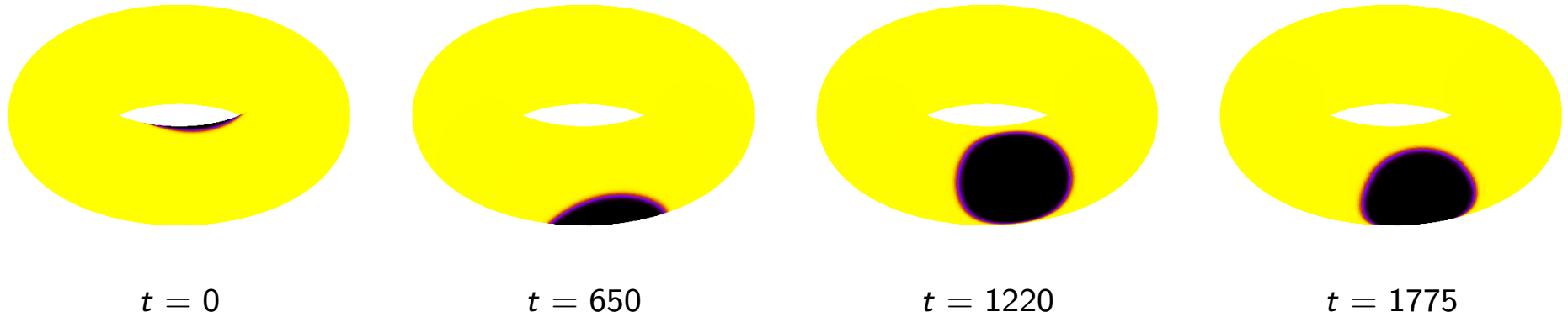
$$\begin{aligned} f_{\kappa}^{(\text{eq})} = n w_{k_{\theta}} w_{k_{\varphi}} \left\{ 1 + \mathbf{p}_{\kappa} \cdot \mathbf{u} + \frac{1}{2} [(\mathbf{p}_{\kappa} \cdot \mathbf{u})^2 - \mathbf{u}^2] \right. \\ \left. + \frac{1}{6} \mathbf{p}_{\kappa} \cdot \mathbf{u} [(\mathbf{p}_{\kappa} \cdot \mathbf{u})^2 - 3\mathbf{u}^2] \right\}. \end{aligned}$$

# Line tension effect: migration of stripes



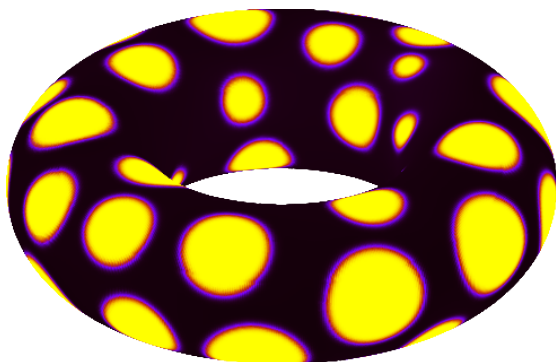
Due to  $\gamma$ , stripes migrate towards  $\theta = \pi$ .

# Curvature effect: droplets migration

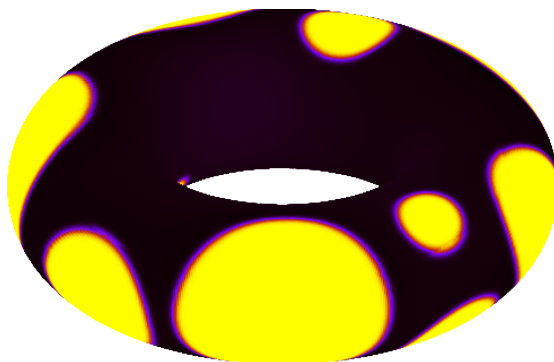


Droplets migrate towards lowest curvature ( $\theta = 0$ ).

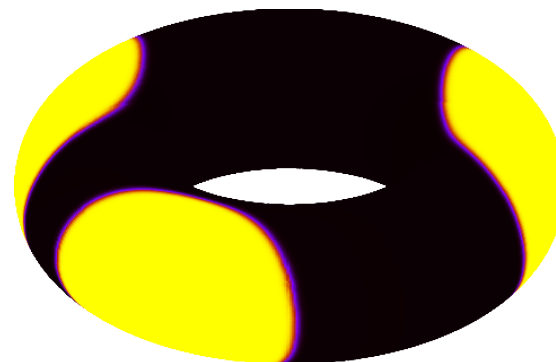
# Separation to droplets



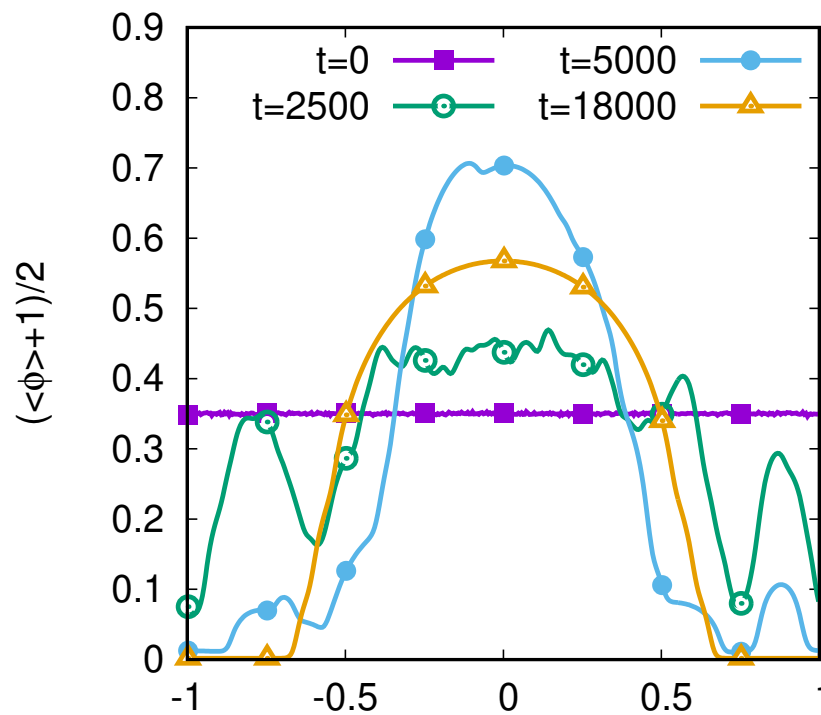
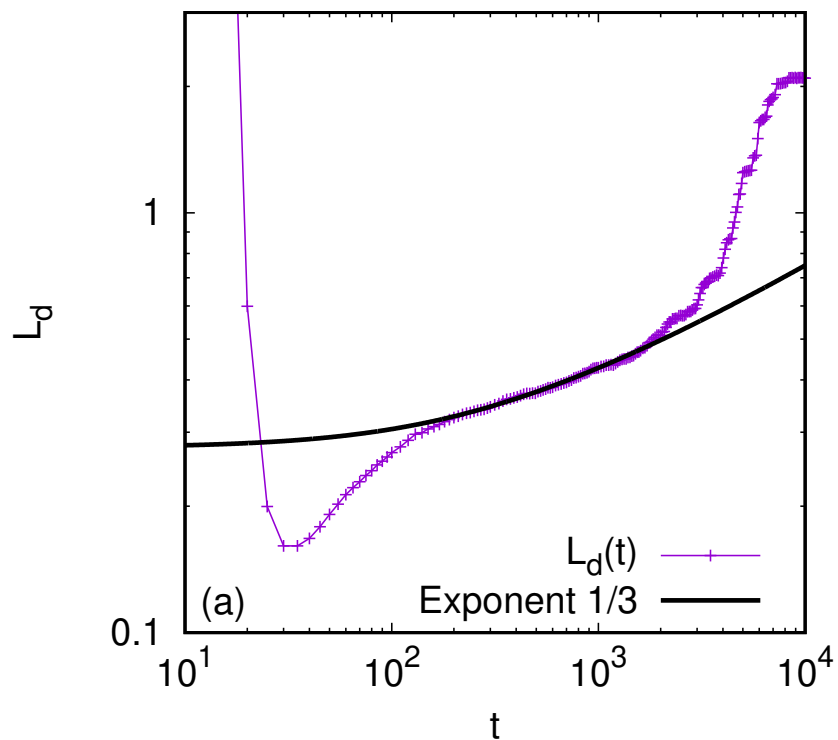
$t = 2500$



$t = 5000$



$t = 18000$



Droplet migration can be quantified using  $\langle \phi \rangle = \int_0^{2\pi} d\varphi \phi$ .

# Multicomponent flows: Conclusions

- ▶ Component segregation can be achieved based on free energy models.
- ▶ The implementation of such models on curved surfaces can be performed using  $Q = 4$  (16 velocities).
- ▶ In order to reduce spurious effects, high order schemes were employed (WENO-5, RK-3, fourth order Laplacian, etc).
- ▶ This methodology opens the door to various complex fluid flow applications (liquid crystals, deformable membranes, etc).

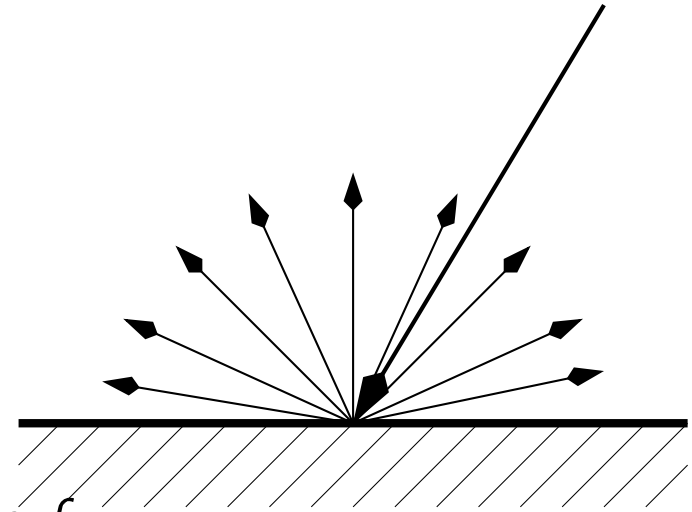


## Section 6

Rarefied gas flows through micro-channels

# Diffuse reflection

- ▶ The interaction between incoming gas molecules and the wall constituents is in general complex.
- ▶ According to the diffuse reflection concept, the incoming flux is reemitted according a MB distribution.
- ▶ Since the incoming flux is essentially arbitrary, this induces a discontinuity in  $f$ .
- ▶ The discontinuity is responsible for microfluidics effects such as slip velocity and temperature jump, which are manifest in the *Knudsen layer*.
- ▶ The Knudsen layer physics can be recovered by using half-range Gauss-Hermite quadratures:

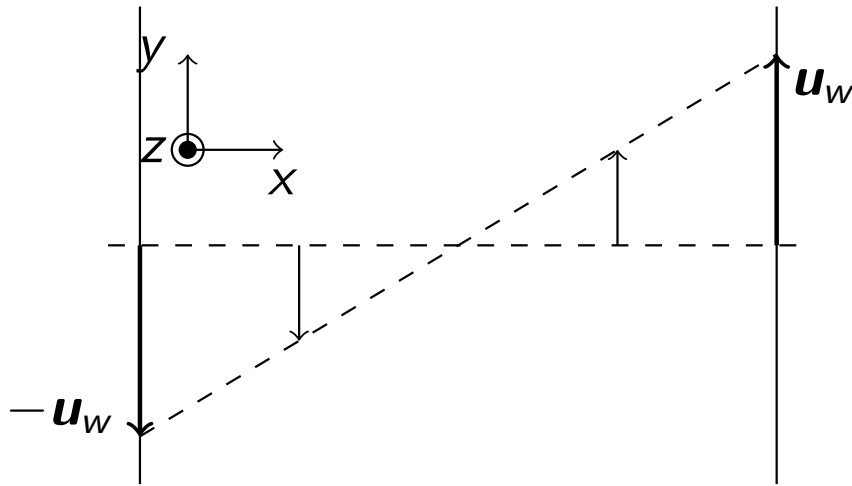


$$\int_0^{\infty} \frac{e^{-x^2/2} dx}{\sqrt{2\pi}} P_s(x) \simeq \sum_{k=1}^Q w_k^h P_s(x_k).$$

---

<sup>1</sup>V. E. Ambruş, V. Sofonea, J. Comput. Phys. **316** (2016) 1–29.

# Linearised theory: Couette flow

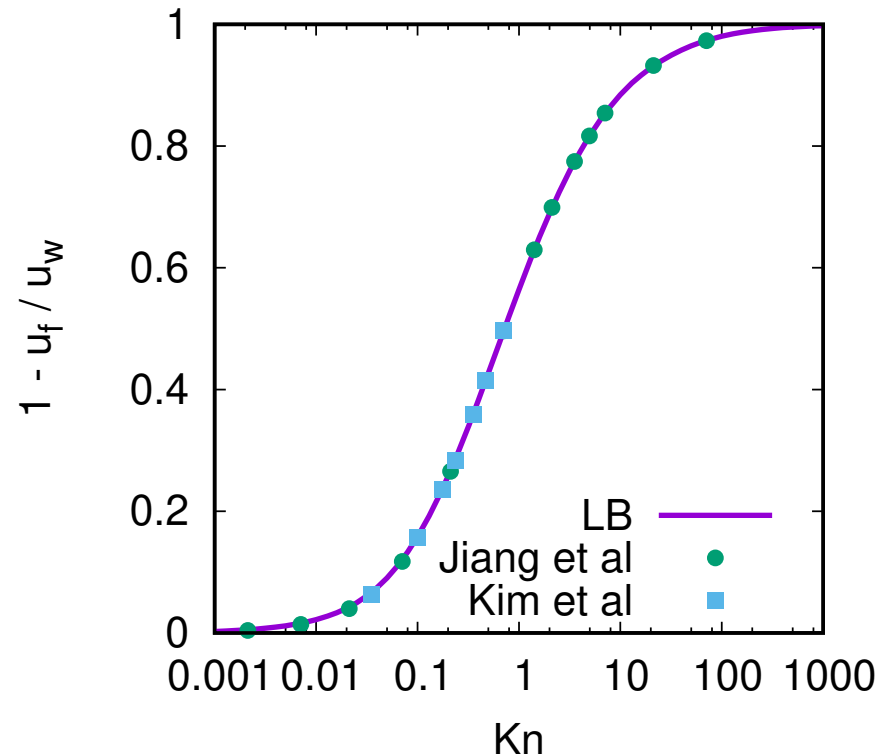
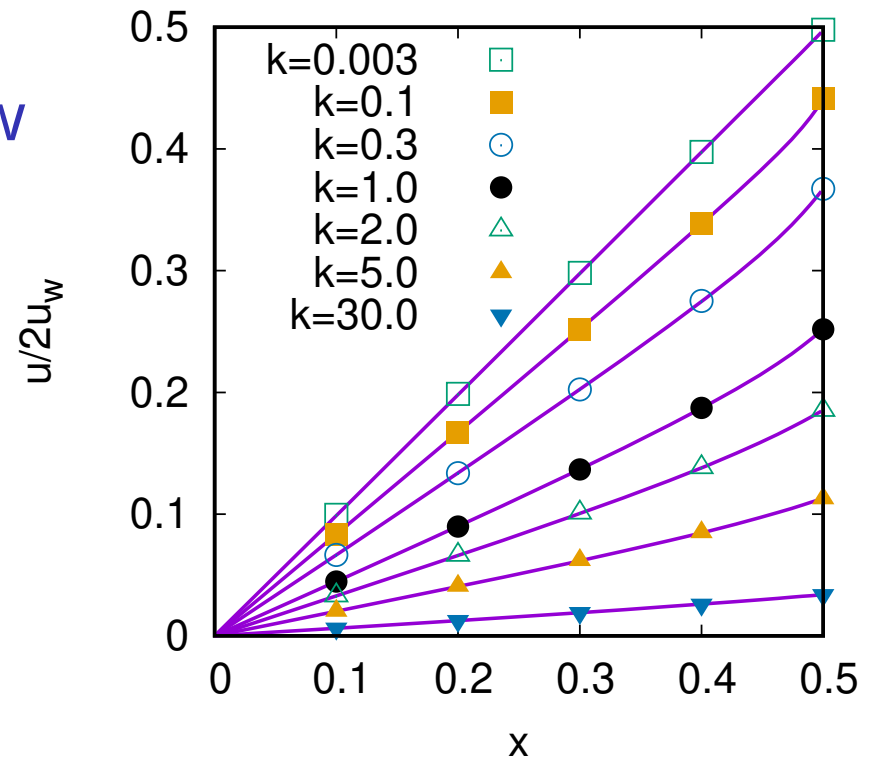


- ▶ In the planar Couette flow, the walls move with  $\pm u_w \mathbf{j}$ .
- ▶ Acc. to Jiang and Luo,<sup>11</sup>

$$u_y(\delta x) = \sum_{n,m=0}^{\infty} c_{n,m} x^n (x \ln x)^m,$$

where  $\delta x$  is the distance to the wall.

- ▶ Due to  $n = 0, m = 1$ ,  $\omega = \partial_x u_y$  diverges at  $\delta x = 0$ .



<sup>12</sup>S. Jiang, L.-S. Luo, J. Comput. Phys **316** (2016) 416–434.

# Model for Maxwell molecules

- ▶ For Maxwell molecules, the viscosity is given by:

$$\eta = \eta_0 \frac{T}{T_0}, \quad (31)$$

where  $\eta_0$  is the viscosity at  $T = T_0$ , while the Prandtl number is

$$\text{Pr} = \frac{c_p \eta}{\kappa} = \frac{2}{3}, \quad c_p = \frac{5K_B}{2m}. \quad (32)$$

- ▶ More generally,  $\eta = \eta_0 (T/T_0)^\omega$  can be implemented by fixing  $\tau$  to:

$$\tau = \frac{\mu_0}{nK_B T_0} \left( \frac{T}{T_0} \right)^{\omega-1}. \quad (33)$$

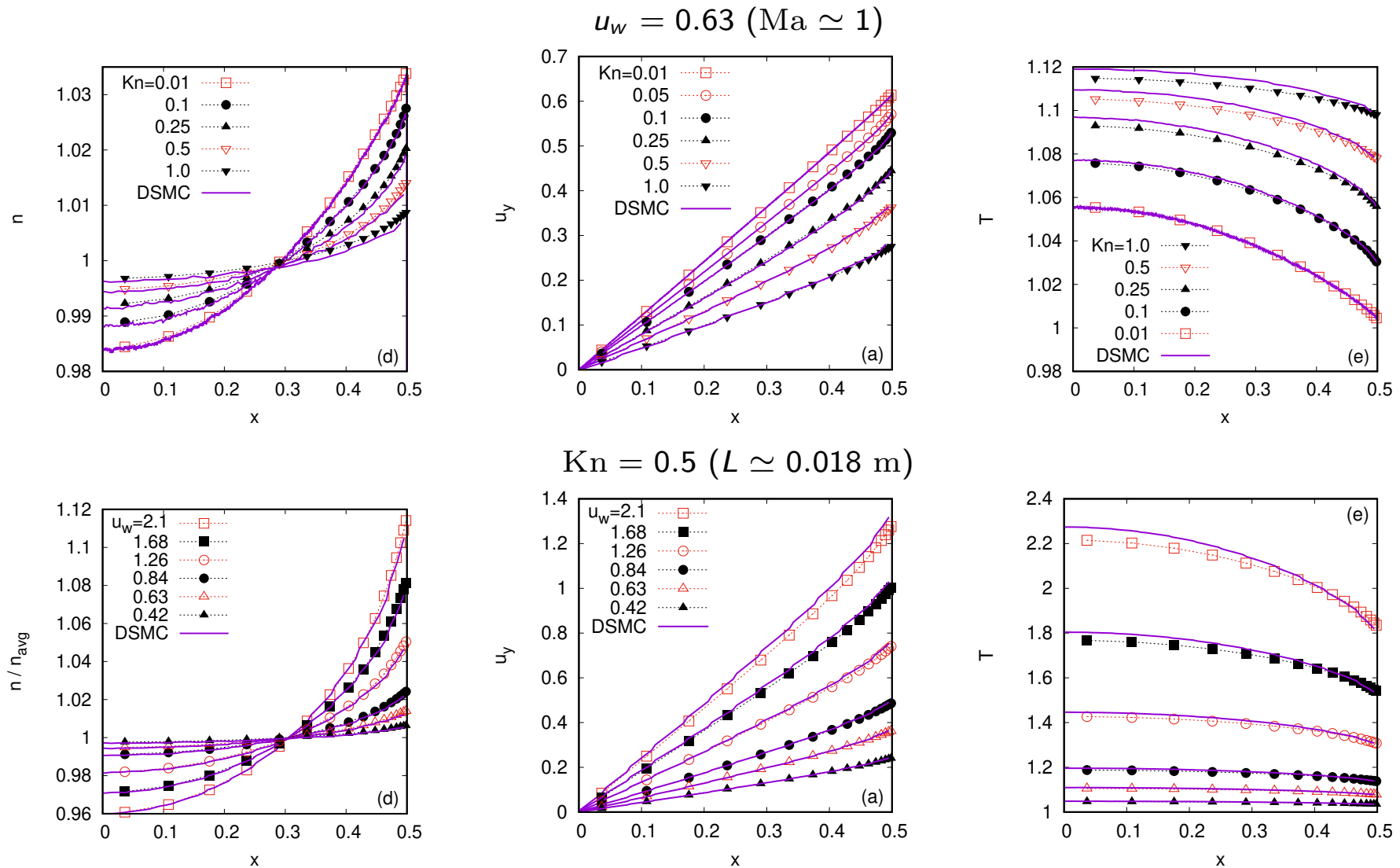
- ▶ In the BGK model,  $\text{Pr} = 1$ .
- ▶  $\text{Pr}$  can be set to  $2/3$  using the Shakhov model:<sup>13</sup>

$$J_{\text{Shakhov}} = -\frac{1}{\tau} [f - f^{(\text{eq})}(1 + \mathbb{S})], \quad \mathbb{S} = \frac{1 - \text{Pr}}{nK_B^2 T^2} \left( \frac{\xi^2}{5mK_B T} - 1 \right) \mathbf{q} \cdot \xi. \quad (34)$$

---

<sup>13</sup>E. M. Shakhov, Fluid Dyn. **3** (1968) 95–96; 112–115.

# Comparison to DSMC (Argon)<sup>15</sup>



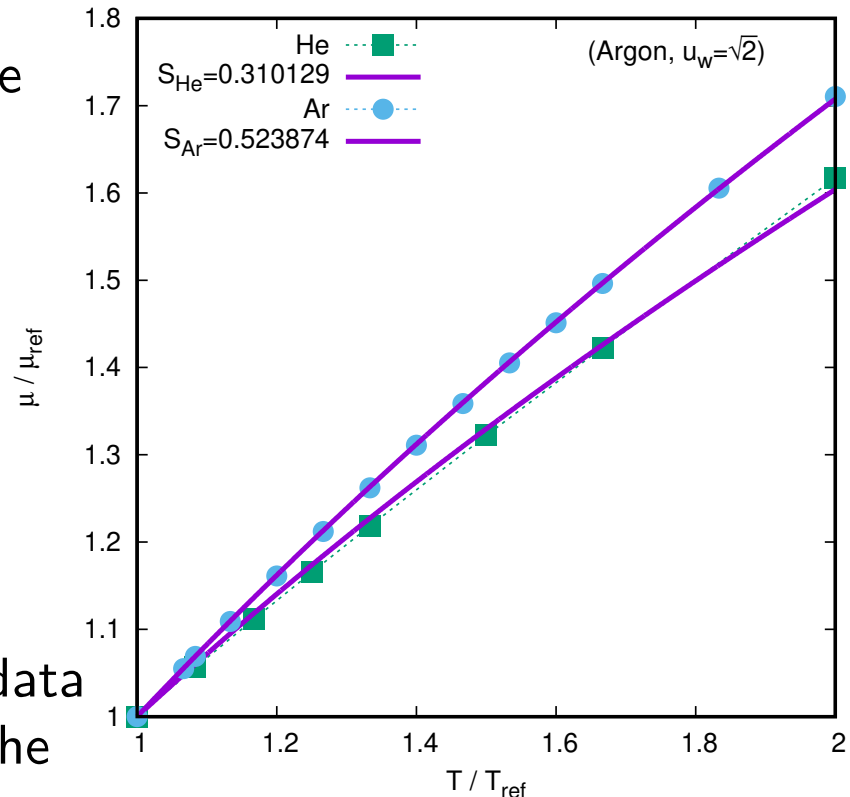
Very good agreement w.r.t. the DSMC results can be seen.<sup>14</sup>

<sup>14</sup>V. E. Ambrus, V. Sofonea, arXiv: 1702:01335 [physics.flu-dyn].

<sup>15</sup>H. Struchtrup, M. Torrilhon, Phys. Rev. Lett. **99** (2007) 014502.

# Model for real (ab initio) potentials<sup>19</sup>

- ▶ The ab initio method allows the interaction potentials to be obtained analytically.
- ▶  $\mu$  and  $\kappa$  can then be computed directly (w/o exp. input).
- ▶ The data for He is tabulated by Cencek et al.<sup>16</sup>
- ▶ The data for Ar is tabulated by Vogel et al.<sup>17</sup>
- ▶ For  $300 \text{ K} \lesssim T \lesssim 600 \text{ K}$ , the data can be well represented using the Sutherland law:<sup>18</sup>



$$\eta = \eta_0 \left( \frac{T}{T_0} \right)^{1/2} \frac{1 + S/T_{\text{ref}}}{1 + S/T}, \quad (35)$$

where the Sutherland constant  $S$  is used to fit Eq. (35) to the data:

$$S_{\text{He}} \simeq 93.04 \text{ K}, \quad S_{\text{Ar}} \simeq 157.16 \text{ K}. \quad (36)$$

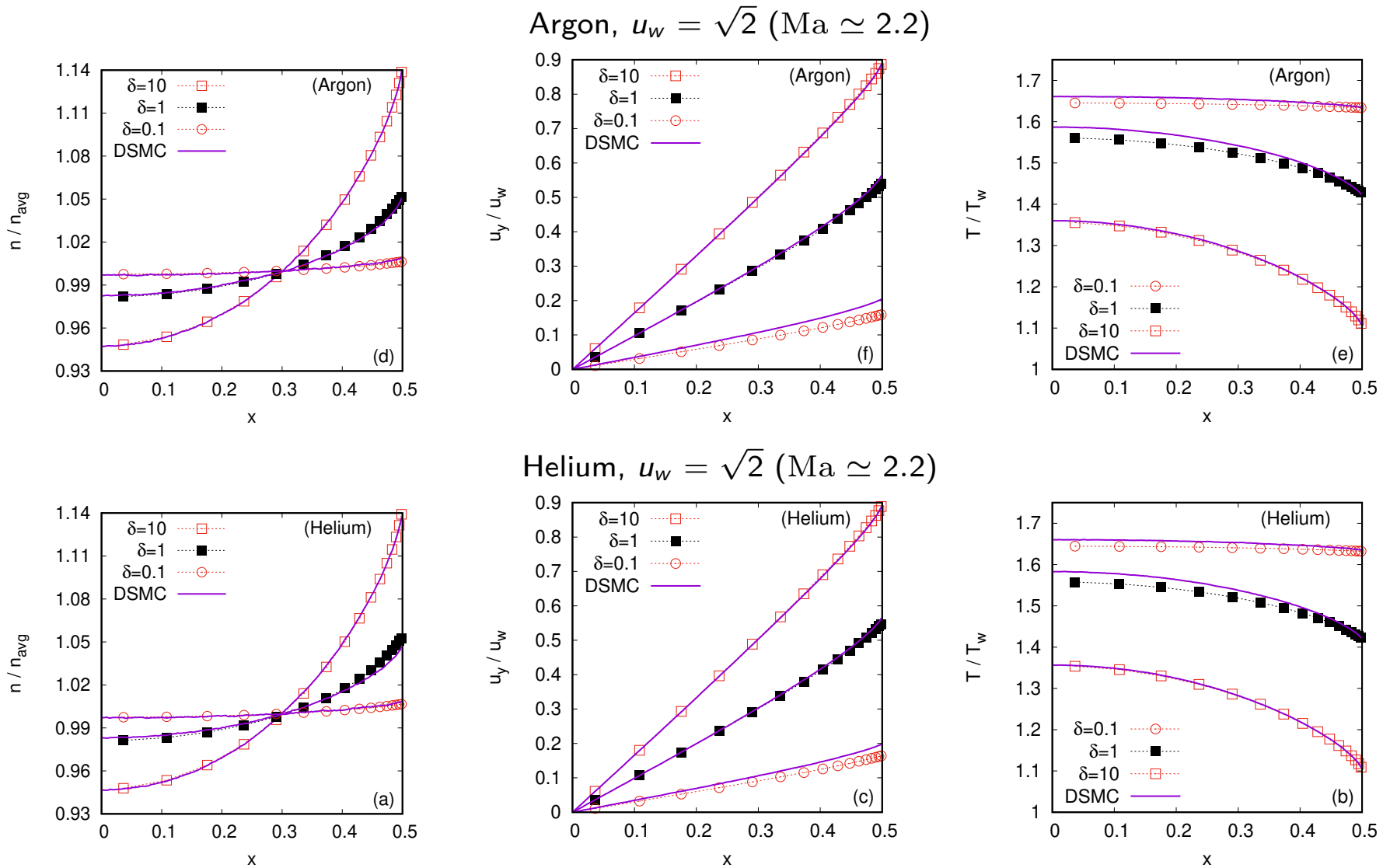
- ▶  $Pr$  is set to  $2/3$  using the Shakhov model.

<sup>16</sup>W. Cencek, M. Przybytek, J. Komasa, J. B. Mehl, B. Jeziorski, and K. Szalewicz, *J. Chem. Phys.* **136** (2012) 224303.

<sup>17</sup>E. Vogel, B. Jäger, R. Hellmann, E. Bich, *Mol. Phys.* **108** (2010) 3335–3352.

<sup>18</sup>M. N. Macrossan, *J. Comput. Phys.* **185** (2003) 612–627.

# Comparison to DSMC for ab initio potentials<sup>21</sup>



Very good agreement w.r.t. the DSMC results can be seen.<sup>20</sup>

<sup>20</sup>V. E. Ambrus, V. Sofonea, arXiv: 1702.01335 [physics.flu-dyn].

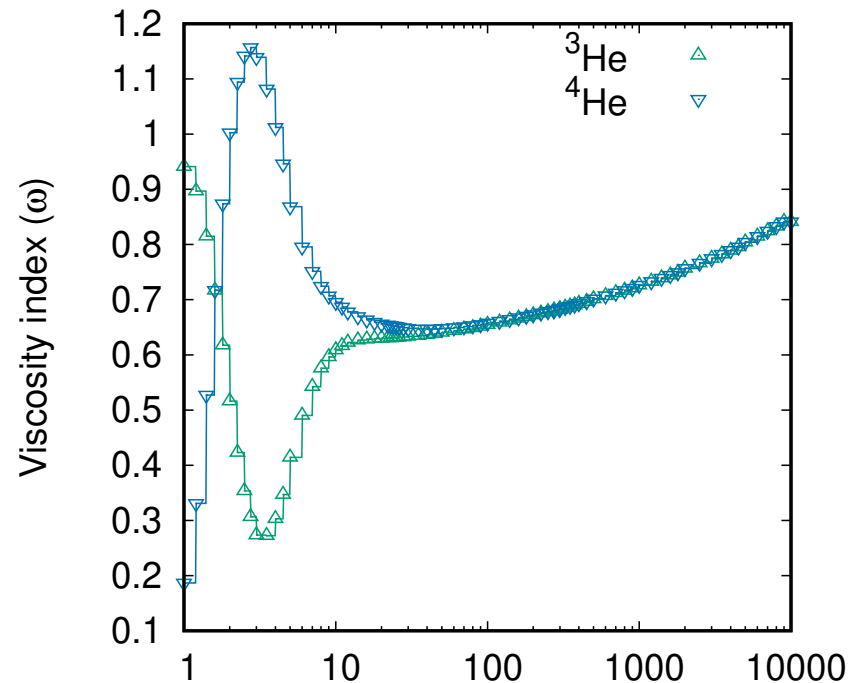
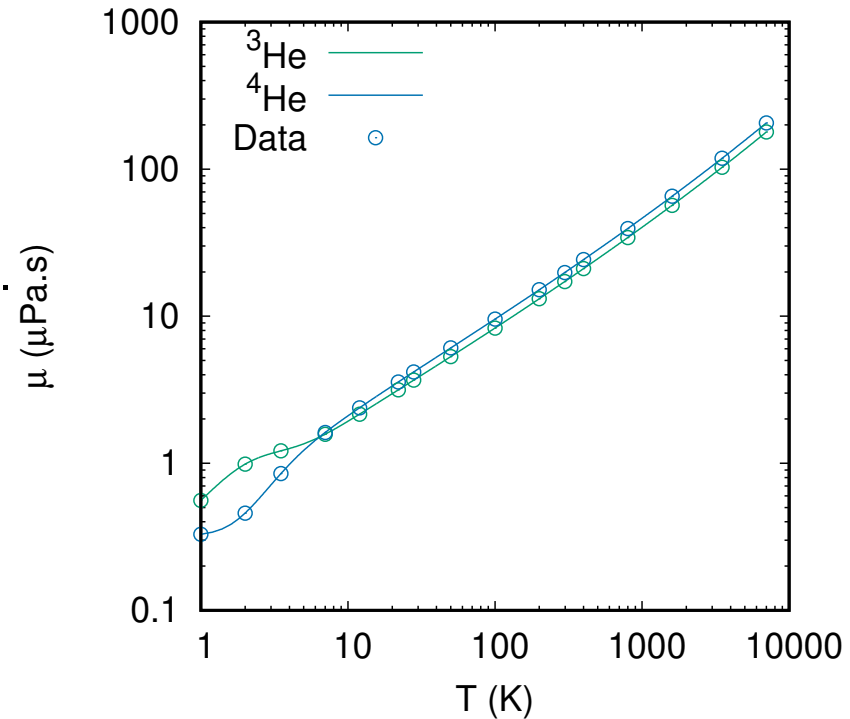
<sup>21</sup>F. Sharipov, J. L. Strapasson, Phys. Fluids **25** (2013) 027101.

# Ab initio over a large temperature range

- ▶ The Sutherland model works for small temperature ranges.
- ▶ The data tabulated by Cencek et al. covers  $1 \text{ K} \leq T \leq 10^4 \text{ K}$ .
- ▶ In order to cover this whole temperature range within one RTA model,  $\tau$  is defined in a piece-wise fashion, based on the law:

$$\eta^{(n)}(T) = \eta_n \left( \frac{T}{T_n} \right)^{\omega_n},$$
$$\omega_n = \frac{\ln(\eta_{n+1}/\eta_n)}{\ln(T_{n+1}/T_n)}.$$

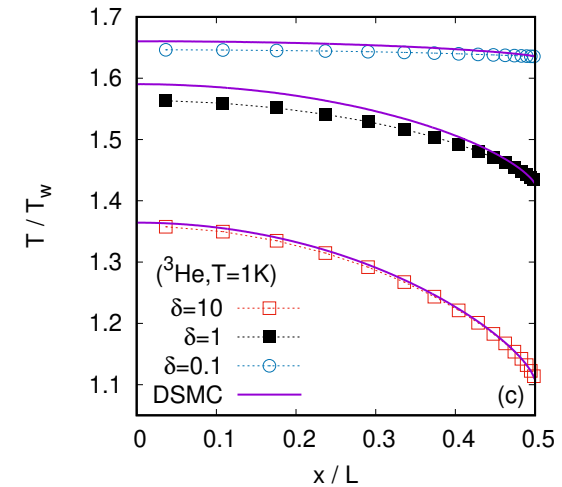
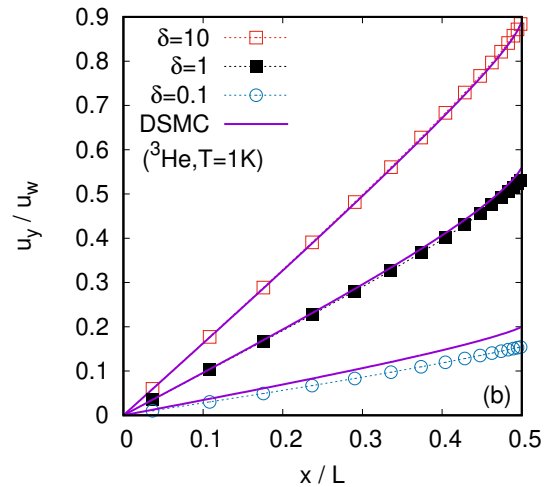
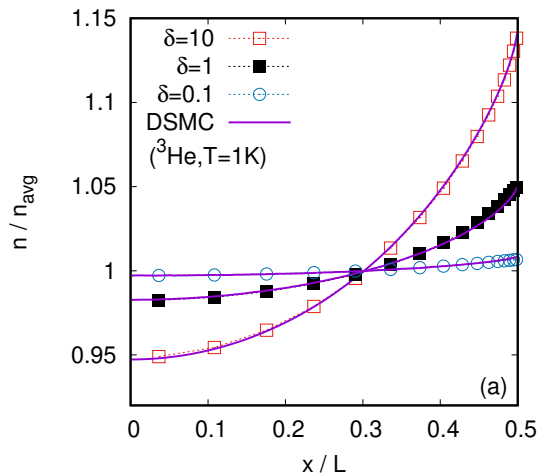
- ▶ The Prandtl number is represented similarly.



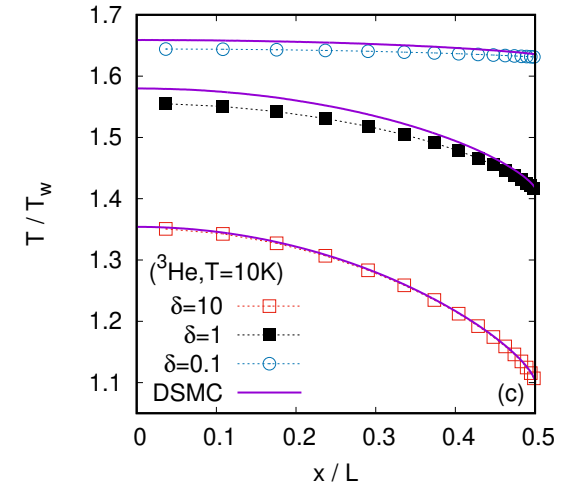
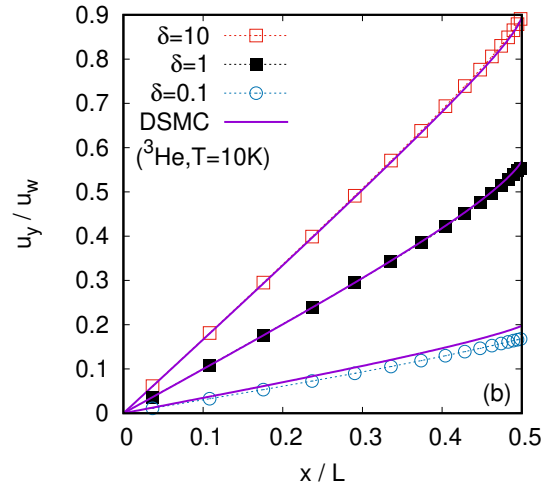
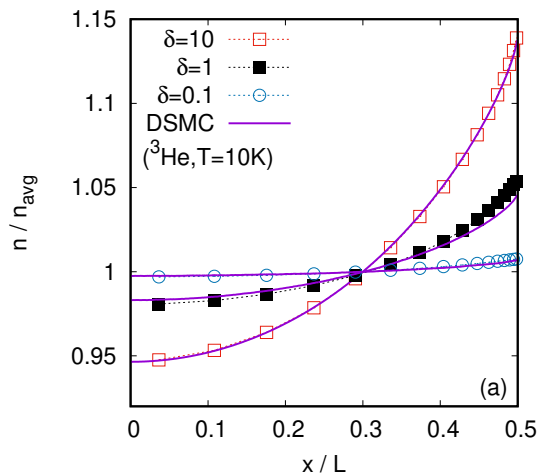


# Comparison to DSMC for ab initio potentials<sup>23</sup>

<sup>3</sup>He,  $u_w = \sqrt{2}$  (Ma  $\simeq 2.2$ ),  $T = 1$  K



<sup>3</sup>He,  $u_w = \sqrt{2}$  (Ma  $\simeq 2.2$ ),  $T = 10$  K



Very good agreement w.r.t. the DSMC results can be seen.<sup>22</sup>

<sup>22</sup>V. E. Ambruş, F. Sharipov, V. Sofonea, arXiv: 1810.07803 [physics.flu-dyn].

<sup>23</sup>F. Sharipov, Physica A **508** (2018) 797–805.

# Rarefied gases: Conclusions

- ▶ The capabilities of the lattice Boltzmann (LB) models based on half-range and full-range Gauss-Hermite quadratures were demonstrated in the context of the Couette flow.
- ▶ In the linearised regime, the ability of our models to capture Knudsen layer effects for the Couette flow was confirmed by comparison with semi-analytic benchmark results.
- ▶ Using the Shakhov collision model together with the implementation of the relaxation time compatible with the viscosity index  $\omega = 0.81$ , our models accurately reproduced DSMC results for the Couette flow of Maxwell molecules for Kn up to 1.0 and for wall velocities up to  $u_w = 2.1$  (approximately 500 m/s).
- ▶ Using the Shakhov model together with the Sutherland model for the viscosity, our models obtained excellent agreement with the DSMC results based on ab initio potentials for Argon and Helium gases, for rarefaction parameter  $\delta$  down to 0.01 ( $Kn \simeq 71$ ) and for wall velocity  $u_w = \sqrt{2}$ .

## Section 7

### Shock wave propagation

# Model for internal degrees of freedom

- ▶ The adiabatic coefficient for an ideal gas is  $\gamma = c_p/c_V = 5/3$ .
- ▶ For, e.g., diatomic molecules,  $\gamma = (5 + 2)/(3 + 2) = 1.4$ .
- ▶ For  $K$  internal degrees of freedom  $\zeta_1, \zeta_2, \dots, \zeta_K$ ,  $f^{(\text{eq})}$  is extended according to the equipartition theorem:

$$f^{(\text{eq})} = \frac{n}{(2\pi m K_B T)^{(3+K)/2}} \exp \left[ -\frac{\xi^2 + \zeta^2}{2m K_B T} \right]. \quad (37)$$

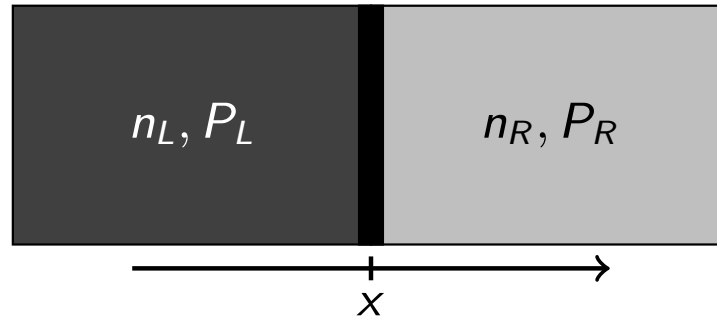
- ▶ In some problems, only  $d < 3$  translational dofs ( $\mathbf{p}$ ) are relevant, since the system is homogeneous along the  $3 - d$  dofs ( $\boldsymbol{\eta}$ ).
- ▶ The system can be described using the reduced distributions  $f'$  and  $f''$ :

$$\begin{pmatrix} f' \\ f'' \end{pmatrix} = \int d^{3-d} p \int d^K \zeta \left( \frac{1}{m} (\zeta^2 + \boldsymbol{\eta}^2) \right) f. \quad (38)$$

- ▶ The reduced equilibrium distribution  $f^{(\text{eq})'}$  is:

$$f^{(\text{eq})'} = \frac{n}{(2\pi m K_B T)^{d/2}} \exp \left[ -\frac{(\mathbf{p} - m\mathbf{u})^2}{2m K_B T} \right]. \quad (39)$$

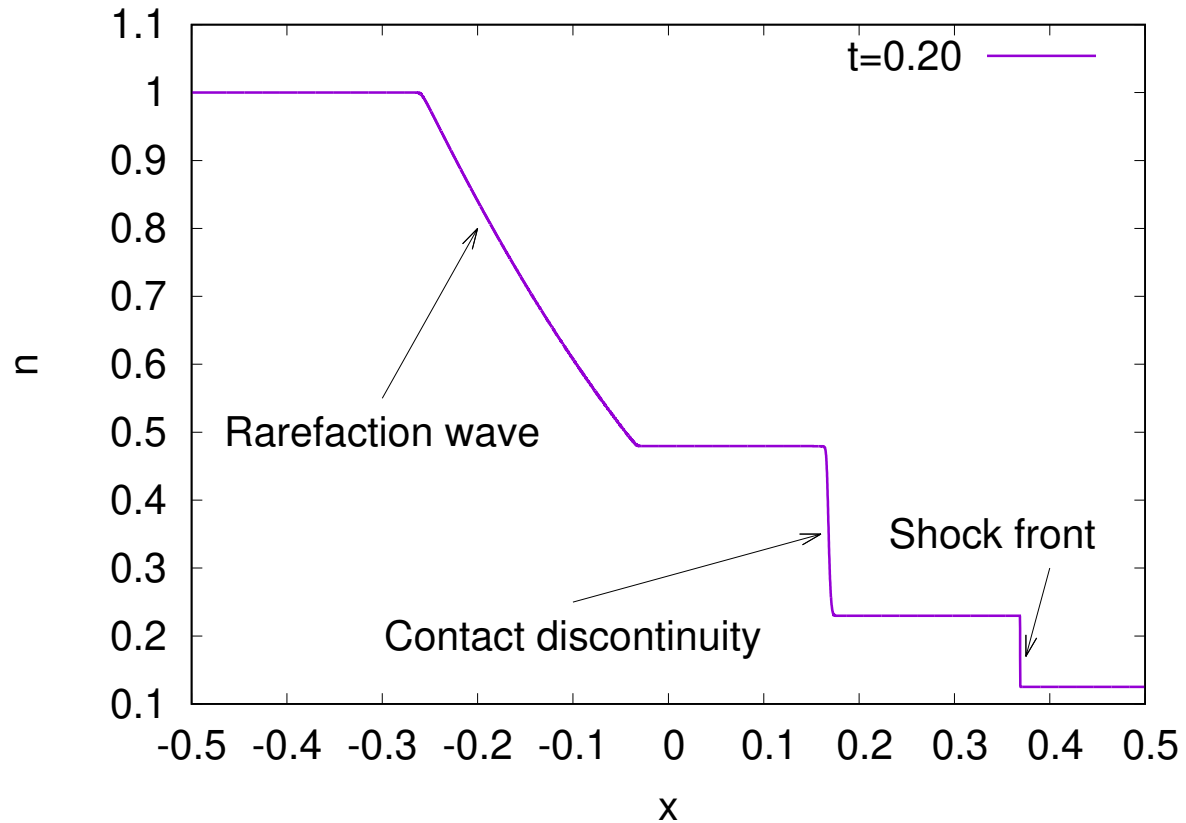
# 1D problem: Sod shock tube



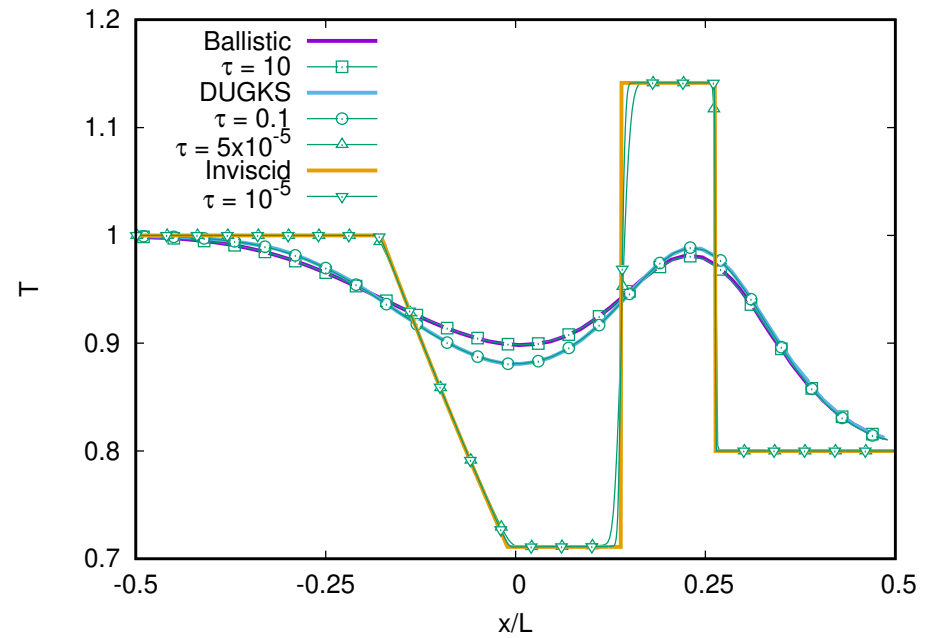
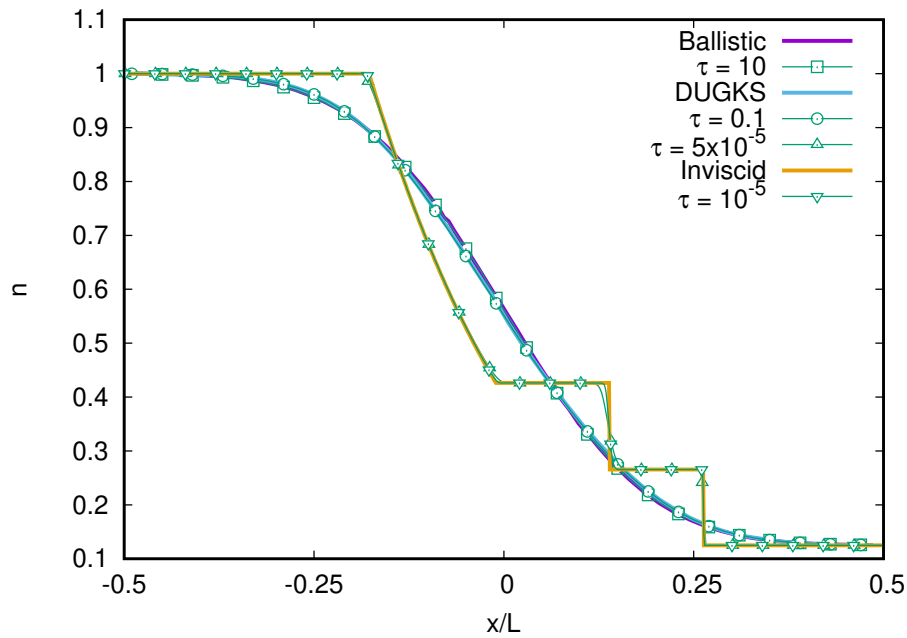
- ▶ At  $t = 0$ , the system consists of two semi-infinite domains separated by a thin membrane at  $x = 0$ .
- ▶ The system is homogeneous along  $y$  and  $z$  ( $d = 1$ ):

$$\partial_t f + \frac{p_x}{m} \partial_x f = J[f]. \quad (40)$$

# Shock wave structure



- ▶ The head of the rarefaction wave propagates at the speed of sound.
- ▶ The contact discontinuity propagates at the velocity on the plateau.
- ▶ The speed of the shock front is supersonic.

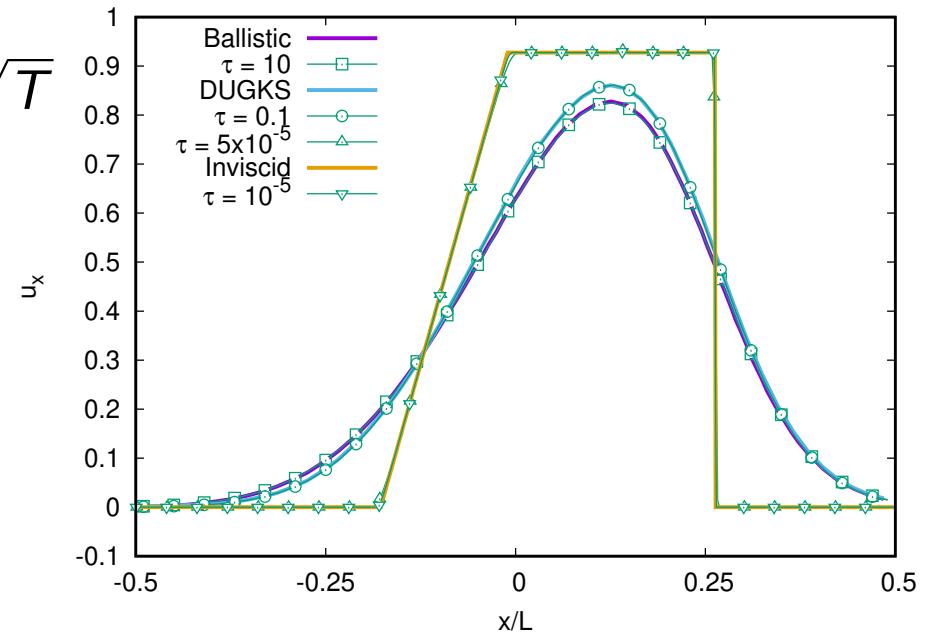


$\gamma = 7/5$ ,  $\text{Pr} = 2/3$ ,  $\tau = \text{Kn}/n\sqrt{T}$   
(HS).

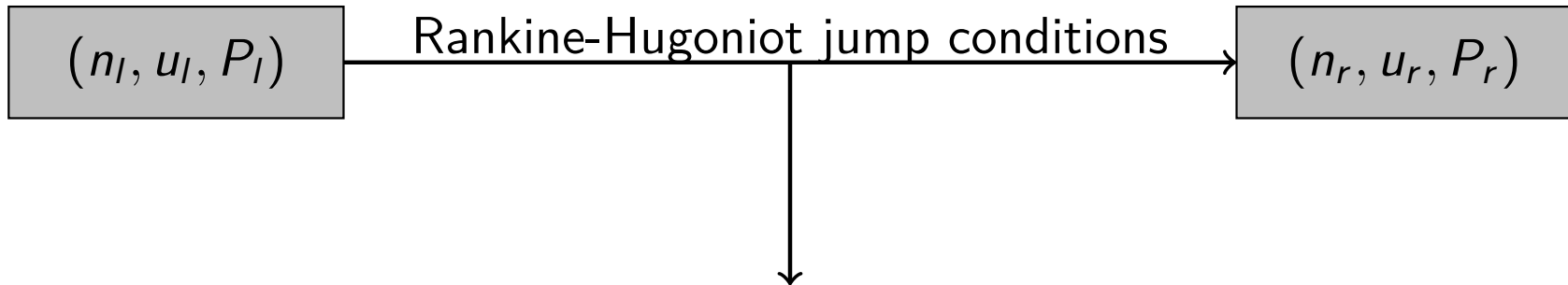
$\text{Kn} = 10^{-5}$ :  $Q = 8$ ,  $N_x = 1000$

$\text{Kn} = 5 \times 10^{-5}$ :  $Q = 8$ ,  $N_x = 400$

$\text{Kn} = 0.1, 10$ :  $Q = 30$ ,  $N_x = 50$



# Standing shock



$$\rho_r \Delta u_r = \rho_l \Delta u_l, \quad (41a)$$

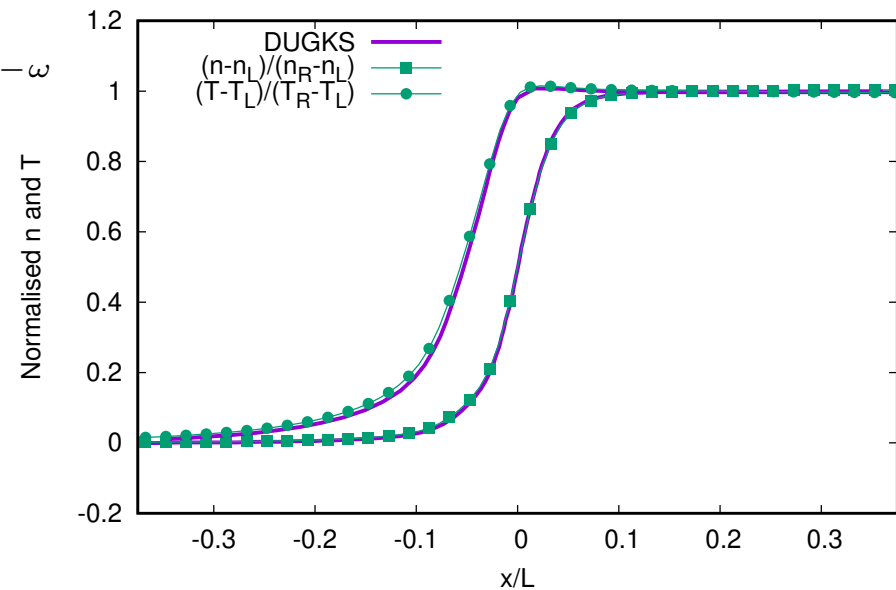
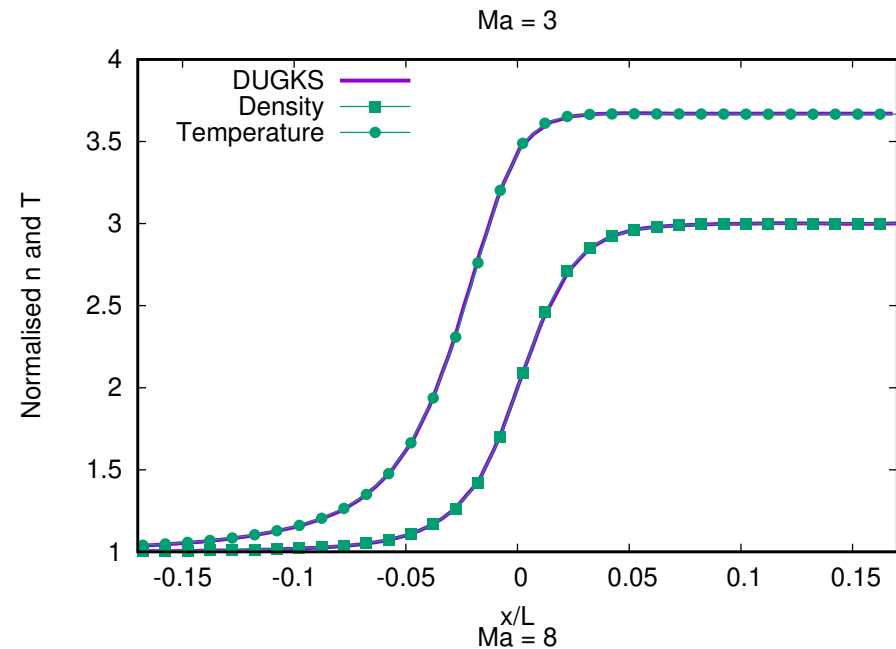
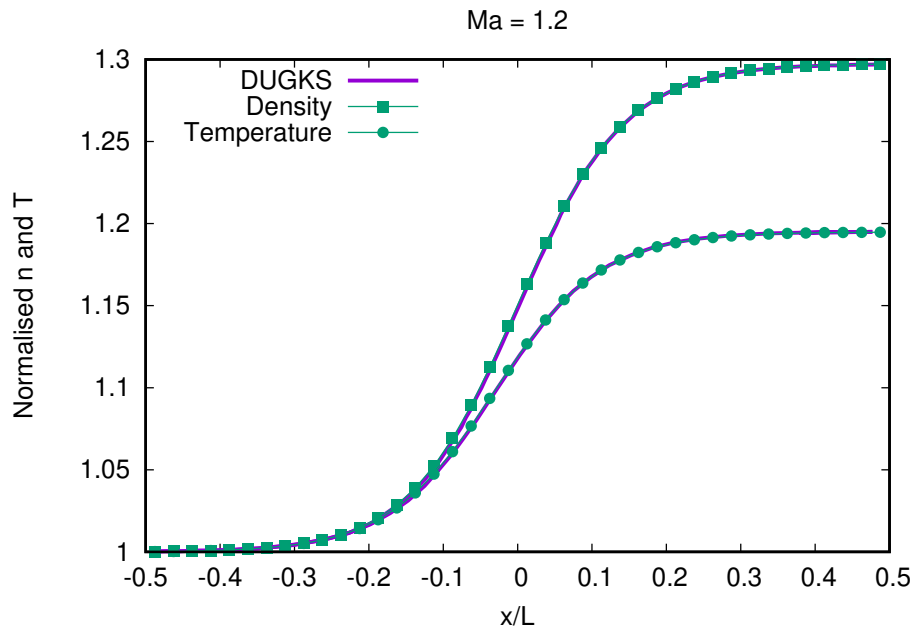
$$\rho_r u_r \Delta u_r + P_r = \rho_l u_l \Delta u_l + P_l, \quad (41b)$$

$$\left( n_r e_r + \frac{1}{2} \rho_r u_r^2 \right) \Delta u_r + u_r P_r = \left( n_l e_l + \frac{1}{2} \rho_l u_l^2 \right) \Delta u_l + u_l P_l, \quad (41c)$$

where  $\Delta u = u - c_s$  and  $c_s$  is the speed of the shock front.



# Comparison to DUGKS<sup>24</sup>



$$\gamma = 5/3, \text{ Pr} = 2/3, \tau = \text{Kn}/nT^{1-\varepsilon}$$

(Kn = 0.02).

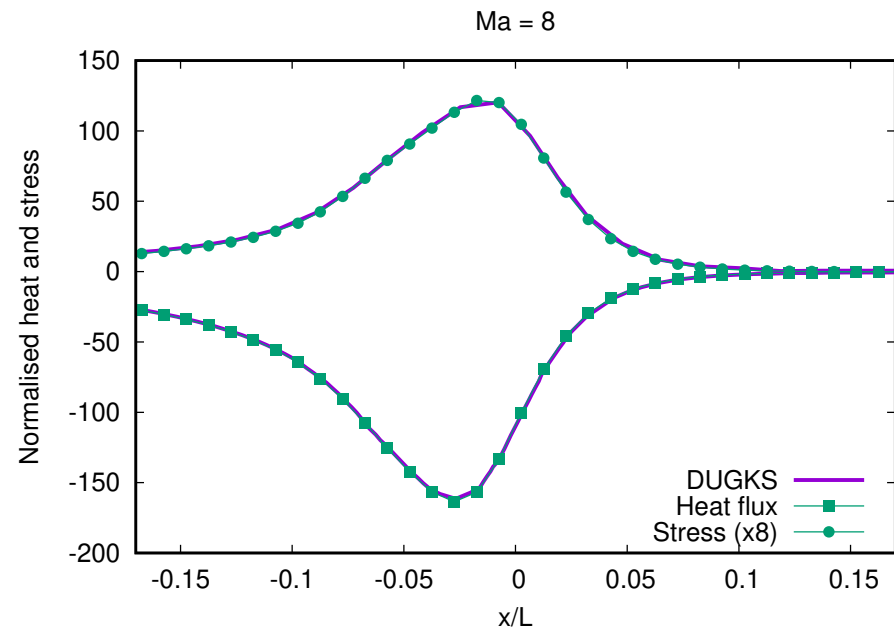
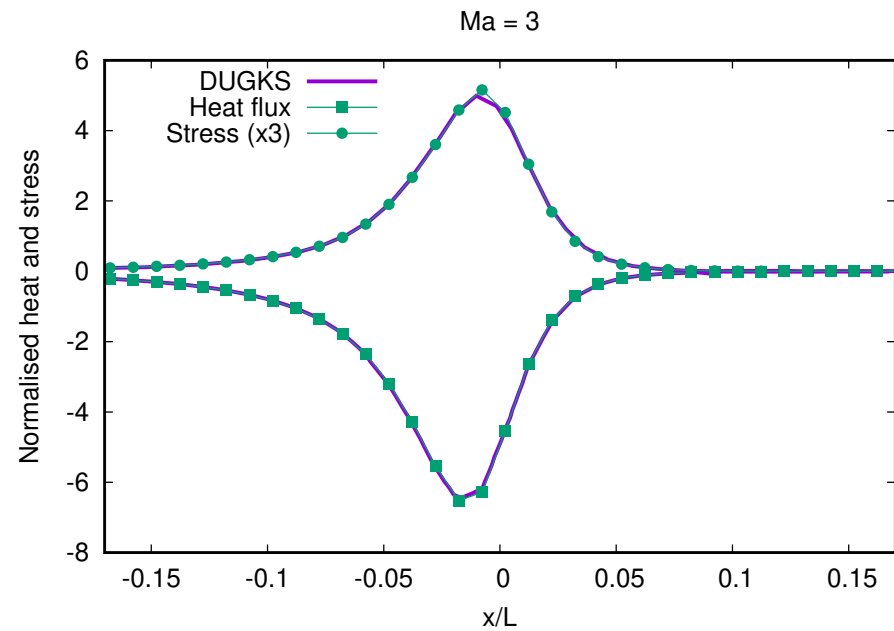
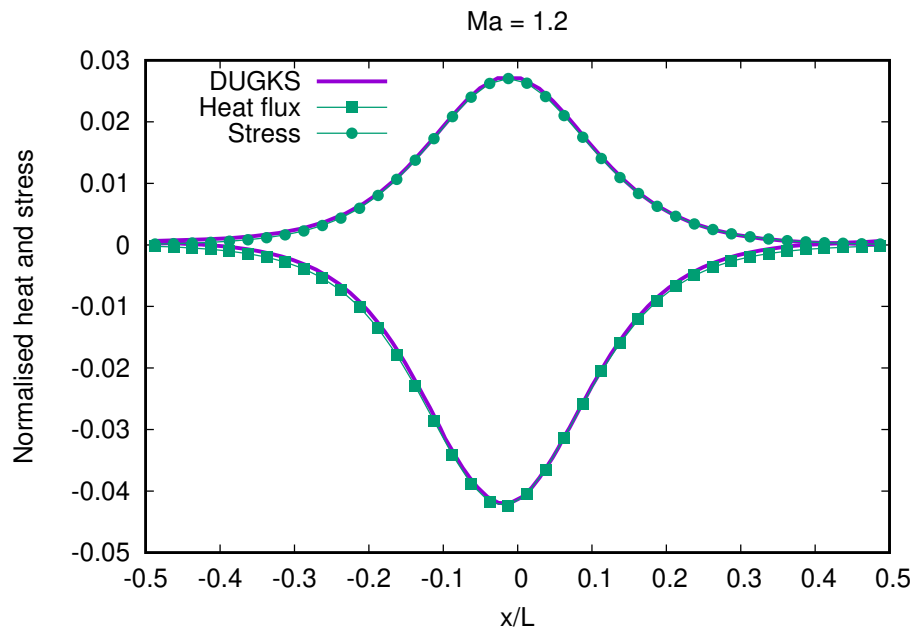
$$\text{Ma} = 1.2: Q = 10, N_x = 40, \omega = 0.5.$$

$$\text{Ma} = 3.0: Q = 20, N_x = 100, \omega = 0.5.$$

$$\text{Ma} = 8.0: Q = 30, N_x = 100, \omega = 0.68.$$

<sup>24</sup>Z. Guo, R. Wang, K. Xu, Phys. Rev. E **91** (2015) 033313.

# Comparison to DUGKS<sup>25</sup>



$$\gamma = 5/3, \text{Pr} = 2/3, \text{Kn} = 0.02.$$

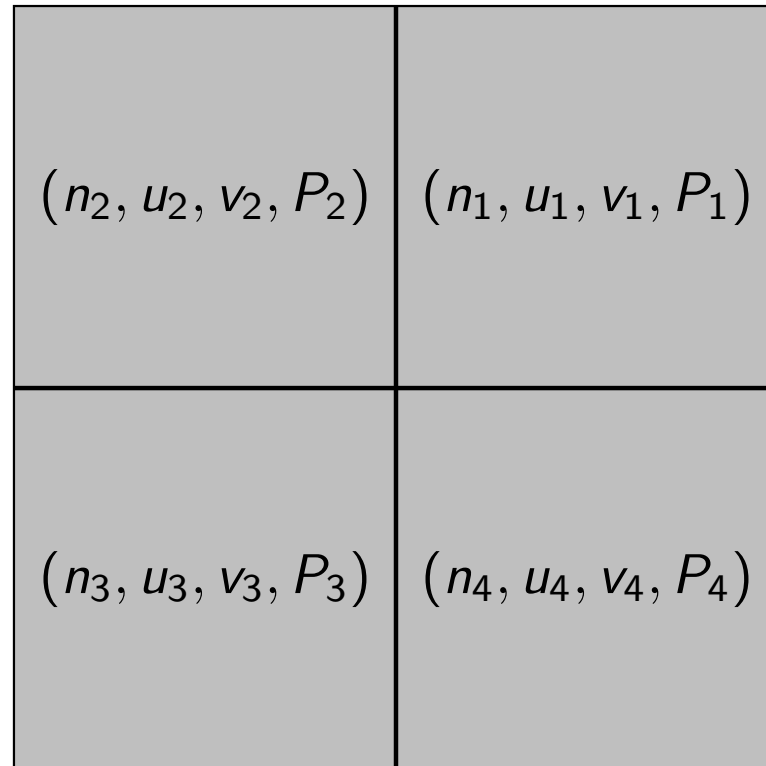
$$\text{Ma} = 1.2: Q = 10, N_x = 40, \omega = 0.5.$$

$$\text{Ma} = 3.0: Q = 20, N_x = 100, \omega = 0.5.$$

$$\text{Ma} = 8.0: Q = 30, N_x = 100, \omega = 0.68.$$

<sup>25</sup>Z. Guo, R. Wang, K. Xu, Phys. Rev. E **91** (2015) 033313.

## 2D Riemann problem.

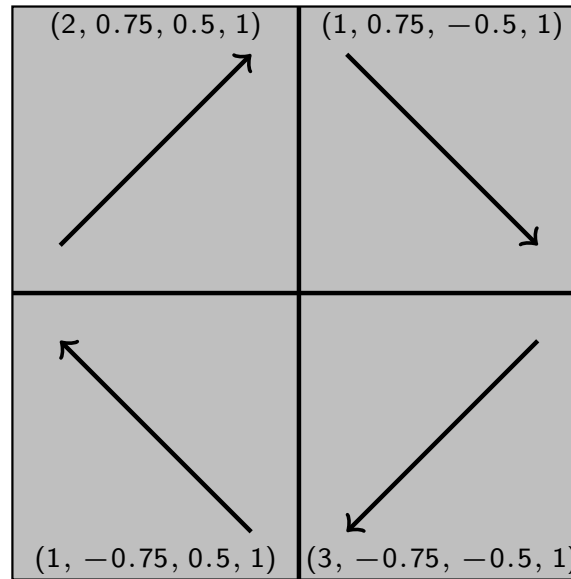


- ▶ In the initial configuration, the fluid properties are constant in each quadrant.
- ▶ Between the quadrants, only elementary waves ( $1D$  shock,  $1D$  rarefaction wave or  $2D$  slip line  $\equiv$  contact discontinuity) can appear.
- ▶ 19 genuinely different configurations emerge.<sup>26</sup>

---

<sup>26</sup>P.D. Lax, X.-D. Liu, SIAM J. Sci. Comput **19** (1998) 319.

# Configuration 6: 4 slip lines



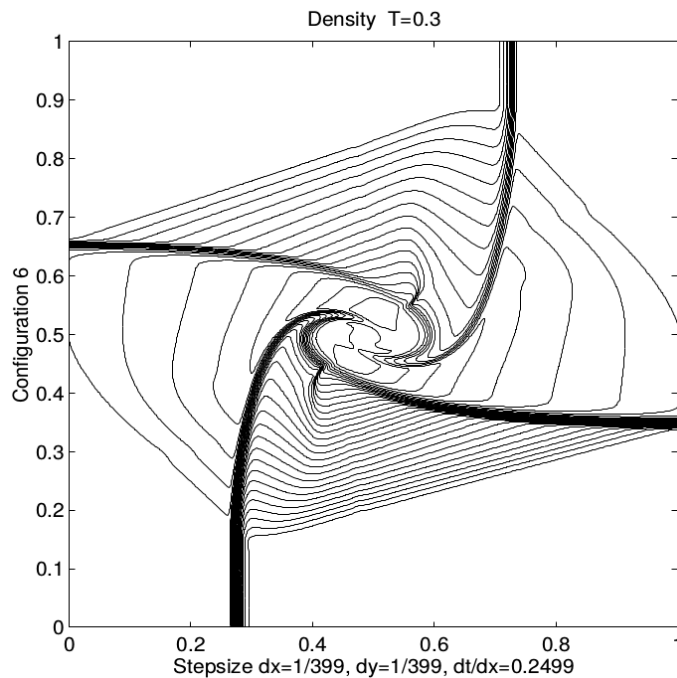
$$\text{Kn} = 5 \times 10^{-5}$$

$$\gamma = 5/3, \text{Pr} = 1$$

$$Q_x = Q_y = 6$$

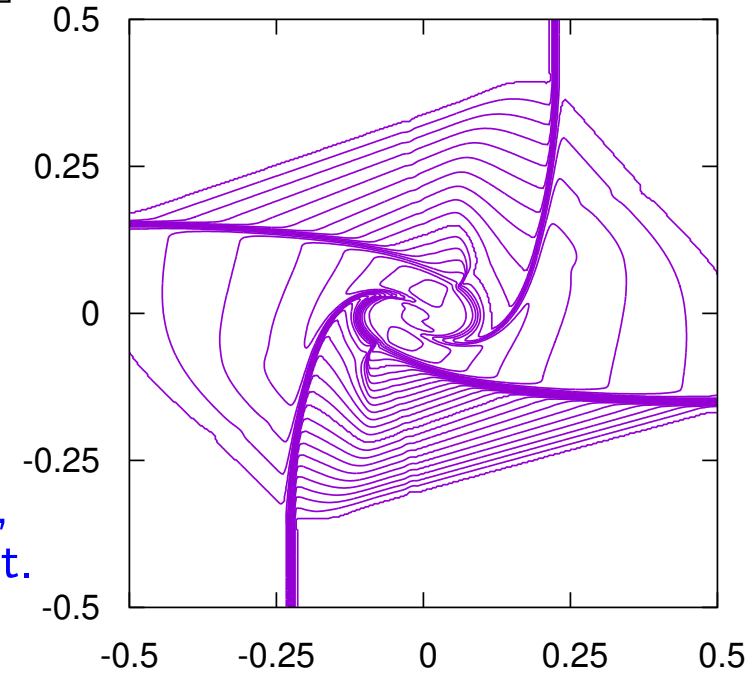
Grid size:  $400 \times 400$

Density contour at  $t = 0.30^*$

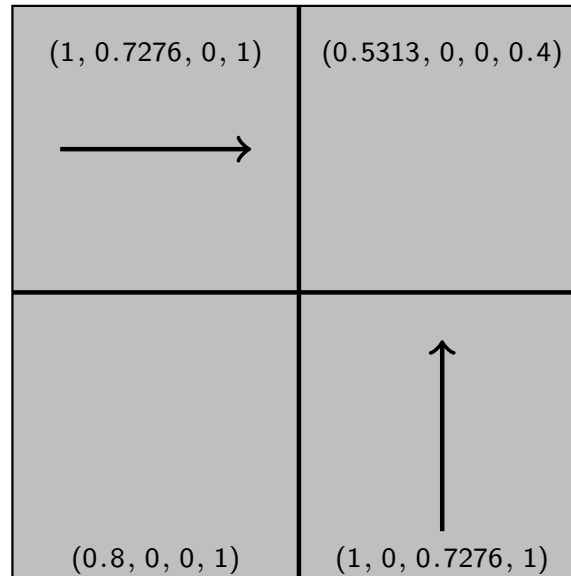


Configuration 6:\*

\*P.D. Lax, X.-D. Liu,  
SIAM J. Sci. Comput.  
**19** (1998) 319.



# Configuration 12: 2 slip lines and 2 shock waves



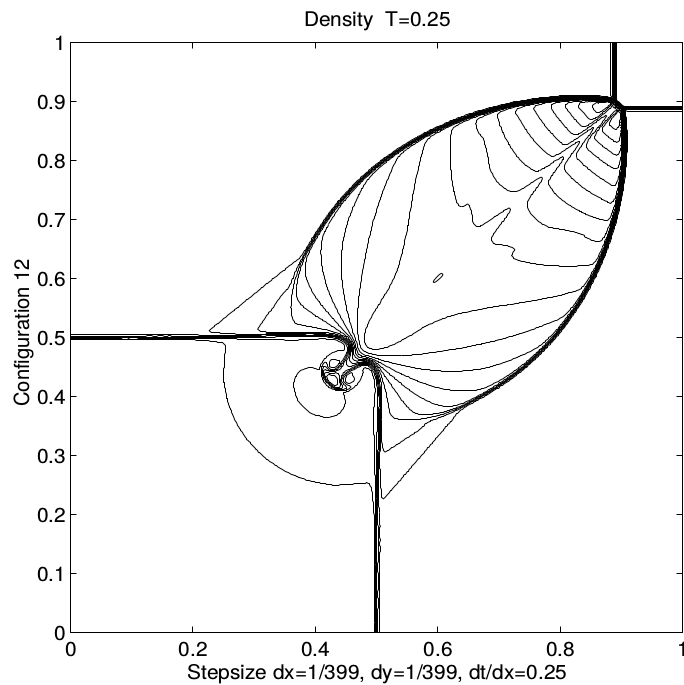
$$\text{Kn} = 5 \times 10^{-5}$$

$$\gamma = 5/3, \text{Pr} = 1$$

$$Q_x = Q_y = 6$$

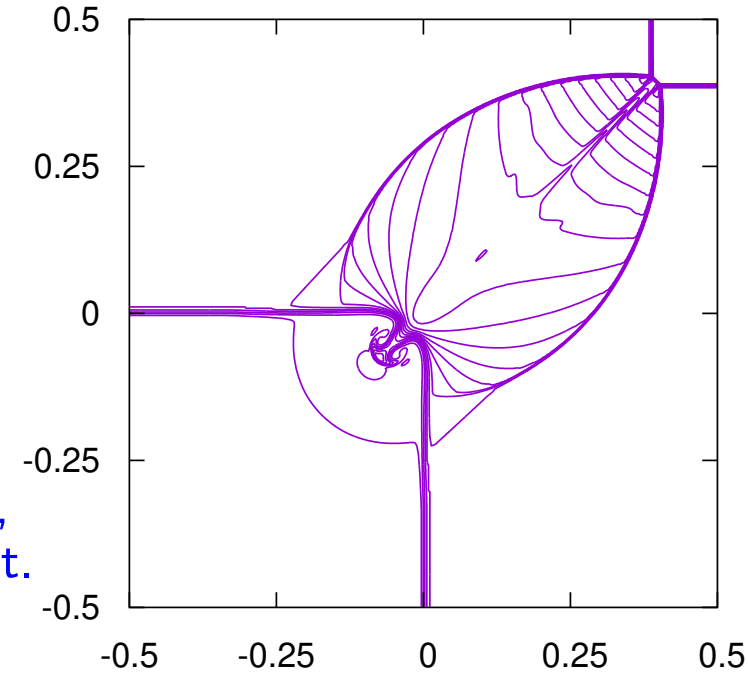
Grid size:  $400 \times 400$

Density contour at  $t = 0.25^*$



Configuration 12:\*

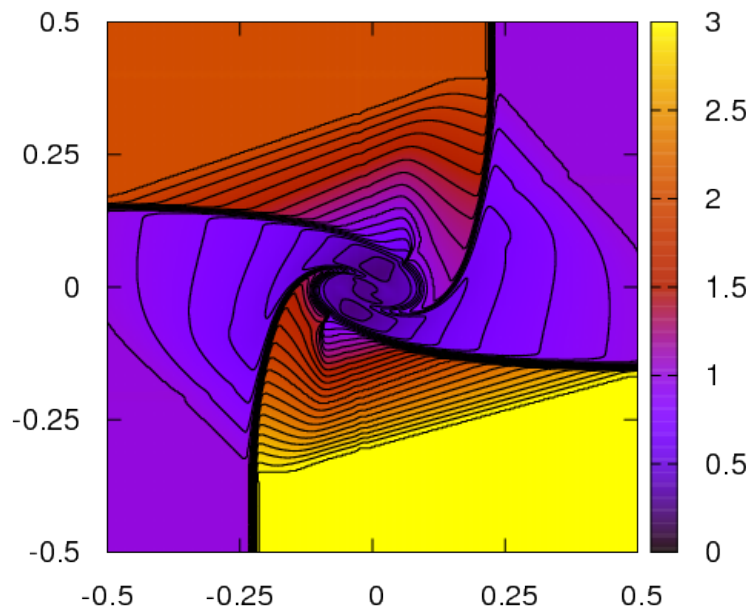
\*P.D. Lax, X.-D. Liu,  
SIAM J. Sci. Comput.  
**19** (1998) 319.



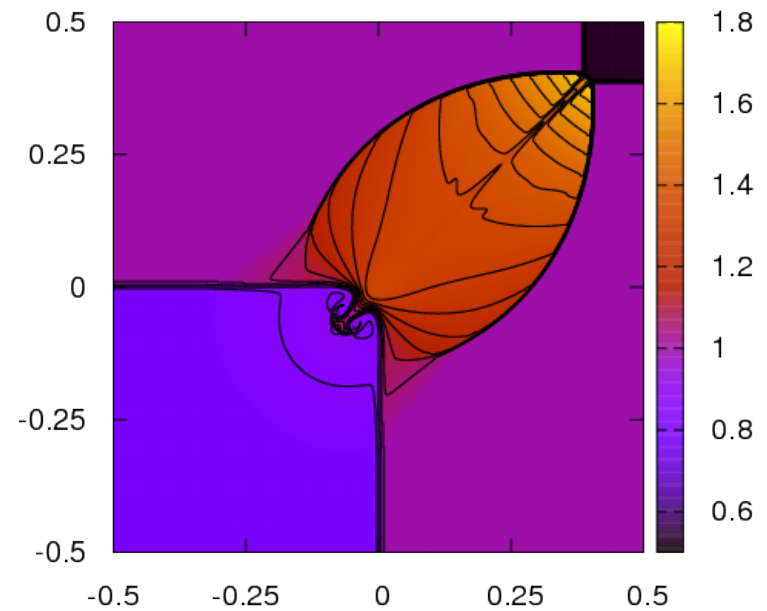
# 2D Riemann problem: animations

$$\text{Kn} = 5 \times 10^{-5}, \gamma = 5/3, \text{Pr} = 1, Q_x = Q_y = 6, 400 \times 400 \text{ nodes}, \\ \delta t = 5 \times 10^{-5}$$

MP9+RK3

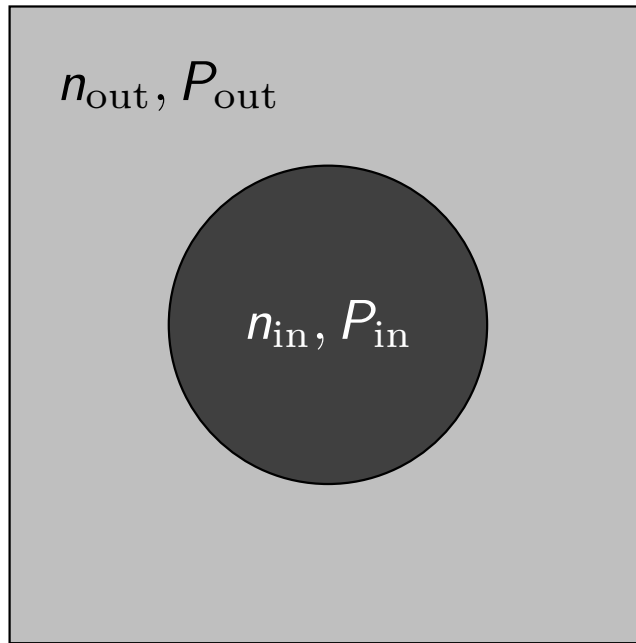


Configuration 6

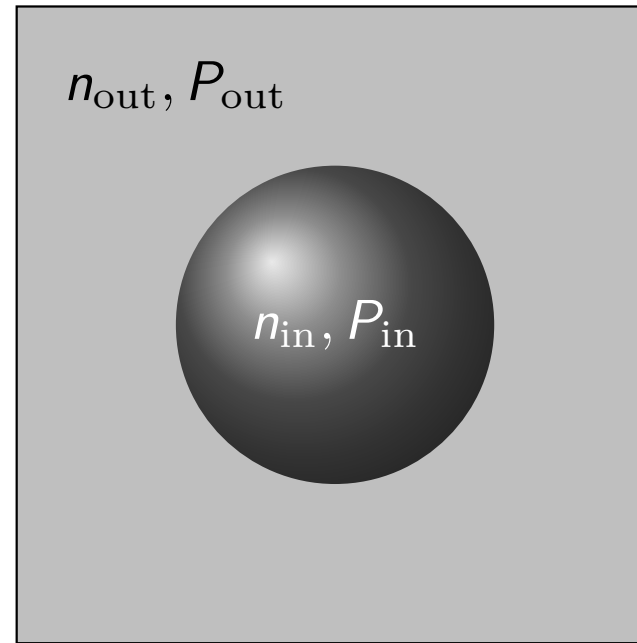


Configuration 12

# Cylindrical and spherical shocks



Cylindrical



Spherical

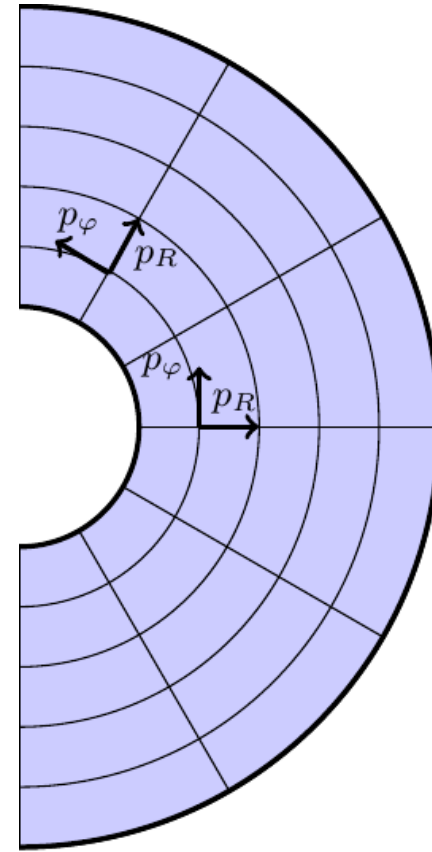
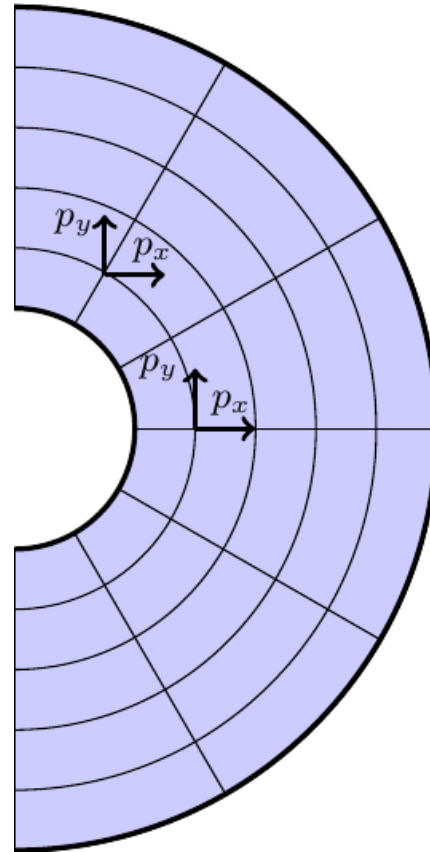
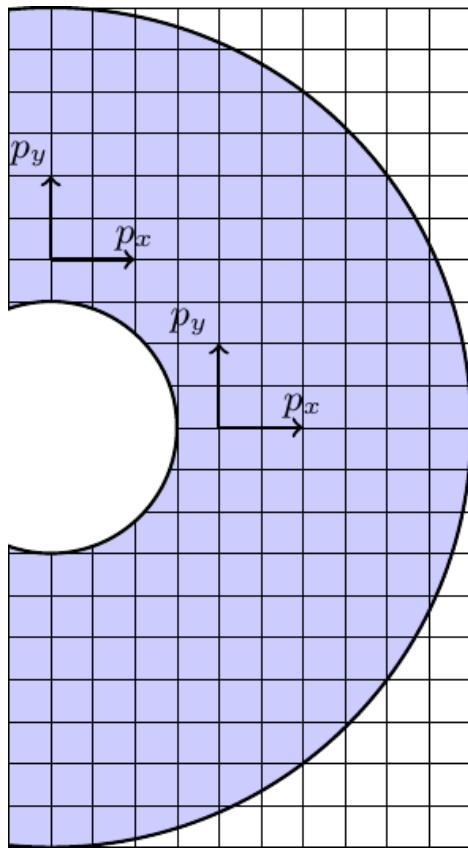
- ▶ Cartesian formulation:

$$\partial_t f + \frac{p_x}{m} \partial_x f + \frac{p_y}{m} \partial_y f + \frac{p_z}{m} \partial_z f = J[f] \quad (42)$$

requires 2 (3) dimensions and high resolution to ensure isotropy.

- ▶ The symmetries of the geometry allow the flow to be described in an essentially 1D manner using the vielbein formalism.

# Curvilinear coordinates and vielbein formalism





# Cylindrical coordinates

- ▶ For the shock with cylindrical symmetry,  $\tilde{x}^i \in \{R, \varphi, z\}$  and

$$\mathbf{e}_{\hat{R}} = \partial_R, \quad \mathbf{e}_{\hat{\varphi}} = R^{-1} \partial_\varphi, \quad \mathbf{e}_{\hat{z}} = \partial_z. \quad (43)$$

- ▶ Setting  $p^{\hat{R}} = p_\perp \cos \phi$  and  $p^{\hat{\varphi}} = p_\perp \sin \phi$ , the Boltzmann equation becomes:

$$\frac{\partial f}{\partial t} + \frac{p_\perp \cos \phi}{mR} \frac{\partial(fR)}{\partial R} - \frac{p_\perp}{R} \partial_\phi(f \sin \phi) = J[f]. \quad (44)$$

- ▶ The  $p^{\hat{z}}$  dof can be integrated out, thus  $d = 2$ .
- ▶ The moments of  $f$  are:

$$\int_0^\infty p_\perp dp_\perp \int_0^{2\pi} d\phi f' p_x^s p_y^r = \sum_{i=1}^{Q_L} \sum_{j=1}^M f'_{ij} p_{\perp,i}^{s+r} (\cos \phi_i)^s (\sin \phi_j)^r. \quad (45)$$

# Spherical coordinates

- ▶ For the shock with spherical symmetry,  $\tilde{x}^i \in \{r, \theta, \varphi\}$  and

$$\mathbf{e}_{\hat{r}} = \partial_r, \quad \mathbf{e}_{\hat{\theta}} = \frac{\partial_\theta}{r}, \quad \mathbf{e}_{\hat{\varphi}} = \frac{\partial_\varphi}{r \sin \theta}. \quad (46)$$

- ▶ Setting  $p^{\hat{r}} = p \sin \vartheta \cos \phi$ ,  $p^{\hat{\theta}} = p \sin \vartheta \sin \phi$ ,  $p^{\hat{\varphi}} = p \cos \vartheta$ , the Boltzmann equation becomes:

$$\frac{\partial f}{\partial t} + \frac{p\xi}{mr^2} \frac{\partial(fr^2)}{\partial r} + \frac{p}{r} \partial_\xi [(1 - \xi^2)f] = J[f], \quad (47)$$

where  $\xi = \cos \vartheta$ .

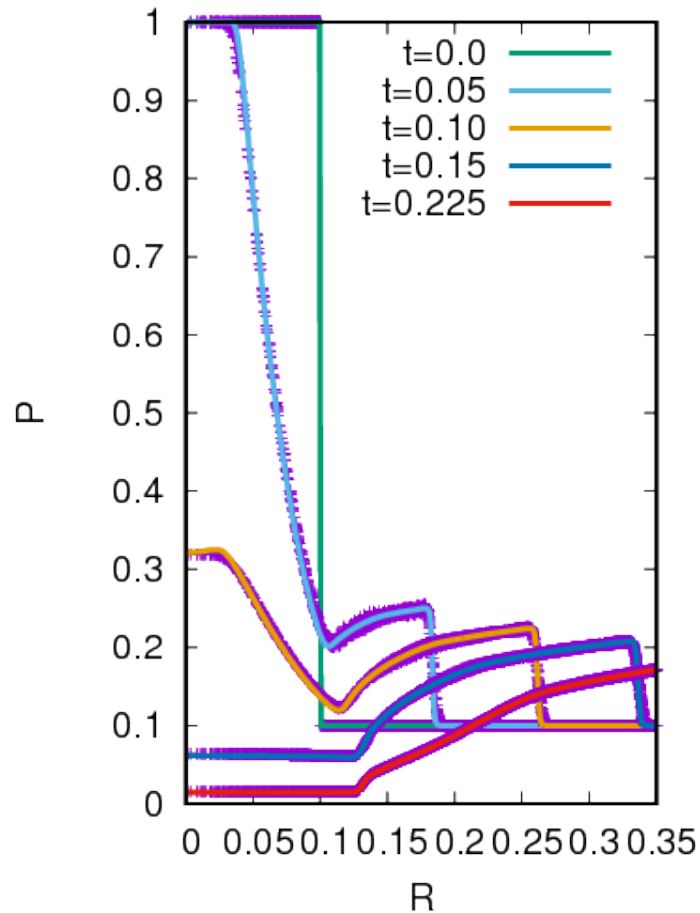
- ▶ The moments of  $f$  are:

$$\int_0^\infty p^2 dp \int_{-1}^1 d\xi \int_0^{2\pi} d\phi f p_x^s p_y^r p_z^q = \sum_{i=1}^{Q_L} \sum_{j=1}^{Q_\xi} f_{ij} p_i^{s+r+q} \xi_j^q (1 - \xi_j^2)^{(s+r)/2} \times \int_0^{2\pi} d\phi (\cos \phi)^s (\sin \phi)^r. \quad (48)$$

where  $P_{Q_\xi}(\xi_j) = 0$  and  $L_{Q_L}^{(1)}(p_i^2) = 0$ .<sup>27</sup>

<sup>27</sup>V.E. Ambruş, V. Sofonea, Phys. Rev. E **86** (2012) 016708.

# Primary shock

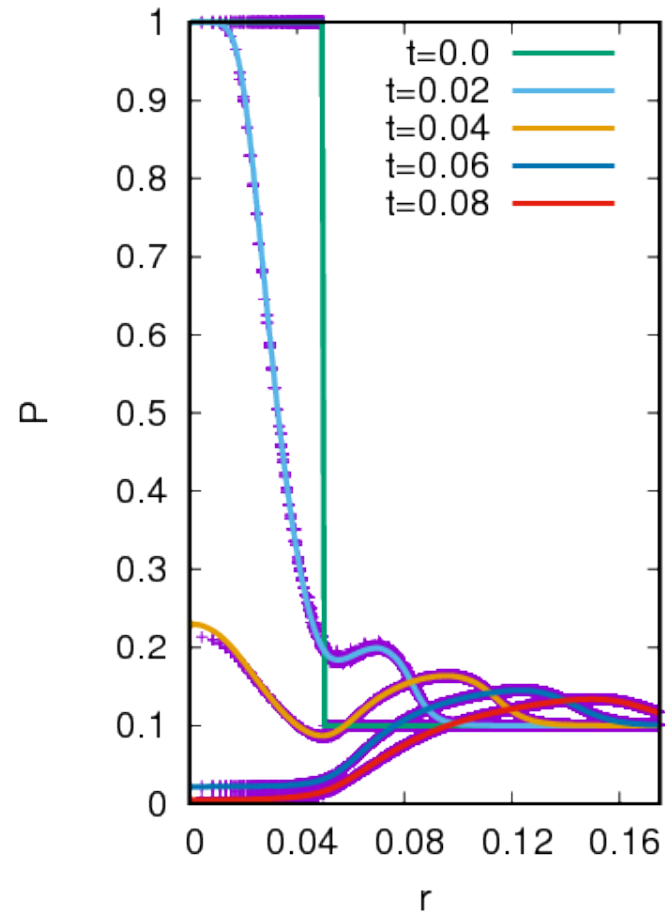


Cylindrical

$Kn = 5 \times 10^{-5}$ ,  $Pr = 1$ ,  $\omega = 0.5$

200  $\times$  200 nodes for Cartesian,

1000 nodes for vielbein



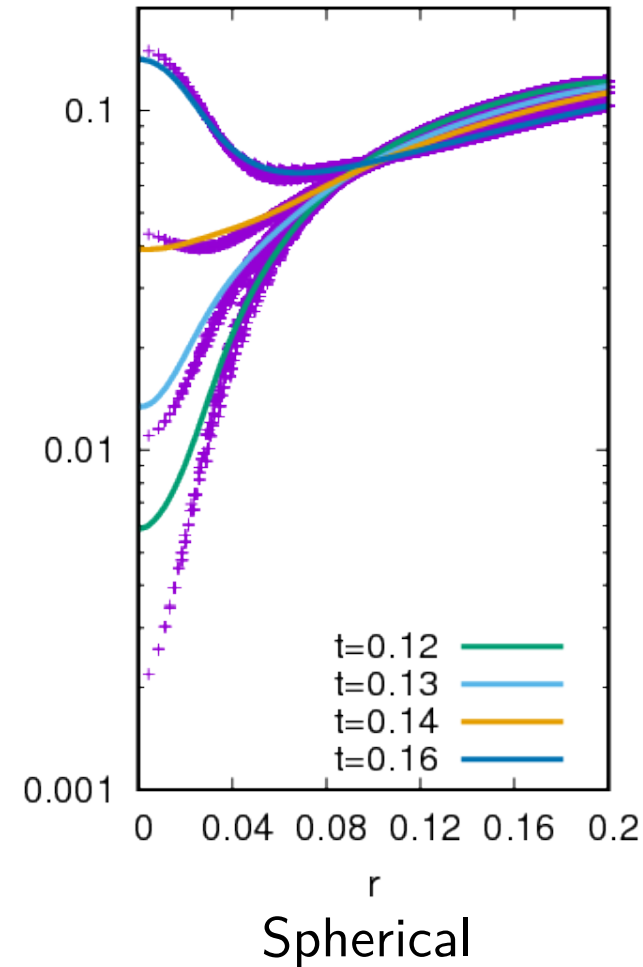
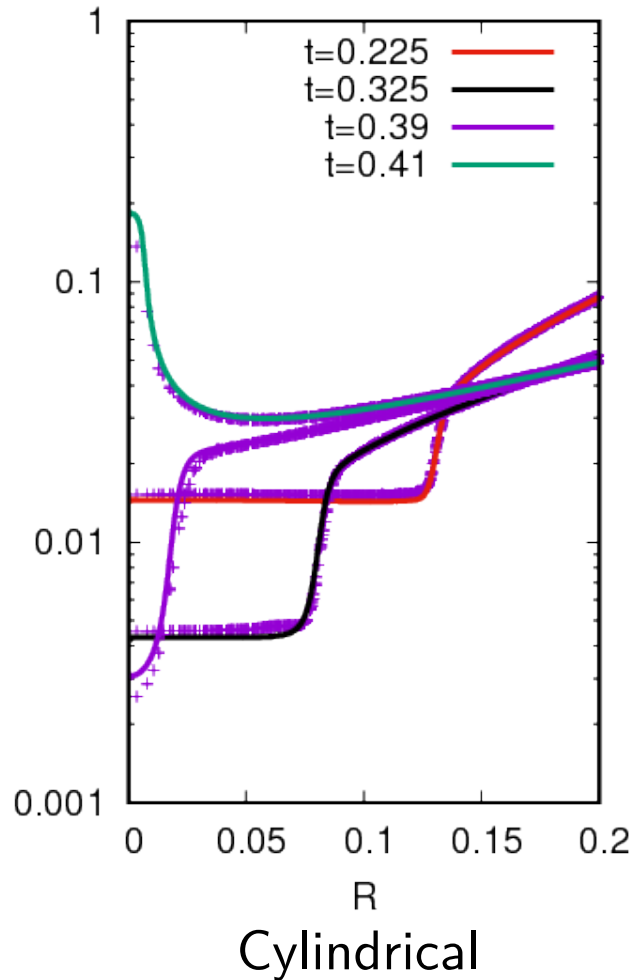
Spherical

$Kn = 5 \times 10^{-4}$ ,  $Pr = 1$ ,  $\omega = 0.5$

96  $\times$  96  $\times$  96 nodes for Cartesian

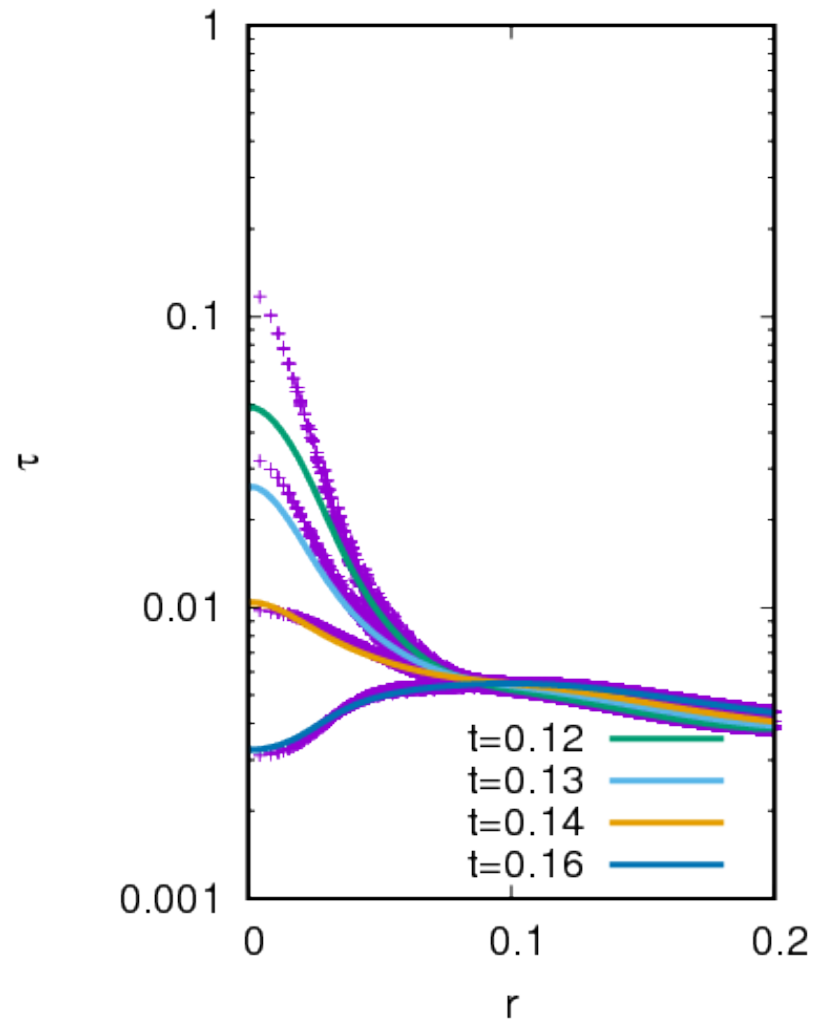
512 nodes for vielbein

# Reverse shock



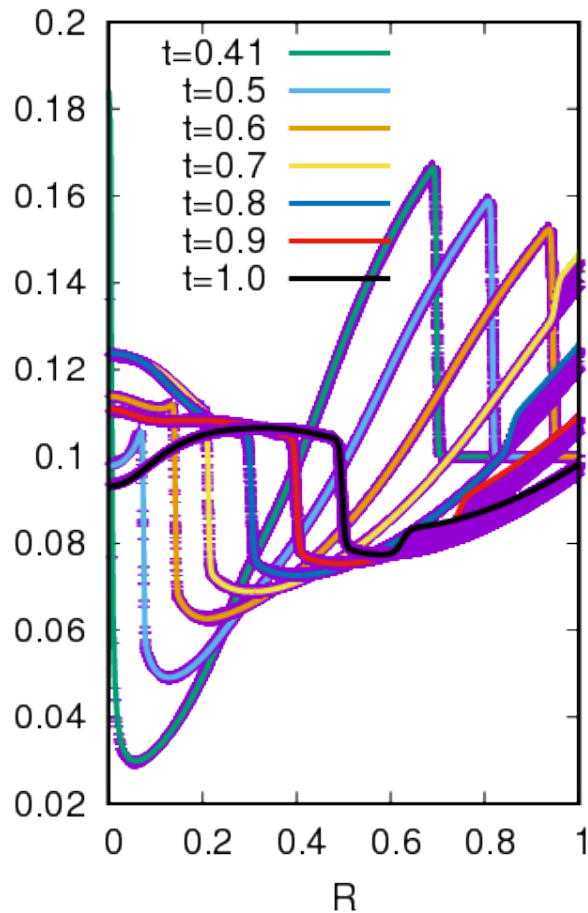
- ▶  $\tau = \text{Kn}/n\sqrt{T} = \text{Kn}\sqrt{T}/P$  becomes large at the origin  $\Rightarrow$  enhanced dissipation due to strong rarefaction.

# Reverse shock



$\tau = \text{Kn}/n\sqrt{T} = \text{Kn}\sqrt{T}/P$  for the spherically symmetric shock.

# Secondary shock

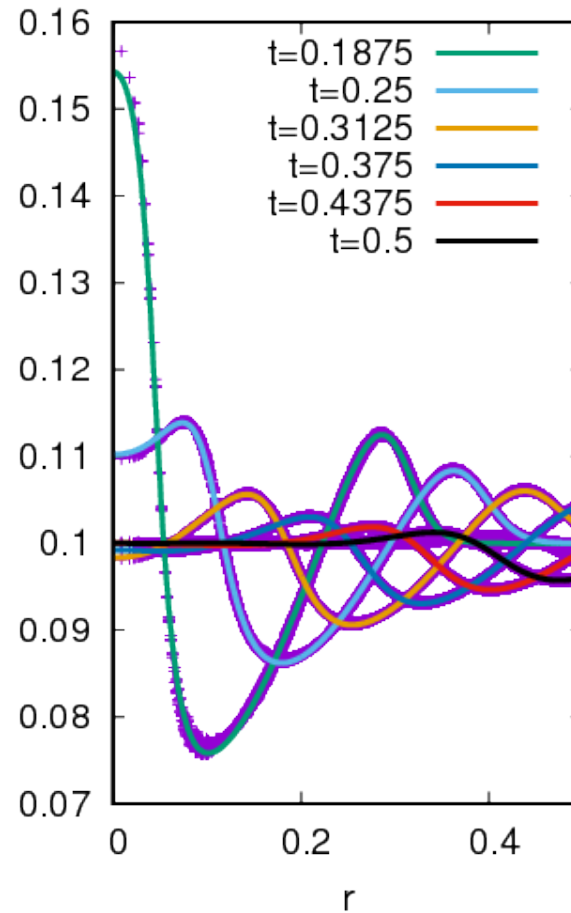


Cylindrical

$Kn = 5 \times 10^{-5}$ ,  $Pr = 1$ ,  $\omega = 0.5$

200 × 200 nodes for Cartesian,

1000 nodes for vielbein



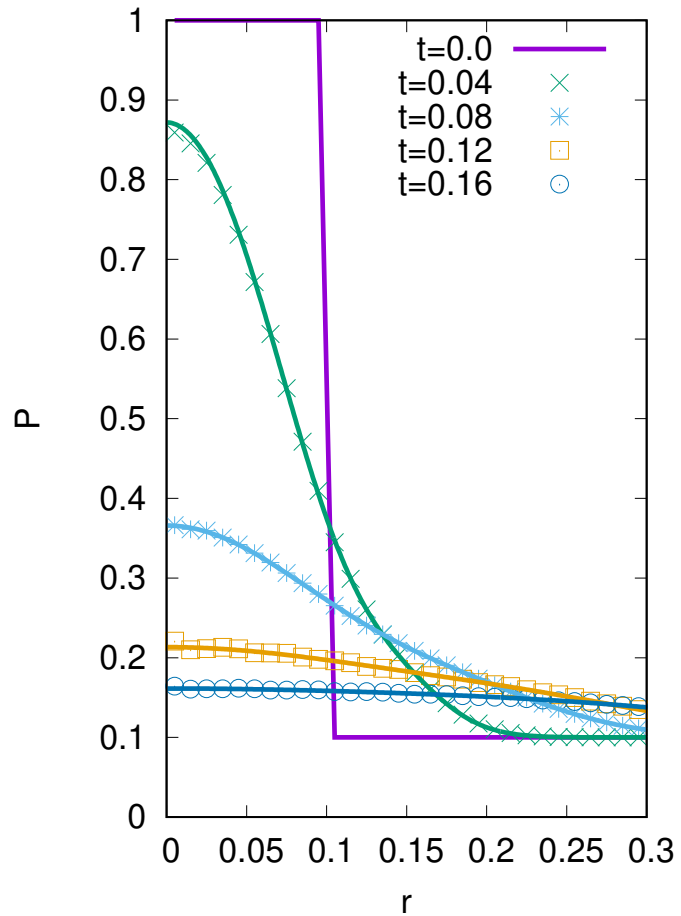
Spherical

$Kn = 5 \times 10^{-4}$ ,  $Pr = 1$ ,  $\omega = 0.5$

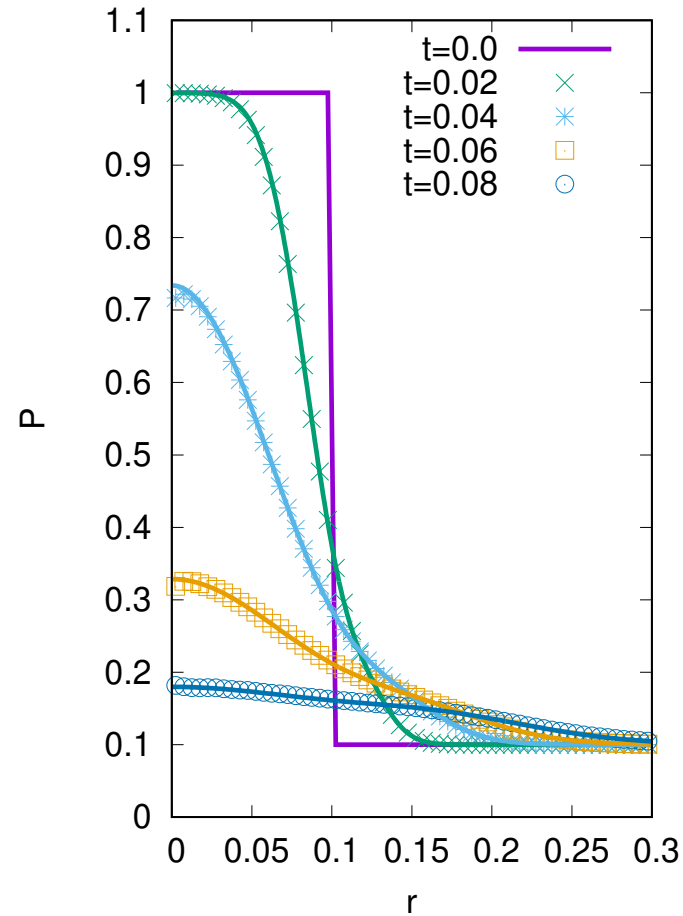
96 × 96 × 96 nodes for Cartesian

512 nodes for vielbein

# Ballistic regime - pressure

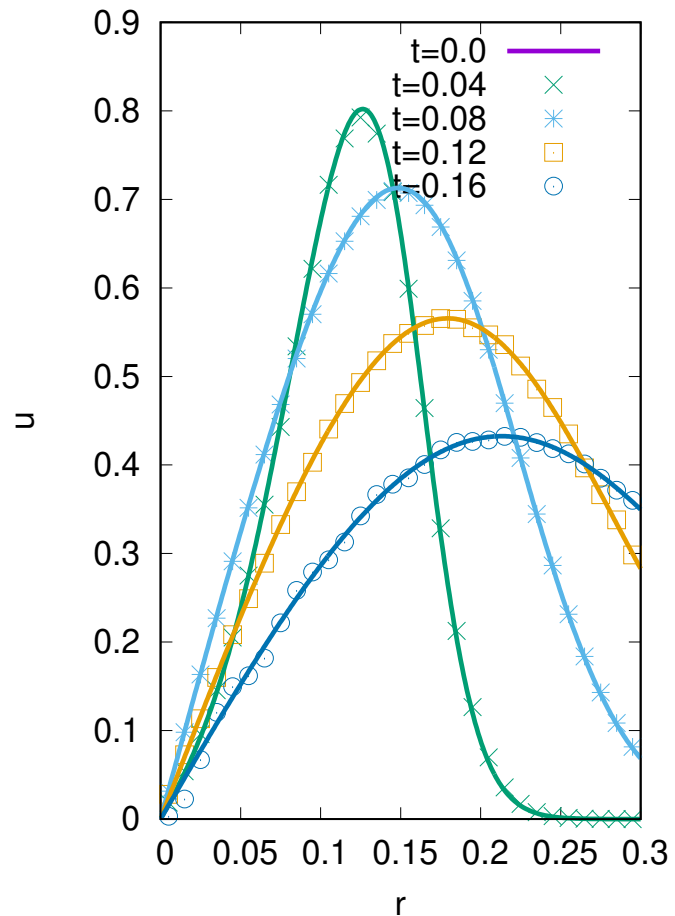


Cylindrical  
50 nodes

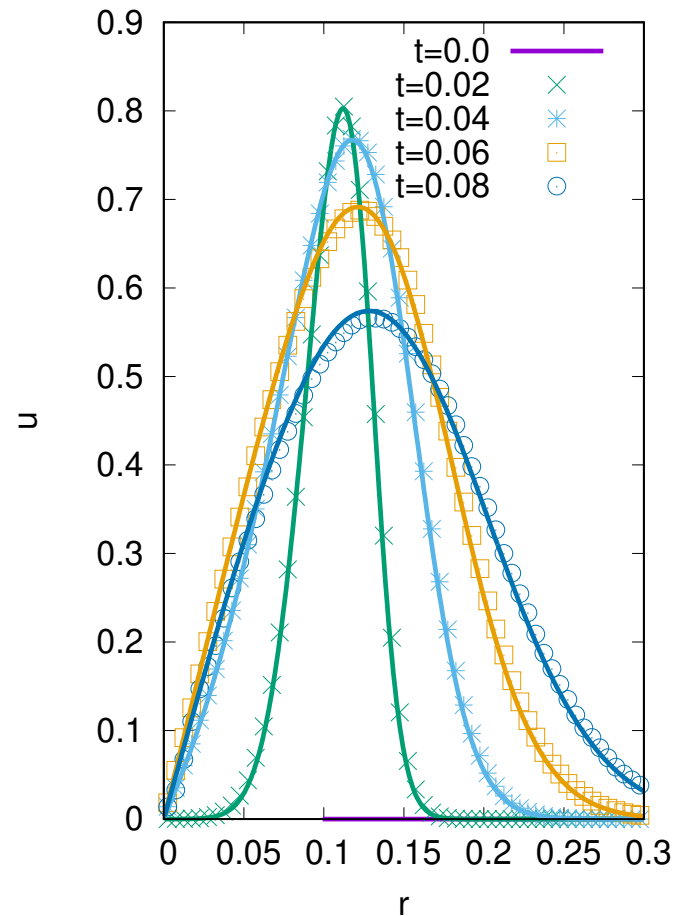


Spherical  
100 nodes

# Ballistic regime - velocity



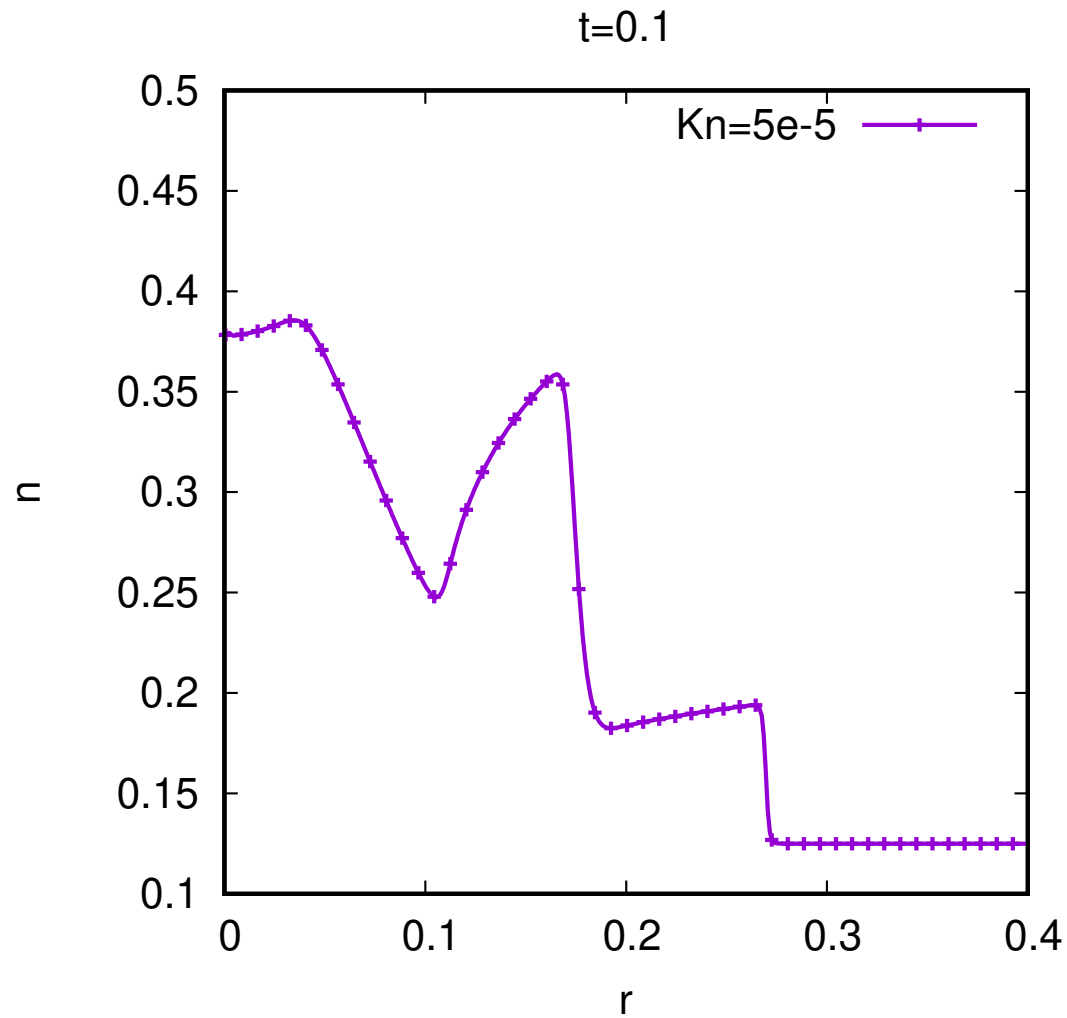
Cylindrical  
50 nodes



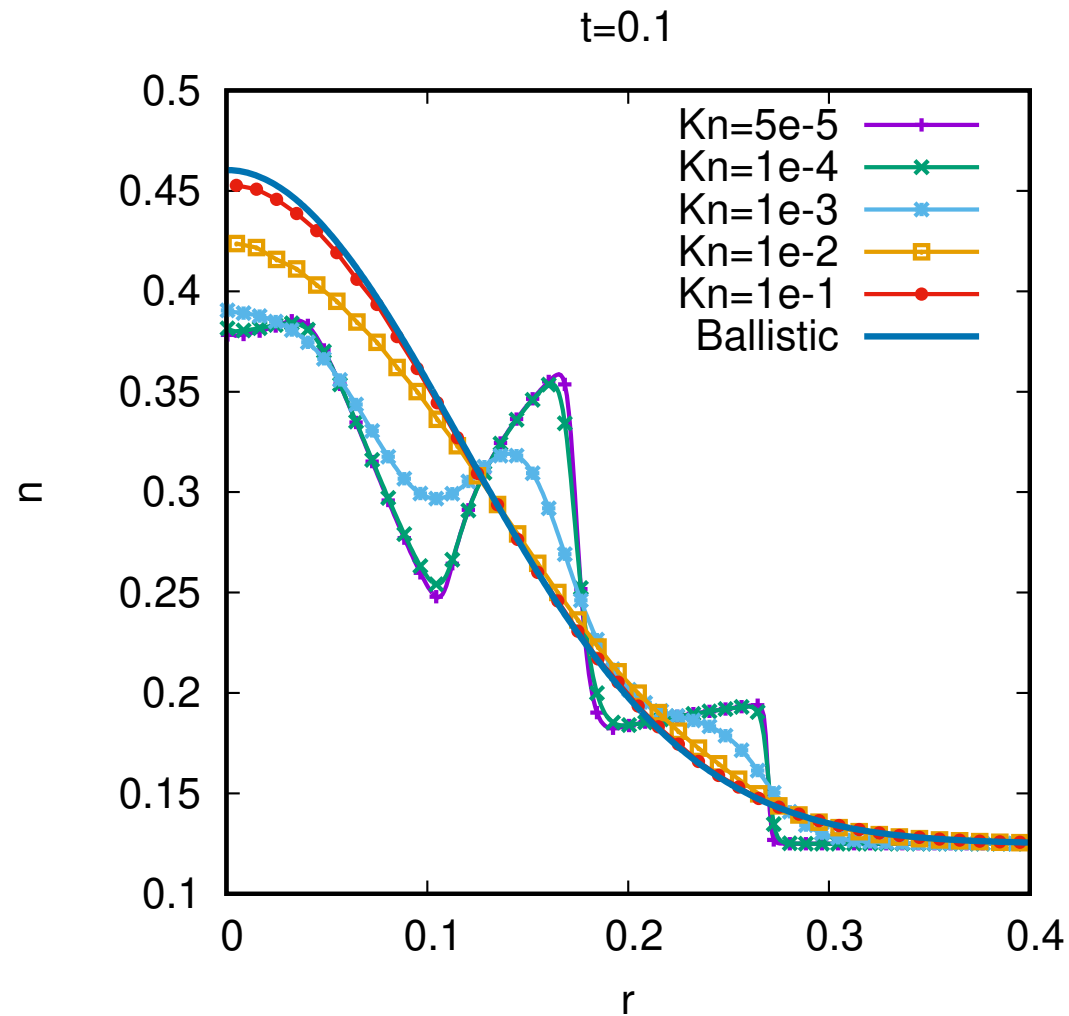
Spherical  
100 nodes



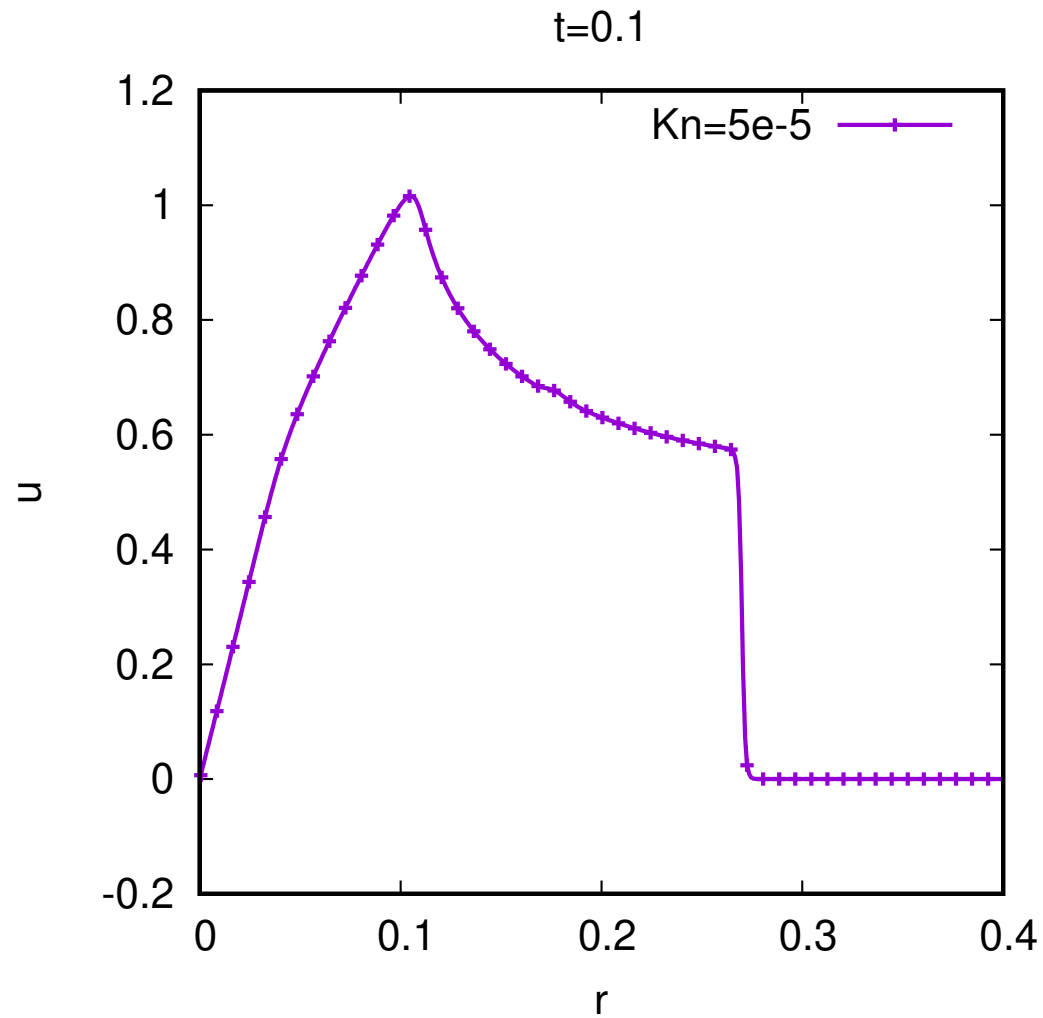
# Cylindrical shock: Transition flow regime - density



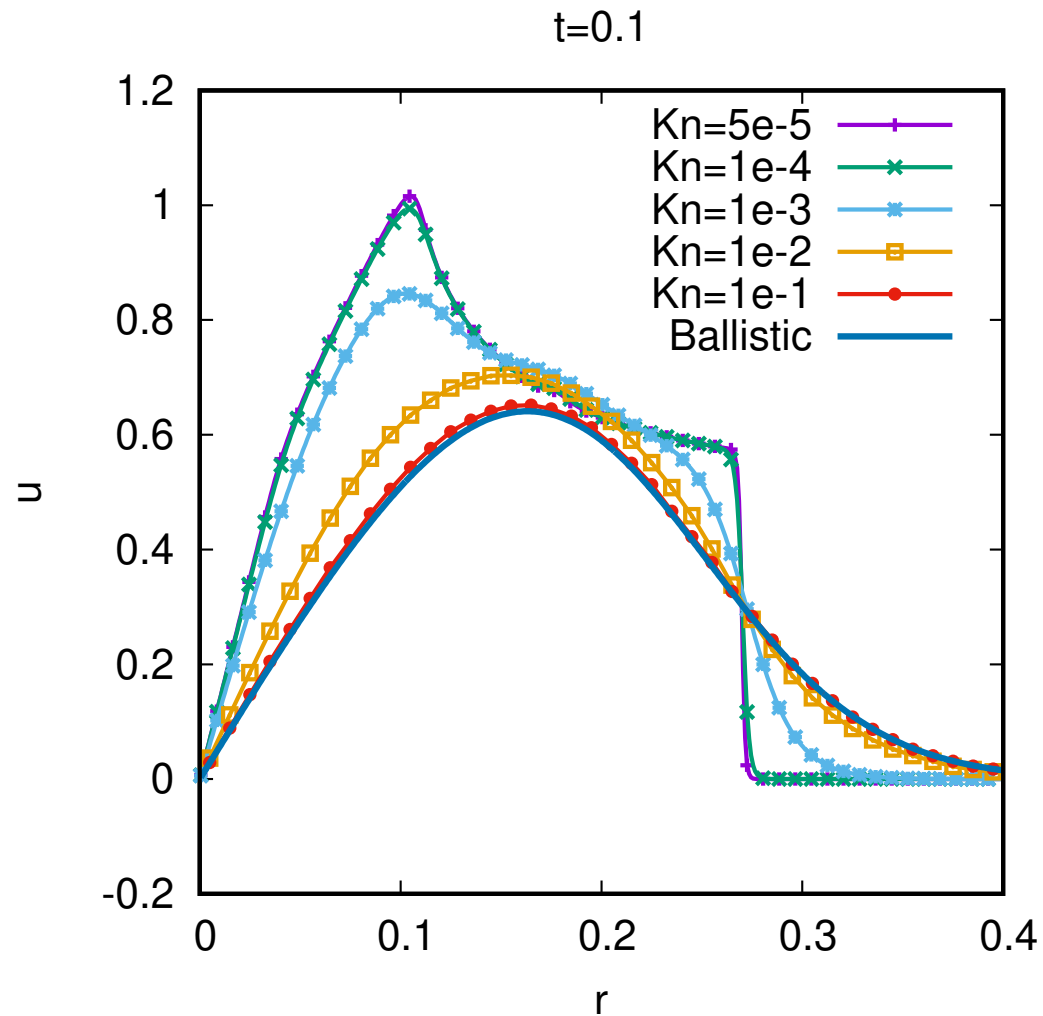
# Cylindrical shock: Transition flow regime - density



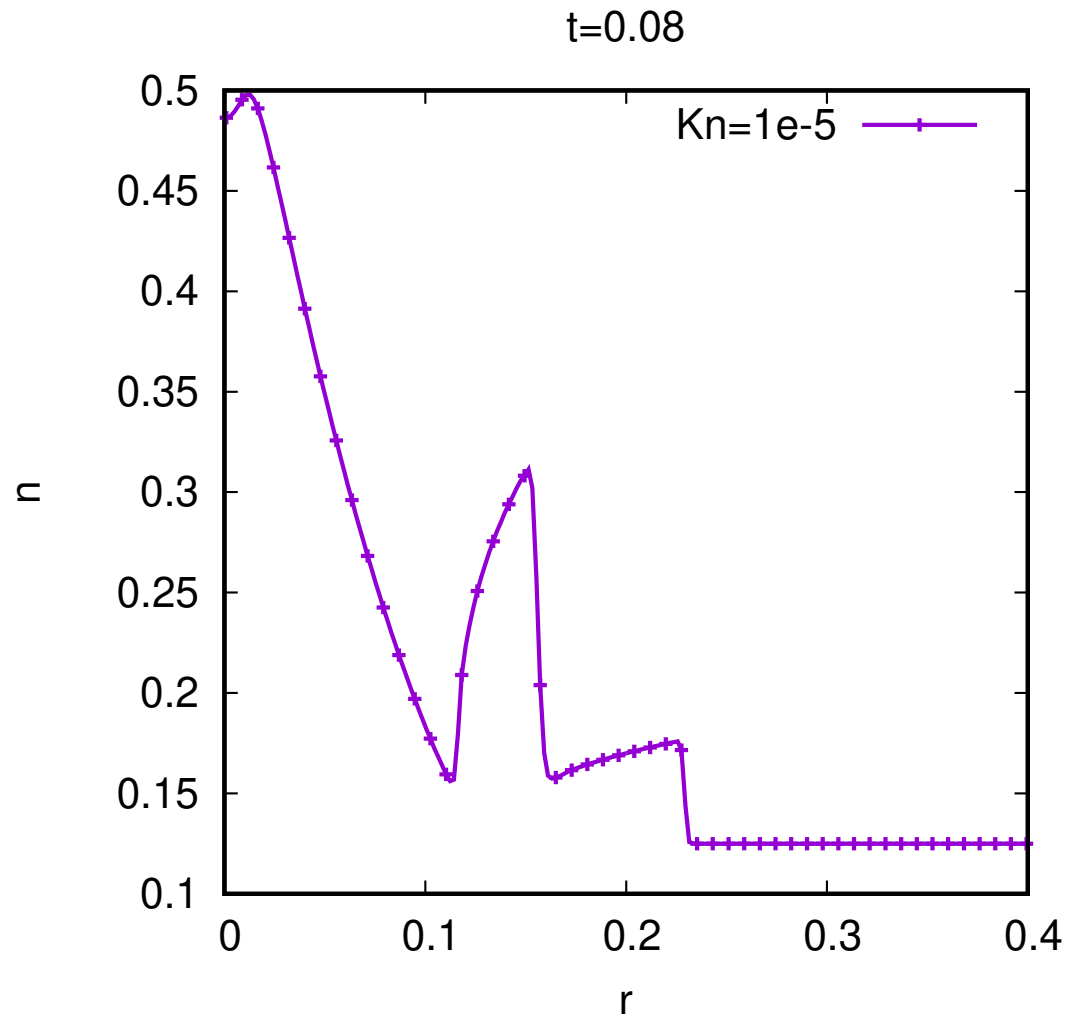
# Cylindrical shock: Transition flow regime - velocity



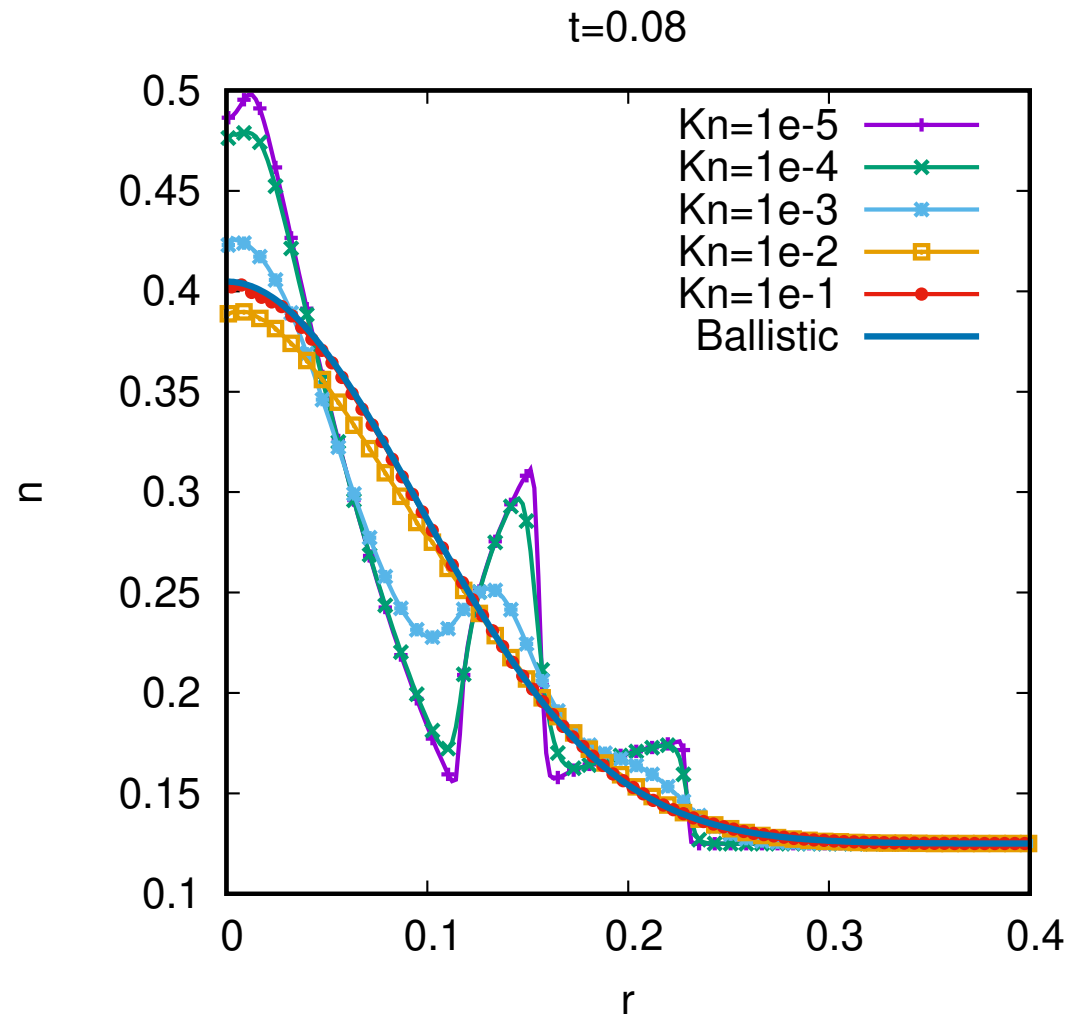
# Cylindrical shock: Transition flow regime - velocity



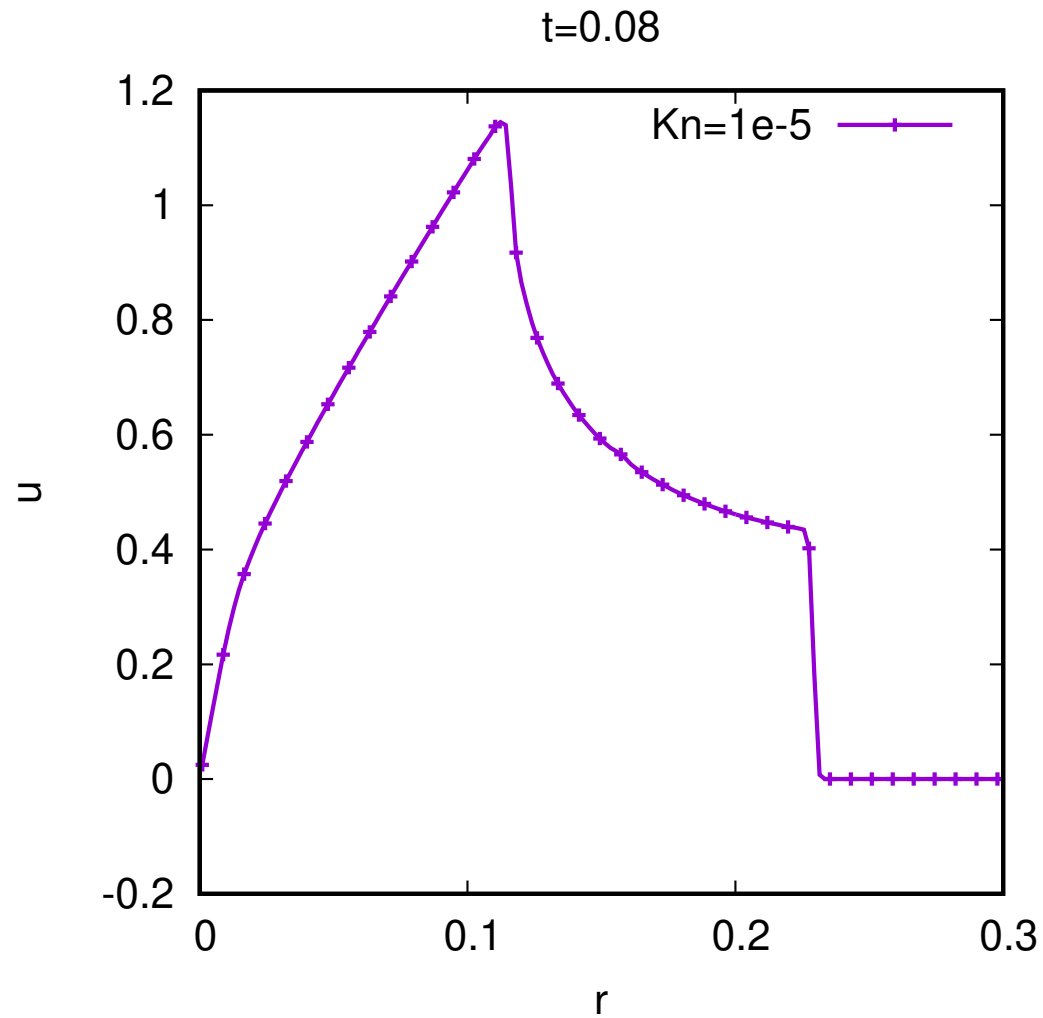
# Spherical shock: Transition flow regime - density



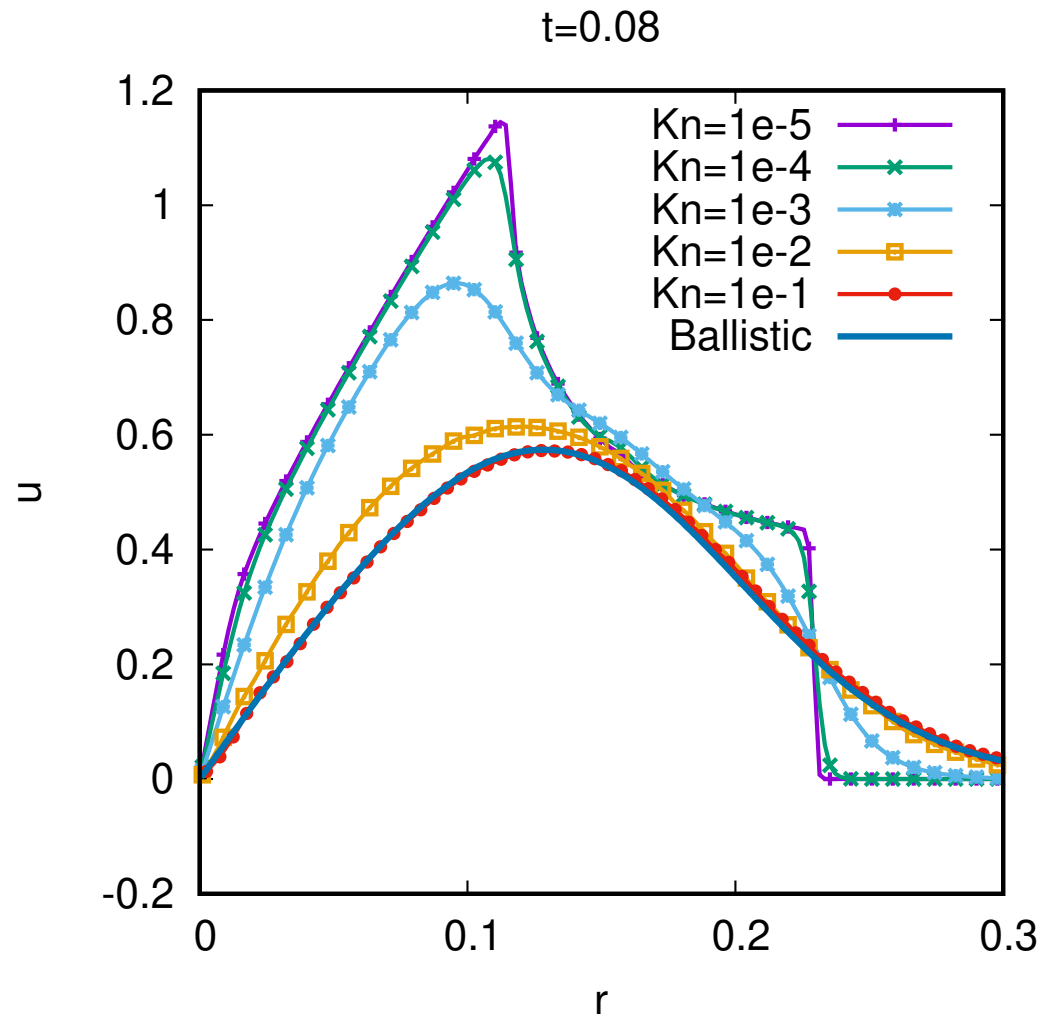
# Spherical shock: Transition flow regime - density



# Spherical shock: Transition flow regime - velocity



# Spherical shock: Transition flow regime - velocity





# Shock wave propagation: Conclusions

- ▶ LB can be applied to study flows from the inviscid to the ballistic regime.
- ▶ The discretisation of the momentum space using Gauss quadratures ensures the exact recovery of the moments of  $f$ .
- ▶ In the context of the Sod shock tube, our results were validated against analytic (inviscid and ballistic) and numerical (DUGKS) results.
- ▶ The rich phenomenology of 2D Cartesian shocks was successfully captured.
- ▶ The vielbein approach takes advantage of the flow symmetries, effectively reducing 3D simulations to 1D systems
- ▶ The cylindrically and spherically symmetric shocks are well described by using the vielbein formalism.
- ▶ Good accuracy ensured by the use of high-order schemes: (RK-3 + MP9).

## Section 8

# Relativistic fluid dynamics

# RTA formulation

- ▶ The relativistic Boltzmann equation with no external forces reads:

$$p^\mu \partial_\mu f = J[f], \quad J[f] = \int \left[ f'_* f' \left( 1 + \varepsilon \frac{f h^3}{g_s} \right) \left( 1 + \varepsilon \frac{f_* h^3}{g_s} \right) - f_* f \left( 1 + \varepsilon \frac{f' h^3}{g_s} \right) \left( 1 + \varepsilon \frac{f_* h^3}{g_s} \right) \right] F \frac{d\sigma}{d\Omega} d\Omega \frac{d^3 p_*}{p_*^0}, \quad (49)$$

where  $F = \sqrt{(p_* \cdot p)^2 - m^4 c^4}$  is the invariant flux,  $d\sigma/d\Omega$  is the differential cross section and  $\varepsilon \in \{-1, 0, 1\}$  for Fermi-Dirac, Maxwell-Jüttner and Bose-Einstein statistics.

- ▶  $J[f]$  admits the collision invariants  $\psi \in \{1, p^\mu\}$ , allowing the following conservation equations to be derived:

$$\partial_\mu N^\mu = 0, \quad \partial_\nu T^{\mu\nu} = 0, \quad (50)$$

where

$$N^\mu = \int \frac{d^3 p}{p^0} f p^\mu, \quad T^{\mu\nu} = \int \frac{d^3 p}{p^0} f p^\mu p^\nu. \quad (51)$$

# RTA: Anderson-Witting model

- ▶ The extension of the BGK model to relativistic and ultrarelativistic particles was proposed by Anderson and Witting:<sup>28</sup>

$$J[f] = \frac{\mathbf{p} \cdot \mathbf{u}}{\tau_{\text{A-W}} c^2} [f - f^{(\text{eq})}], \quad (52)$$

where  $u^\mu$  is the fluid four-velocity.<sup>29</sup>

- ▶ In order to preserve the collision invariants,  $f^{(\text{eq})}$  is restricted to satisfy:

$$u_\mu (N^\mu - N_{\text{eq}}^\mu) = 0, \quad u_\nu (T^{\mu\nu} - T_{\text{eq}}^{\mu\nu}) = 0. \quad (53)$$

- ▶ The second relation suggests that  $u^\mu$  should be defined in the Landau frame:

$$T^\mu{}_\nu u^\nu = -E u^\mu, \quad (54)$$

while the first relation fixes  $n_{\text{eq}} = -u_\mu N^\mu$  to be the particle number density in the Landau frame.

---

<sup>28</sup>J. L. Anderson, H. R. Witting, *Physica* **74** (1974) 466–488; 489–495.

<sup>29</sup>The signature convention is  $(-, +, +, +)$ .

# Decomposing $N^\mu$

- ▶ For the ideal fluid,  $N^\mu$  has 4 independent components, while  $T^{\mu\nu}$  has only 2 (1 for massless particles).
- ▶ In general,  $T^{\mu\nu}$  has 10 independent components which can be interpreted physically using so-called decomposition frames.
- ▶ Let  $u^\mu$  be a timelike vector  $u^2 = -1$  (the macroscopic velocity).
- ▶ The most general decomposition for  $N^\mu$  is:<sup>30</sup>

$$N^\mu = nu^\mu + V^\mu, \quad (55)$$

where  $u_\mu V^\mu = 0$  by construction.

- ▶ The particle number density  $n$  and the flow of particles in the local rest frame  $V^\mu$  are recovered as follows:

$$n = -u_\mu N^\mu, \quad V^\mu = \Delta^{\mu\nu} N_\nu, \quad (56)$$

where  $\Delta^{\mu\nu} = u^\mu u^\nu + g^{\mu\nu}$  is the projector on the hypersurface orthogonal to  $u^\mu$ .

---

<sup>30</sup>I. Bouras et al, Phys. Rev. C **82** (2010) 024910.

# Decomposing $T^{\mu\nu}$

- ▶ For *perfect fluids*,  $T^{\mu\nu} = T_{\text{eq}}^{\mu\nu} = (E + P)u^\mu u^\nu + P\eta^{\mu\nu}$ .
- ▶ In general,  $T^{\mu\nu}$  can be decomposed as follows:<sup>31</sup>

$$T^{\mu\nu} = Eu^\mu u^\nu + (P + \bar{\omega})\Delta^{\mu\nu} + W^\mu u^\nu + W^\nu u^\mu + \Pi^{\mu\nu}, \quad (57)$$

where  $W^\mu u_\mu = 0$ ,  $\Pi^{\mu\nu} u_\nu = 0$  and  $\Pi^{\mu\nu} u_\mu = 0$  by construction.

- ▶ The constituents of the SET can be obtained as follows:
  - ▶ The energy density  $E = u_\mu T^{\mu\nu} u_\nu$ ;
  - ▶ The isotropic pressure  $P + \bar{\omega} = \frac{1}{3}\Delta_{\mu\nu} T^{\mu\nu}$ ;
  - ▶ The flow of energy-momentum in the LRF  $W^\mu = -\Delta^{\mu\nu} u^\lambda T_{\nu\lambda}$ ;
  - ▶ The shear-stress (pressure deviator) tensor  $\Pi^{\mu\nu}$ :

$$\Pi^{\mu\nu} = T^{\langle\mu\nu\rangle} = \left[ \frac{1}{2} (\Delta^{\mu\lambda} \Delta^{\nu\kappa} + \Delta^{\nu\lambda} \Delta^{\mu\kappa}) - \frac{1}{3} \Delta^{\mu\nu} \Delta^{\lambda\kappa} \right] T_{\lambda\kappa}.$$

- ▶ The combination  $q^\mu = W^\mu - \frac{E+P}{n} V^\mu$  represents the heat flux.

---

<sup>31</sup>I. Bouras et al, Phys. Rev. C **82** (2010) 024910.

# The Eckart decomposition<sup>35</sup>

- ▶ In the Eckart (particle) frame,  $V^\mu = 0$  such that  $u_\mu$  is parallel to  $N^\mu$ :

$$N^\mu = n_e u_e^\mu, \quad (58)$$

where  $n_e = -u_e^\mu N_\mu$ .

- ▶ In the Eckart decomposition,  $q^\mu = W^\mu$ , such that  $T^{\mu\nu}$  becomes:

$$T^{\mu\nu} = E_e u_e^\mu u_e^\nu + (P_e + \bar{\omega}_e) \Delta_e^{\mu\nu} + (q_e^\mu u_e^\nu + q_e^\nu u_e^\mu) + \pi_e^{\mu\nu}. \quad (59)$$

- ▶ Eckart frame – pros:

- ▶ Intuitive:  $N^\mu$  and  $u^\mu$  are parallel;
- ▶  $\nabla_\mu N^\mu = \nabla_\mu (n u^\mu)$  has a simple form;
- ▶ Employed to construct the Marle RTA collision model.<sup>32</sup>

- ▶ Eckart frame – cons:

- ▶ Quote:<sup>33</sup> *For systems with vanishing net baryon number, as approximately realised in relativistic heavy ion collisions at very high energies, the Eckart frame is not well defined (the quark contribution to the energy flux diverges in the limit of vanishing baryon number density).*<sup>34</sup>
- ▶ Defining the Eckart frame requires knowledge of  $N^\mu$ .

---

<sup>32</sup>C. Marle, Annales de l'I. H. P. Physique théorique **10** (1969) 67.

<sup>33</sup>L. Rezzolla, O. Zanotti, *Relativistic hydrodynamics* (OUP, 2013).

<sup>34</sup>P. Danielewicz, M. Gyulassy, Phys. Rev. D **31** (1985) 53–62.

<sup>35</sup>C. Eckart, Phys. Rev. **58** (1940) 919.

## The Landau (energy) frame<sup>37</sup>

- ▶  $E_L$  and  $u_L^\mu$  are obtained by solving the eigenvalue equation:

$$T^\mu{}_\nu u_L^\nu = -E_L u_L^\mu. \quad (60)$$

- ▶ Because of this definition of  $u_L^\mu$ ,  $W^\mu = 0$  such that:

$$T^{\mu\nu} = E_L u_L^\mu u_L^\nu + (P_L + \bar{\omega}_L) \Delta_L^{\mu\nu} + \pi_L^{\mu\nu}. \quad (61)$$

- ▶ The heat flux  $q^\mu = -\frac{E+P}{n} V^\mu$  is now fully contained in  $N^\mu$ :

$$N^\mu = n_e u_e^\mu = n_L u_L^\mu - \frac{n_L}{E_L + P_L} q_L^\mu, \quad (62)$$

where

$$q_L^\mu = (E_L + P_L) \left( u_L^\mu + \frac{u_e^\mu}{u_e \cdot u_L} \right) \quad (63)$$

- ▶ The Landau quantities are in general not equal to the Eckart ones.
- ▶ Preferred for the Anderson-Witting model for the collision term.<sup>36</sup>

---

<sup>36</sup>J. L. Anderson, H. R. Witting, *Physica* **74** (1974) 466–488.

<sup>37</sup>L. D. Landau, E. M. Lifshitz, *Fluid mechanics*, 2nd ed. (1987).



## Ultrarelativistic ideal gases: 1D flows

- ▶ In the ultrarelativistic regime,  $p^2 = -(p^0)^2 + \mathbf{p}^2 = 0$ .
- ▶ This prompts the use of spherical coordinates, such that  $p^0 = p$ .
- ▶ If, in addition, the flow is along  $z$ , the M-J distribution reduces to:

$$f^{(\text{eq})} = \frac{n}{8\pi T^3} \exp\left[\frac{\mathbf{p} \cdot \mathbf{u}}{T}\right] = \frac{n}{8\pi T^3} \exp\left[-\frac{p\gamma}{T}(1 - \beta\xi)\right], \quad (64)$$

since  $u^\mu = \gamma(1, 0, 0, \beta)$ .

- ▶ The relativistic Boltzmann-Anderson-Witting eq. becomes:

$$\partial_t f + \xi \partial_z f = -\frac{\gamma(1 - \beta\xi)}{\tau_{\text{A-W}}} [f - f^{(\text{eq})}]. \quad (65)$$

- ▶ Due to the orthogonality relations  $u \cdot q = 0$  and  $\Pi^{\mu\nu} u_\nu = 0$ ,  $q^\mu$  and  $\Pi^{\mu\nu}$  can be expressed as:

$$q^\mu = q \begin{pmatrix} \beta \\ 0 \\ 0 \\ 1 \end{pmatrix}, \quad \Pi^{\mu\nu} = \Pi \begin{pmatrix} \beta^2 \gamma^2 & 0 & 0 & \beta \gamma^2 \\ 0 & -\frac{1}{2} & 0 & 0 \\ 0 & 0 & -\frac{1}{2} & 0 \\ \beta \gamma^2 & 0 & 0 & \gamma^2 \end{pmatrix}. \quad (66)$$

# Validation 1: Longitudinal wave damping

- ▶ Let us consider the propagation of infinitesimal perturbations through a background, homogeneous fluid of density  $n_0$ , pressure  $P_0$  and vanishing velocity.
- ▶ Writing  $n = n_0 + \delta n$  and  $P = P_0 + \delta P$  and considering that  $\delta n$ ,  $\delta P$ ,  $\Pi$  and  $q$  are of order  $\beta$ , the linearised limit of the cons. eqs. in the Eckart frame is:

$$\begin{aligned}\partial_t \delta n + n_0 \partial_z \beta &= 0, \\ 3\partial_t \delta P + 4P_0 \partial_z \beta + \partial_z q &= 0, \\ 4P_0 \partial_t \beta + \partial_t q + \partial_z \delta P + \partial_z \Pi &= 0.\end{aligned}\tag{67}$$

- ▶ In the (2nd order) hydrodynamic regime, the following constitutive eqs. can be written for  $q$  and  $\Pi$ :

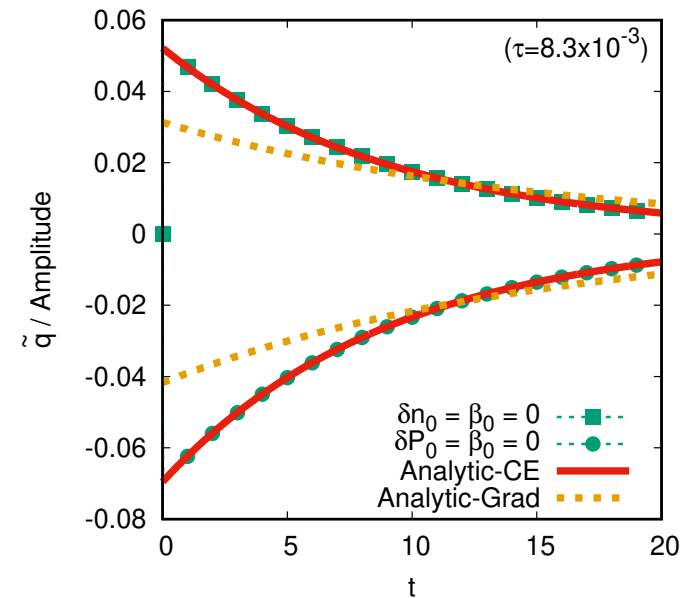
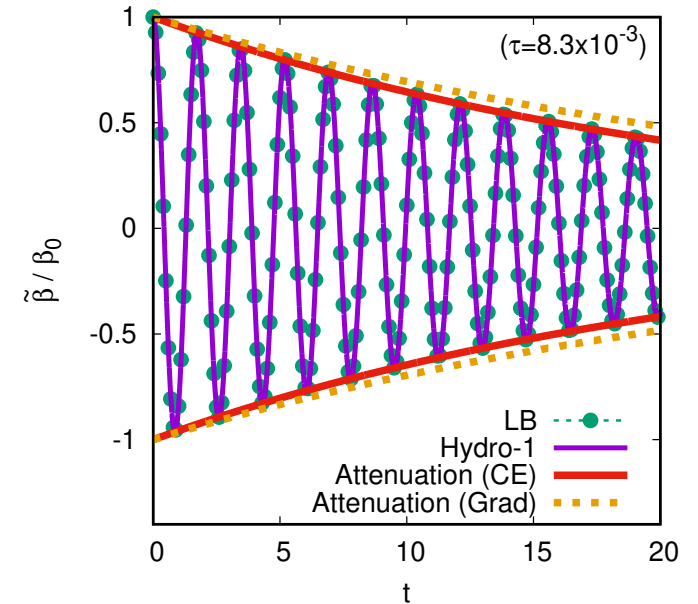
$$\begin{aligned}\tau_q \partial_t q + q &= -\frac{\lambda P_0}{4n_0} \left( \frac{3\partial_z \delta P}{P_0} - \frac{4\partial_z \delta n}{n_0} \right), \\ \tau_\Pi \partial_t \Pi + \Pi &= -\frac{4\eta}{3} \partial_z \left( \beta + \frac{q}{4P_0} \right).\end{aligned}\tag{68}$$

# First-order hydro

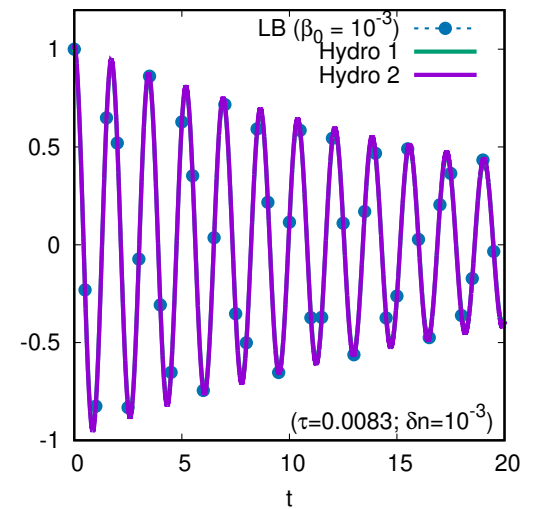
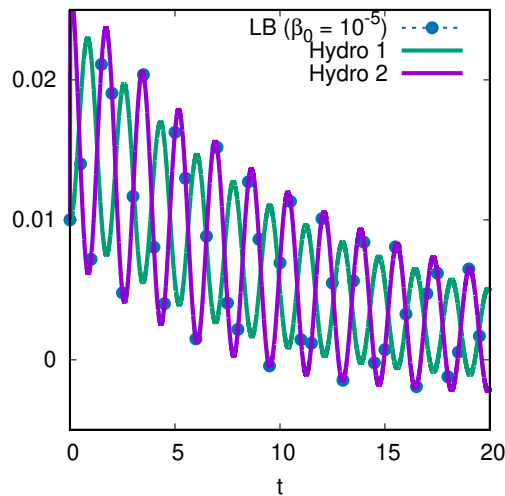
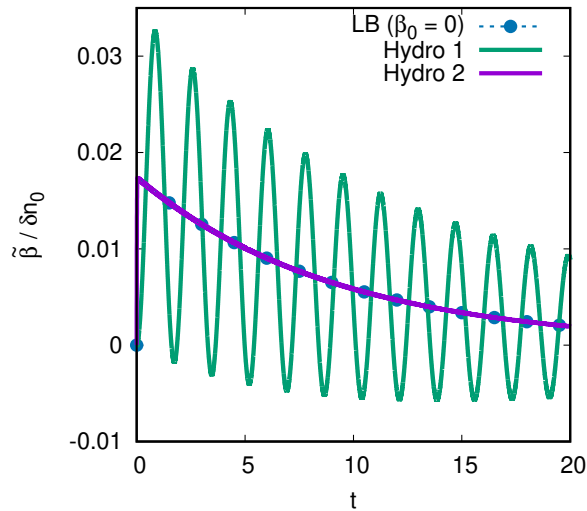
- Writing  $M(t, z) = \tilde{M}(t) \times \cos(kz)$  or  $\sin(kz)$ , the solution of 1st order hydro ( $\tau_q = \tau_\Pi = 0$ ) is:

$$\begin{pmatrix} \tilde{\beta} \\ \tilde{\delta n} \\ \tilde{\delta P} \\ \tilde{q} \\ \tilde{\Pi} \end{pmatrix} = e^{-\nu_\lambda kt} \begin{pmatrix} \beta_\lambda \\ \delta n_\lambda \\ 0 \\ q_\lambda \\ 0 \end{pmatrix} + e^{-\nu_d kt} \times \left[ \begin{pmatrix} \beta_c \\ \delta n_c \\ \delta P_c \\ 0 \\ \Pi_c \end{pmatrix} \cos \nu_o kt + \begin{pmatrix} \beta_s \\ \delta n_s \\ \delta P_s \\ 0 \\ \Pi_s \end{pmatrix} \sin \nu_o kt \right],$$

where  $\nu_\lambda = k\lambda/4n_0$ ,  $\nu_d = k\eta/6P_0$  and  $\nu_o \simeq \frac{1}{\sqrt{3}}$  is the speed of sound.



# First order not enough!



- ▶ Let us consider the case  $\beta_0 = \delta P_0 = 0, \delta n_0 \neq 0$ .
- ▶  $\tilde{\beta}$  is given in H1 through:

$$\frac{\tilde{\beta}_{H1}}{\delta n_0} = \nu_\lambda \left[ e^{-\nu_\lambda kt} - e^{-\nu_d kt} \left( \cos \nu_d kt - \frac{\nu_d}{\nu_o} \sin \nu_d kt \right) \right].$$

- ▶ The second order solution is:

$$\frac{\tilde{\beta}_{H2}}{\delta n_0} = \nu_\lambda \left[ e^{-\nu_\lambda kt} - e^{-t/\tau_q} \right].$$

- ▶ H1 has “insufficient modes”!
- ▶  $Q_L \times Q_\xi = 2 \times 6 = 12$  velocities required for this investigation!

# Simulations for the QGP fluid

- ▶ In the QGP fluid, it is expected that the ratio  $\eta/s$  between the shear viscosity and the entropy density is constant.
- ▶ Noting that in the A-W model for ultrarelativistic particles,

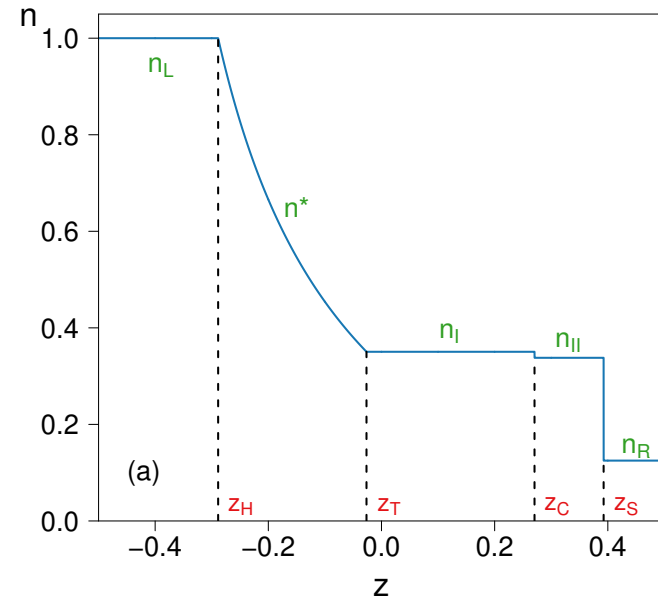
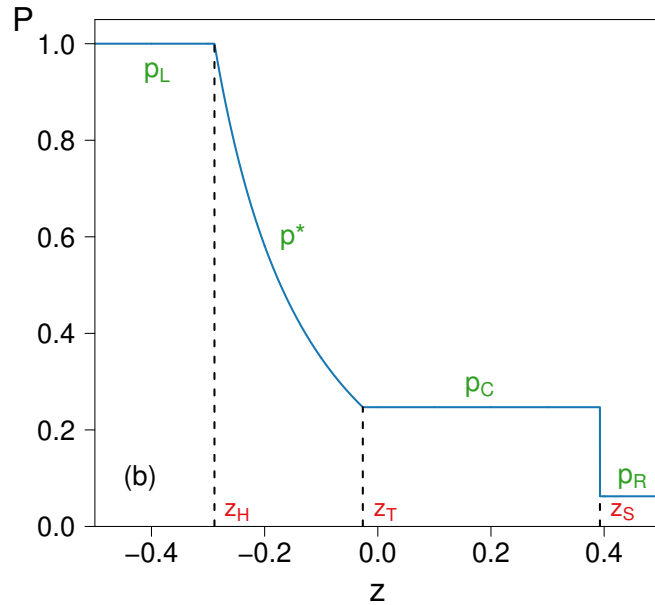
$$\eta = \frac{4}{5}\tau_{\text{A-W}}P, \quad s = n(4 - \ln \lambda), \quad \lambda = \frac{\pi^2 n}{g_s} \left( \frac{\hbar c}{K_B T} \right)^3, \quad (69)$$

a constant  $\eta/s$  ratio can be achieved by implementing  $\tau_{\text{A-W}}$  as follows:

$$\tau_{\text{A-W}} = \frac{\tau_{\text{A-W};0}}{T} \left[ 1 - \frac{1}{4} \ln(\bar{\lambda} \lambda_{\text{ref}}) \right], \quad \tau_{\text{A-W};0} = 5 \frac{\hbar c}{K_B T_{\text{ref}} L_{\text{ref}}} (\overline{\eta/s}), \quad (70)$$

where the quantities denoted with ref are computed at the reference values used in the non-dimensionalisation, while  $\bar{\lambda} = n/T^3$  is the relative fugacity.

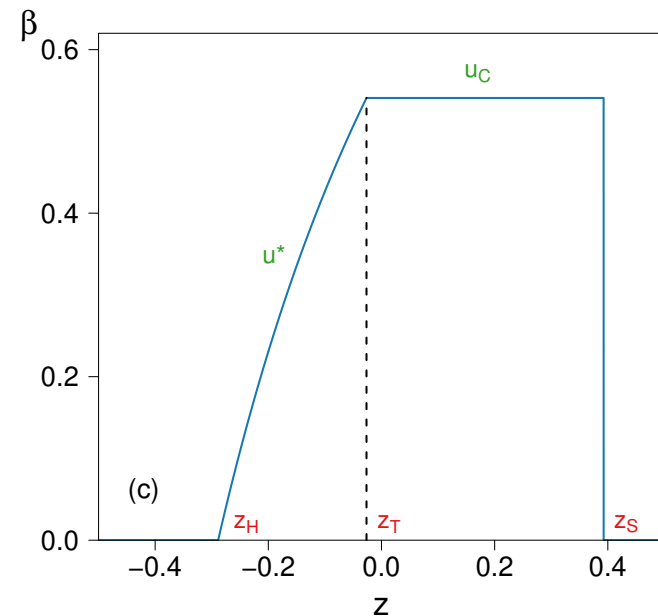
# Relativistic Sod shock tube



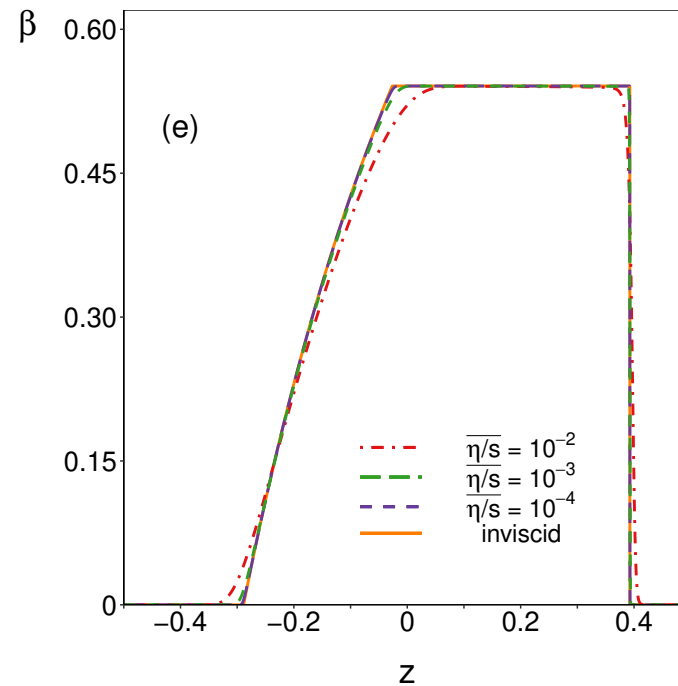
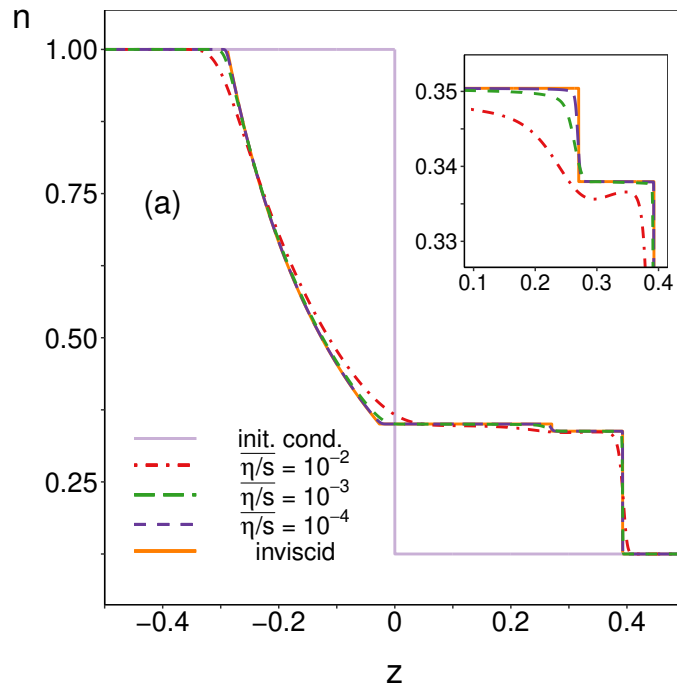
- ▶ The system consists of two semiinfinite domains separated by a membrane at  $z = 0$ :

$$(P, n, \beta) = \begin{cases} (P_L, n_L, 0), & z < 0, \\ (P_R, n_R, 0), & z > 0. \end{cases}$$

- ▶ The reference quantities are chosen to be those in the left state.



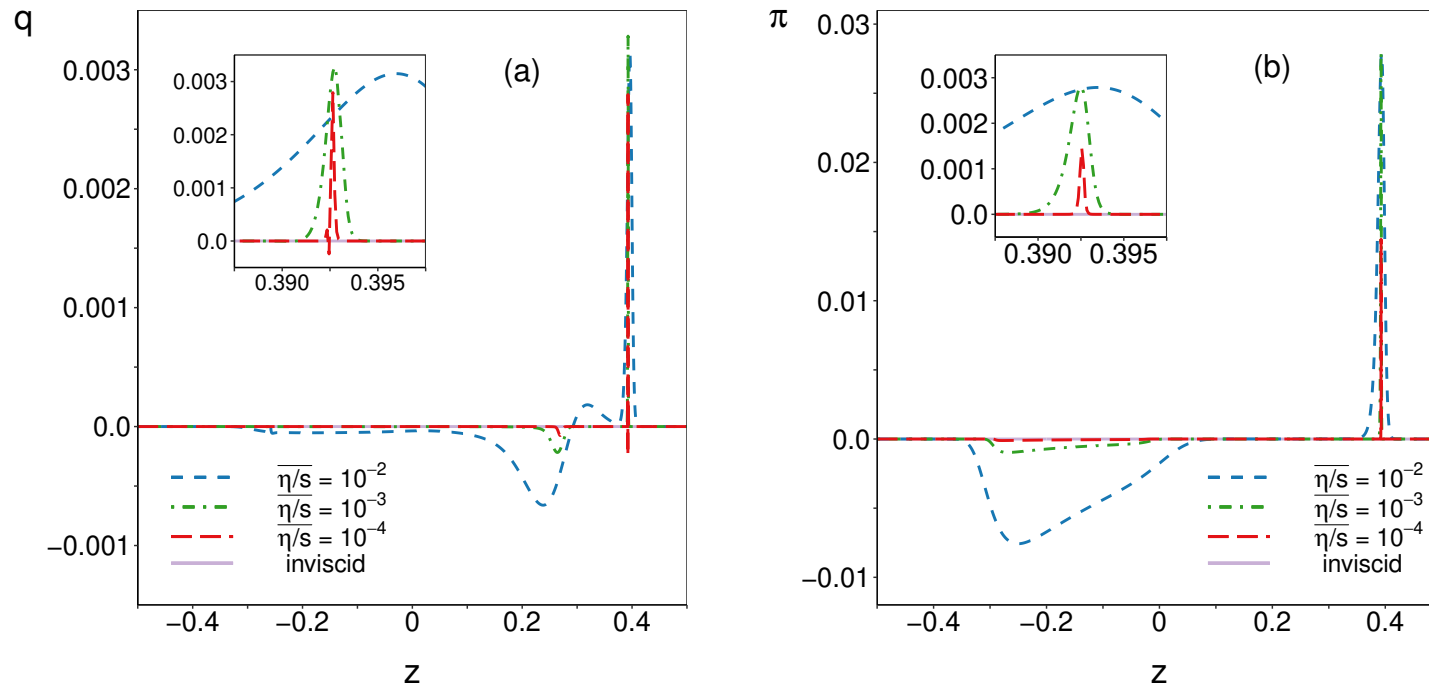
# Inviscid regime



- ▶ The inviscid regime can be solved analytically.<sup>38</sup>
- ▶ Since in the kinetic (RTA) approach,  $\tau_{A-W}$  can never vanish, the inviscid regime is reached only asymptotically.
- ▶ Even at  $\tau_{A-W} = 10^{-4}$ , a small deviation from the inviscid solution can be seen.

<sup>38</sup>L. Rezzolla, O. Zanotti, *Relativistic hydrodynamics* (OUP, 2013).

# Non-equilibrium quantities



- $q$  and  $\Pi$  are related to the gradients of  $n$ ,  $\beta$  and  $P$ :

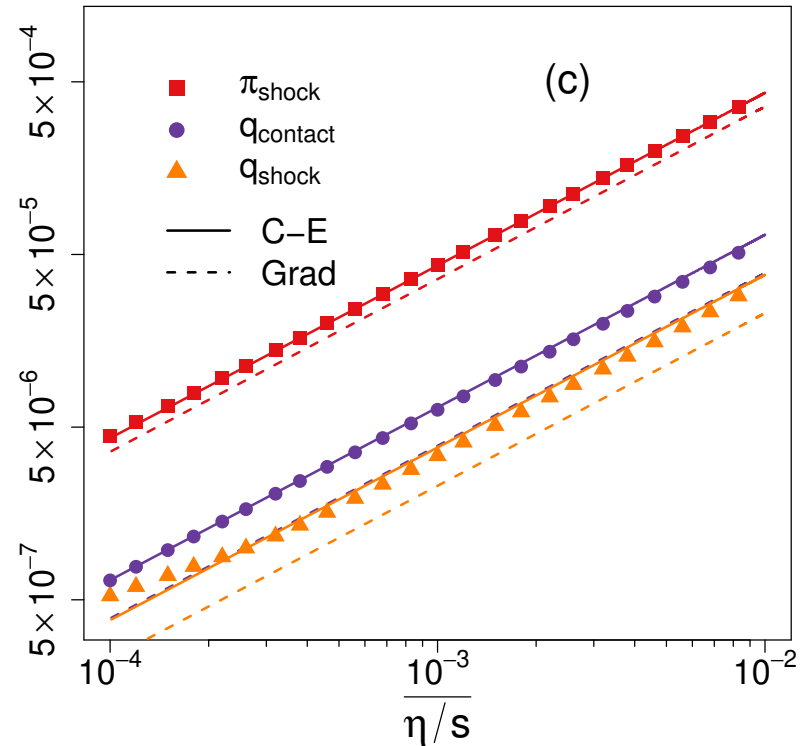
$$q = \frac{\lambda T \gamma^2}{4t} (1 - \beta \zeta) \partial_\zeta \ln \bar{\lambda}, \quad \Pi = -\frac{4\eta}{3t} (1 - \beta \zeta) \partial_\zeta (\beta \gamma), \quad (71)$$

where  $\zeta = z/t$  is the similarity variable for the inviscid regime.

- Near the shock front and contact discontinuity, these gradients tend to  $\infty$ .



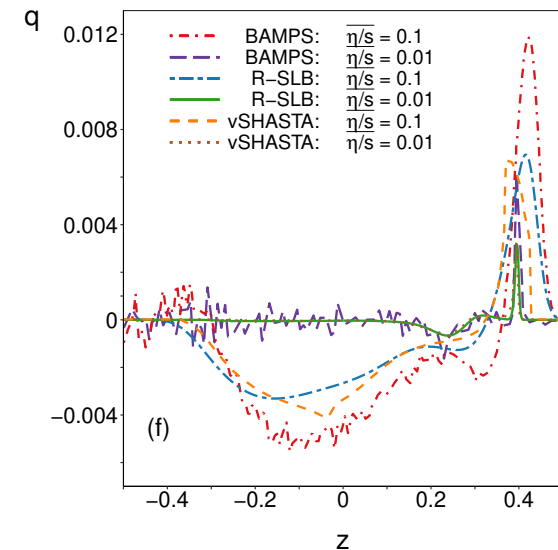
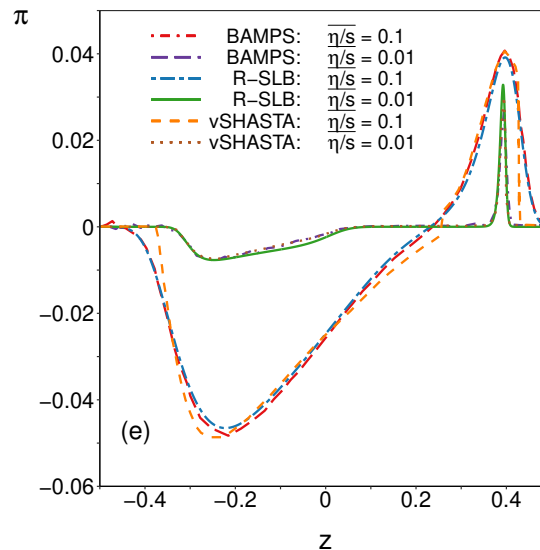
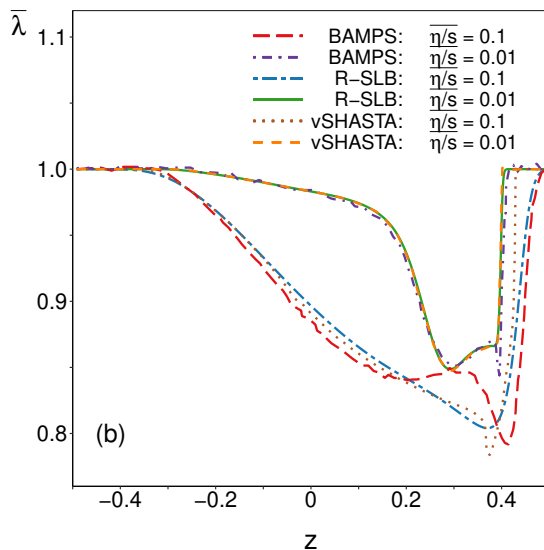
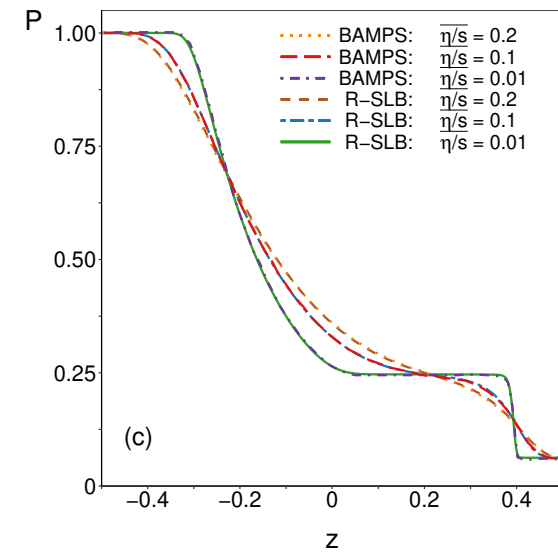
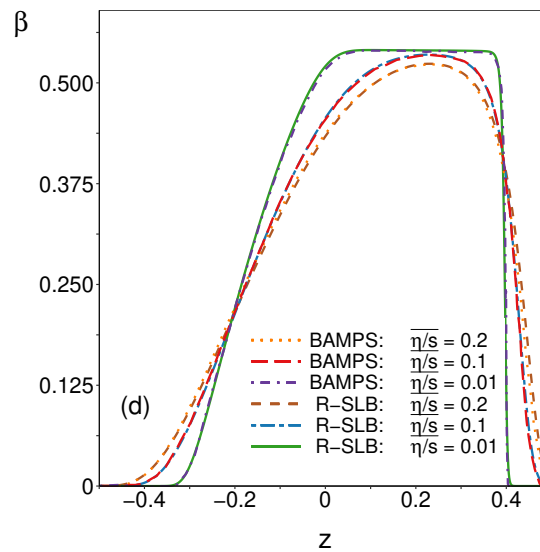
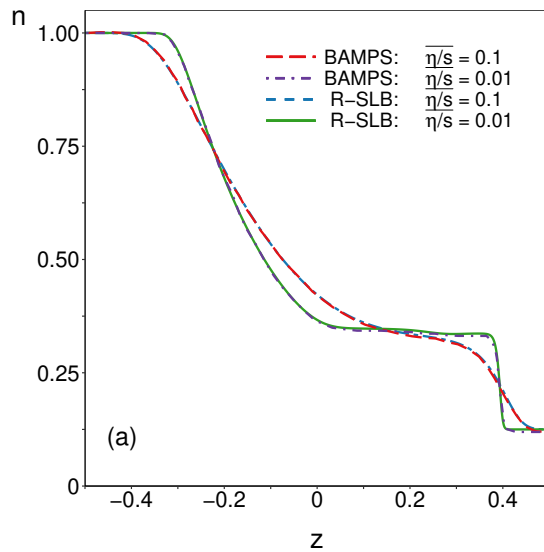
# Validation of transport coefficients



- ▶ The “spike” can be quantified by integrating  $q$  and  $\Pi$  around the discontinuity.
- ▶ For  $q$  around the contact discontinuity:

$$\int_{z_C - \delta z}^{z_C + \delta z} q \, dz = \frac{1}{8} (\lambda_{\text{heat},I} T_I + \lambda_{\text{heat},II} T_{II}) \ln \frac{\bar{\lambda}_{II}}{\bar{\lambda}_I}. \quad (72)$$

# Validation against BAMPS



- ▶ Very good agreement w.r.t. BAMPS is observed, even for  $\Pi$ .
- ▶ The disagreement in  $q$  is due to the incorrect value of  $\lambda$  given by the RTA.

# Relativistic fluid dynamics: Conclusions

- ▶ Comparing numerical (LB) and analytic results confirms the C-E values for  $\eta$  and  $\lambda$  for the AWB equation.
- ▶ Insufficient degrees of freedom in the H1 formulation results in inaccurate solutions for  $\beta$  even at small  $\tau$ .
- ▶ The LB model is very efficient at small (only 8 velocities required for  $\tau_{A-W} \lesssim 0.001$ ) to moderate (12 velocities required for  $\tau_{A-W} \lesssim 0.1$ ) values of  $\tau_{A-W}$ .
- ▶ Good agreement with BAMPS was observed, except for  $q$ , due to the incorrect recovery of the thermal conductivity in the AWB model.